MASTER THESIS

HØGSKOLEN I ÅLESUND
Aalesund University College

TITLE:
Computional Fluid Dynamics(CFD) Study on Free Surface Anti-Roll Tank and Experimental Validation

CANDIDATE NAME:			
Yue Li			
DATE:	COURSE CODE:	COURSE TITLE:	RESTRICTION:
29/05/2015	IP501909	Master thesis	
STUDY PROGRAM:		PAGES/APPENDIX:	LIBRARY NO.:
Master in ship design		65/10	

SUPERVISOR(S):
Karl Henning Halse

ABSTRACT:

The excessive motion of a ship can seriously degrade the performance of machinery and personnel. Anti-roll tanks are tanks fitted onto ships in order to improve their response to roll motion, which is typically the largest amplitude of all the degrees of freedom. In this thesis project, a numerical model based on Volume of Fluid (VOF) is introduced to simulate the liquid sloshing inside a free surface tank (FST). And this particular model is suitable for a general thermostatic incompressible sloshing problem.

Through the simulation of the model, the performance of the FST is fully investigated when the tank is excited by different periods and different amplitudes. Besides, different tank filling levels are studied to find out the optimal filling level. The results are proved by the existing experimental database.

Furthermore, a model platform is designed and established to give further validation to the numerical model. The comparisons between the model tests and simulations have shown good consistency. Further improvements are proposed in the end.

Keywords: Volume of Fluid (VOF), free surface tank (FST), model tests, validation

This thesis is submitted for evaluation at Ålesund University College.

Postal adress: Høgskolen i Ålesund N-6025 Ålesund Norway
Visit adress Larsgårdsvegen 2
Internett www.hials.no
Telephone 70 16 12 00
E-mail postmottak@hials.no
Fax 70 16 13 00
Bank 7694 05 00636
Enterprise no. NO 971 572 140

MASTER THESIS 2015
FOR
STUD.TECHN. 130513

COMPUTATIONAL FLUID DYNAMICS (CFD) STUDY ON FREE SURFACE ANTI-ROLL TANK AND EXPERIMENTAL VALIDATION

The excessive motion of a ship can seriously degrade the performance of machinery and personnel. Anti-roll tanks are tanks fitted onto ships in order to improve their response to roll motion, which is typically the largest amplitude of all the degrees of freedom.

The thesis shall investigate the designs of different anti-roll tanks and mainly focus on free surface tank. Results of computer simulations of the water motion in free surface tank are compared with experimental data. The numerical computations are done with Star CCM+. Part of experimental data comes from ShipX. Besides, model tests are designed and implemented at Aalesund University College.

- Pre-study
  - Current Anti-roll tanks designs, Pros and Cons of each design
  - Principle of anti-roll tank and wave patterns inside
  - Knowledge of numerical analysis method
- CFD Simulation on free surface tank
  - Define model architecture, parameters and motion
  - Investigation on mesh selection
  - Investigation on time marching scheme, including model selection and time step
  - Investigation on turbulence modelling
  - Comparison between 2D and 3D flow
  - The natural period of the free surface tank
- Tank performance discussion
  - Investigation on different excitation amplitudes
  - Investigation on different filling levels and the optimal filling level
  - Cover influence
- Experimental validation
  - Design of a physical model test platform (1 DOF roll motion)
  - Model tests of the free surface tank
  - Comparison between the results from simulation and model test
  - The results are compared to the database in ShipX
- Discussion and closure

The scope of work may prove to be larger than initially anticipated. Subject to approval from the advisor, topics from the list above may be deleted or reduced in extent.

The thesis should be written as a research report with summary, conclusion, literature references, table of contents, etc. During preparation of the text, the candidate should make efforts to create a well arranged and well written report. To ease the evaluation of the thesis, it is important to cross-reference text, tables

and figures. For evaluation of the work a thorough discussion of results is needed. Discussion of research method, validation and generalization of results is also appreciated.

In addition to the thesis, a research paper for publication shall be prepared.

Three weeks after start of the thesis work, a pre-study have to be delivered. The pre-study have to include:

- Research method to be used
- Literature and sources to be studied
- A list of work tasks to be performed
- An A3 sheet illustrating the work to be handed in.

A templates and instructions for thesis documents and A3-poster are available on the Fronter website under MSc-thesis. Please follow the instructions closely, and ask your supervisor or program coordinator if needed.

The thesis shall be submitted in electronic version according to new procedures from 2014. Instructions are found on the college web site. In addition one paper copy of the full thesis with a CD including all relevant documents and files shall be submitted to your supervisor.

Supervision at AAUC: Karl H. Halse,
Contact at : Aalesund University College

Karl H. Halse
Supervisor

Delivery: 29.05.2015 Signature candidate: Yue Li

PREFACE

This master thesis was written at the Aalesund University College, Faculty of Maritime Technology and Operations (AMO), to earn the degree Master of Science.

The present work constitutes the graduation in the 2 Years International Master Programme in Ship design. The thesis has been made solely by the author; some contents used in the project, however, is based on previous works of others. Through reference has been made accordingly.

The thesis project contains CFD simulations as well as physical model tests and verification. Experimental platform design, establishment and tests are also part of the thesis.

My special thanks go to Associated Prof. Karl Henning Halse who was willingly supervising me. I appreciate his guidance and support throughout the entire thesis composition. The new ideas inspired and new fields of knowledge introduced by him has always been fruitful to me.

Thanks to Geir Åge Øye from Rolls-Royce Marine AS for sharing his experience within this field.

I would also like to thank Professor Vilmar Ærøy, Phd candidate Grotle Erlend Liavåg for their assistance on platform design and establishment. Thank Stig Morten Skaar, Nikolas Myklebostad, Anders Sætersmoen and Wei Li for assisting the model platform manufacturing and running.

No less thanks to my parents who enabled my studies and supported me in many respects. Thanks to my friends who made the time here in Norway so special.

Aalesund University College

May. 2015

Yue Li

ABSTRACT

The excessive motion of a ship can seriously degrade the performance of machinery and personnel. Anti-roll tanks are tanks fitted onto ships in order to improve their response to roll motion, which is typically the largest amplitude of all the degrees of freedom. In this thesis project, a numerical model based on Volume of Fluid (VOF) is introduced to simulate the liquid sloshing inside a free surface tank (FST). And this particular model is suitable for a general thermostatic incompressible sloshing problem.

Through the simulation of the model, the performance of the FST is fully investigated when the tank is excited by different periods and different amplitudes. Besides, different tank filling levels are studied to find out the optimal filling level. The results are proved by the existing experimental database.

Furthermore, a model platform is designed and established to give further validation to the numerical model. The comparisons between the model tests and simulations have shown good consistency. Further improvements are proposed in the end.

Keywords: Volume of Fluid (VOF), free surface tank (FST), model tests, validation

Table of contents

TERMINOLOGY

Symbols

A	Excitation amplitude [deg]
b	Tank width [m]
C_N	Courant number [-]
h	water level [m]
h/b	Tank filling ratio [-]
H	Tank height [m]
i	Mode number [-]
Lpp	Length between perpendiculars [m]
M	Damping moment [Nm]
t	Time step [s]
T_n	Natural period [s]
u_i	Flow velocity [m/s^2]
x_i	Grid spacing at node i [m]

Abbreviations

ART	Anti-roll tank
CFD	Computational Fluid Dynamics
FST	Free surface tank
LNG	Liquid Natural Gas
RAO	Response Amplitude Operator
RSM	Reynolds-stress model
SST	Shear Stress Transport
VERES	ShipX Vessel Responses program
VCG	Vertical center of gravity
VOF	Volume of Fluid

1 INTRODUCTION

In former times ships were stabilised in the wind by their huge sails and large keels. When ships began sailing with motor power they started to use bilge keels but these were not sufficient enough to compensate for the upcoming roll motions. It was already in 1880 when Watts and Froude suggested the use of water tanks for damping as reported by (Bosch 1966). Nowadays, roll stabilizing tanks are widely used on offshore supply vessels and fishing vessels to provide a better and safer working environment. Tanks of different shape exist and they can be passively or actively controlled.

The movement of water within a container is called sloshing. Sloshing appears in almost every moving vessel which contains liquids with a free surface in a partially filled tank. (O. T. Faltinsen 2009) pointed out that the liquid will move severely from one side to the other as a result of resonant excitation motions from the ship. As examined later, sloshing has a strong influence on the dynamic stability of a vessel.

Ship motions excited by waves can evoke sloshing in a tank which in turn will influence the ship motions from inside the ship. Ships equipped with a specially tuned tank utilize this effect to dampen their roll motions.

1.1 Motivation and Objective

Since the 1960´s first liquid natural gas (LNG) tankers were built to serve Europe and Japan with a new carrier of energy. It became apparent that sloshing in cargo tanks resulted in one of the most critical ship loads. Until today these generated loads have remarkable influence on the tank walls and the supporting ship structure as reported by (O. M. Faltinsen 1974) and (Solaas 1995). Spherical and membrane tanks are the two mainly used geometries. A failure of such a tank can lead to brittle fracture of the surrounding structure due to a low temperature shock of the escaping liquid. Besides the risk of explosion the repair costs and out-of-service costs are high.

The phenomenon of sloshing appears not only in ships but also in many different applications and vehicles. Recently sloshing in seismically excited tanks is investigated that (Goudarzi 2012). Other storage tanks are installed on floating offshore units for oil and gas production. Tanks of well boats contain living fish which has to be transported carefully to fish farms. Solaas (1995) mentioned sloshing in railway tanks. One can also find many articles written about sloshing in fuel tanks of rockets.

As can be seen from the described cases, cargo tanks apply manifold and sloshing becomes an important aspect. According to Solaas (1995), sloshing can involve large fluid motions with turbulences, braking waves and spray. These are highly nonlinear phenomenon and sloshing itself is therefore difficult to predict.

Besides the undesired sloshing in cargo tanks, sloshing is required in roll damping tanks to a certain amount. Still, many model tests are conducted to find the best configuration for a roll damping tank. On the other hand, recently studies have tried to perform numerical simulations of the complicated 3D motion of water in tanks together with the sloshing at the free surface. Different numerical methods have been tested by researchers.

This report considers the suitability of a commercial Navier Stokes Computational Fluid Dynamics software for the simulation of free surface tank. As CFD is a relatively new method of simulating fluid dynamics problems, there is as yet no consensus as to the most suitable approach. Given the assortment of possible solution strategies available, it is necessary to study the influence of user choice on the accuracy of the obtained solution. This report seeks to establish the significance of model-specific computational parameters and develop guidelines for future CFD sloshing models. Besides, computational solutions are compared to experimental tests at Aalesund University College. In this study the following are investigated:

- Summary of current ship anti-roll tanks;

- Grid (mesh) independence;
- Time marching scheme;
- Turbulence modelling (K- Epsilon & K-Omega);
- 2D flow and 3D flow;
- Natural period of the tank;
- Tank performance at different excitation amplitudes;
- Tank performance at different filling levels;
- Optimal filling level;
- The influence of cover panel.

1.2 Thesis structure

In the following chapters the theoretical aspects of a free surface tank will be discussed first. This will be done by describing the mechanism of the tank and how this kind of tank works. Then it summarized the current anti-roll tank designs and the numerical methods to this particular problem.

The second part of the report will focus on the CFD simulations. It aims to develop guidelines for a generic anti-roll tank simulation model. Therefore, major considerations are discussed including the mesh independence, time marching scheme, time step control, turbulence modelling and 2D/3D flow difference. And this particular model is suitable for a general thermostatic incompressible sloshing problem.

Chapter 4 will study the the anti-roll tank performance. Firstly, the natural period of the partially filled tank is investigated and discussed. Then different excitation amplitudes will be studied. Tank performance at different filling levels are also of interest. Besides, a small investigation on cover panel effect is included.

The last part of the report will focus on the model tests. It will compare the results from simulations with the exsiting experimental database. The model tests, which designed and performed by the author, have been used to provide validations for the numerical simulations as well.

2 BACKGROUND AND THEORETICAL BASIS

The subject of roll stabilisation has been investigated for many years by Naval Architects and designers. The main reason for this continued interest is that for roll, unlike pitch or other degrees of freedom, the forces required to create a stabilising effect are relatively small. So far, different stablizing devices have been designed such as Bilge keel, fin stabilizer and anti-roll tank. Figure 1 shows the typical Roll response of a ship with and without a passive roll damping tank.

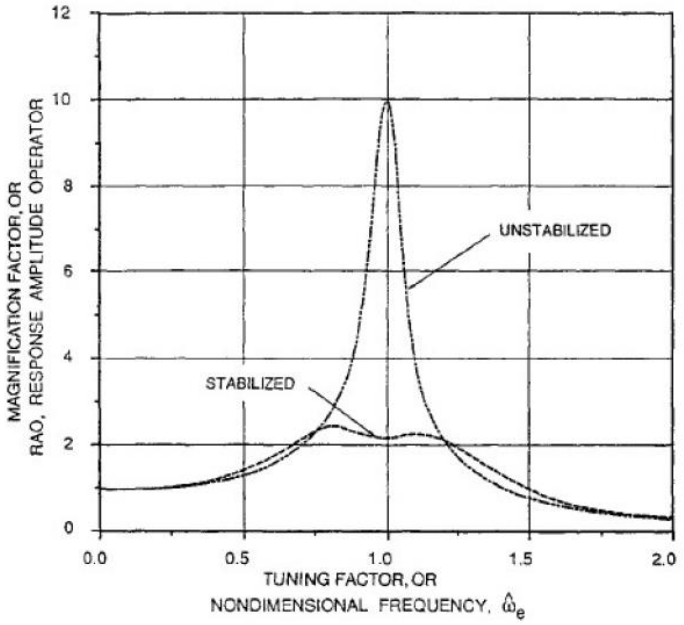

Figure 1. Roll response of a ship with and without a passive roll damping tank (Lewis 1989)

2.1 Mechanism of anti-roll tanks

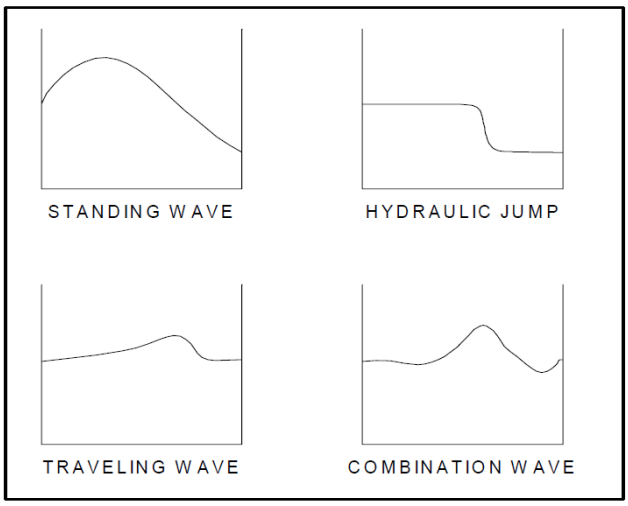

Figure 2. Wave patterns inside a free surface tank

The mechanism by which the flowing water can affect a vessel motion is a combination of various wave phenomena, as shown in Figure 2. Firstly, and most importantly, the variation in water mass from one side of the tank to the other can create an additional moment about the roll-centre, the phase difference between the motion of the water and the ship roll determining whether the effect is to increase or reduce the roll amplitude. Secondly the turbulent flow of water within the tank can be used to reduce roll by

removing kinetic energy from the ship's motion. This is achieved by the formations of hydraulic jumps and turbulence. The creation of hydraulic jumps, or wave bores, within the tank at certain depths and roll frequencies can also result in a considerable impulse when the bore hits the tank wall. This, coupled with the mass of water moving harmonically across the tank, can have a significant effect on the ship motion.

There are a great number of roll stabilisation devices available for use on vessels today. Many of these were initially developed for use on large ships but are increasingly being installed on smaller vessels where the subsequent benefit to the vessel's motions is often more apparent. This is due to the relatively high transverse stability, and short natural roll periods of smaller vessels (Martin 1994). The prevalence of shorter waves also means that smaller vessels are more likely to encounter resonant wave conditions and thus violent rolling.

Hydraulic jump

Due to roll motions of the ship, the fluid in the tank will flow from one side to the other across the tank. The shifting mass will exert an own roll moment on the ship. By a smart design of the tank this roll moment can be used as a damping moment which counteracts the initial roll motion of the ship as stated by (Moaleji 2007). Thereby a so called hydraulic jump occurs when the lowest natural frequency of the tank is near the excitation frequency. The flow motion with a hydraulic jump is schematically illustrated by Faltinsen and Timokha (2009) in Figure 3.

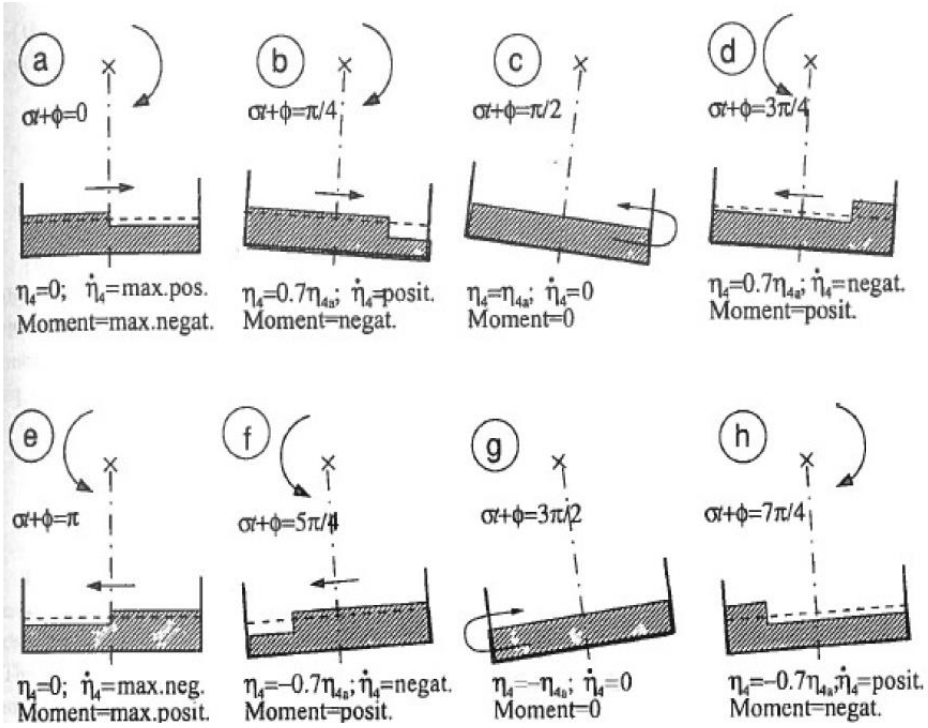

Figure 3. Psition of the hydraulic jump during one period of roll at tank resonance

Standing wave

Henderson (2014) pointed out that waves can be reflected in a way such that the water seems to stand still at certain locations in the tank while the surrounding medium is moving up and down. These nodal points are illustrated in Figure 4 and a so called standing wave pattern is formed.

Nodal and antinodal vertical lines pass through the liquid volume. A liquid particle moves only horizontally at a nodal line, whereas the motions are only vertical at an antinodal line. The lowest natural mode (i=1) has a node in the middle of the tank and antinodal

lines coinciding with the vertical walls. The number of nodal lines is equal to the mode number, i. The nodes divide the interval $[-\frac{1}{2}b, +\frac{1}{2}b]$ into i+1 subintervals.

Figure 4 illustrates that the motion of a liquid particle associated with small-amplitude freestanding waves by a natural mode is rectilinear, which differs from linear harmonic long-crested propagating wave.

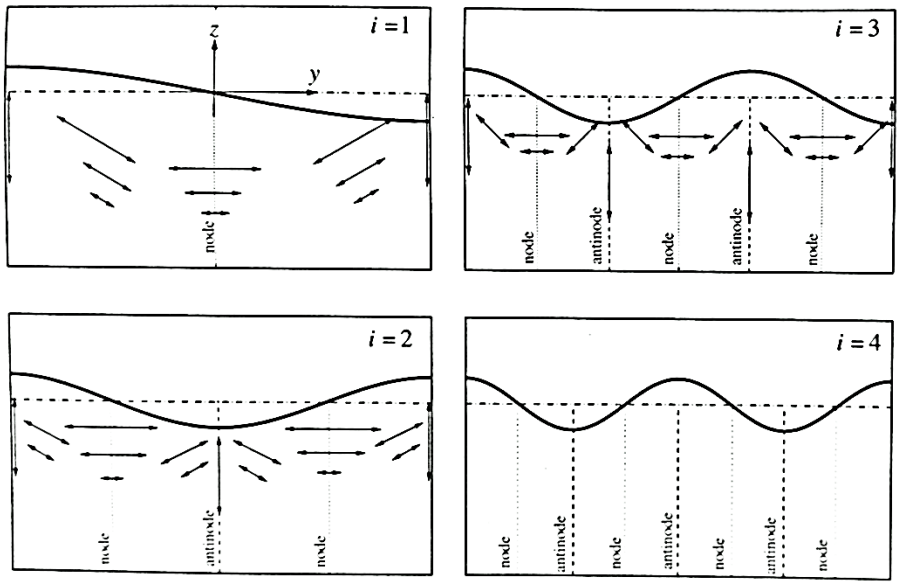

Figure 4. Standing waves corresponding to natural modes for sloshing in rectangular tank

2.2 Development of ship anti-roll tanks

2.2.1 Free surface tank (FST)

In 1875 Watts first introduced the free surface anti-roll tank as a passive method of damping rolling motions. He proposed a large, uniform cross section tank partly filled with water, placed athwartships and usually located well above the centre of gravity, see Figure 5. The principle was based on the work by (Froude 1861) who was the first to frame the effect of waves on the rolling motion of ships.

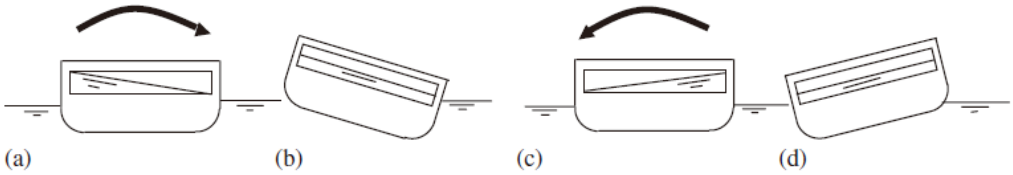

Figure 5. Ideal motion of water in the tank

More recent experimental work was done by (Ikeda 1991) in which the coupling effect on the performance of a rectangular anti-rolling tank was investigated. The results of the bench test of an anti-rolling tank including the effect of sway motion as well as roll motion demonstrated that the sway motion reduced the reduction of the roll angle by the anti-rolling tank and lengthened the natural period of the tank.

It was observed that the performance of free-surface tanks is maximized when the natural frequency of the tank is tuned to be close to the roll natural frequency of the ship. This is mainly done by altering the water level inside the tank. This confirmed the findings of Watts and Froude from a century earlier. Different responses of tanks can be

obtained by changing their shapes, two modifications of such tanks are presented in Figure 6.

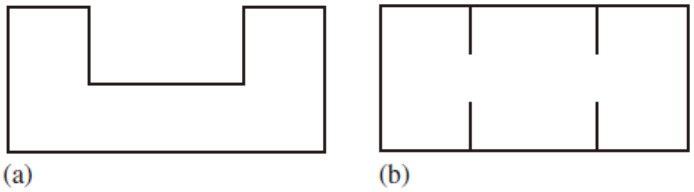

Figure 6. Plan view of modified tanks (a) C-shape tank and (b) rectangular tank with baffles

One disadvantage of rectangular tanks is that it is difficult to control the water, rushing freely from side to side in the tank, threatening the safety of the ship in rough weather. Sometimes a limited control is exerted over the motion of the fluid by installing a restriction or baffle in the center of the tank. Lee and Vassalos (1996) experimentally showed that the performance characteristics of an anti-roll tank could be 'tailor-made' by a judicious application of flow obstructions.

2.2.2 U-shape tank

The simple free surface tank has three practical problems; two due to the sloshing of the large free surface and the third to its location. Sloshing makes it difficult to control the water and adversely affects stability while the tanks required location, above the centre if gravity and near the centre of the ship, is prime usable space. These problems were solved simultaneously with the U-shaped tank suggested by Frahm (1911).

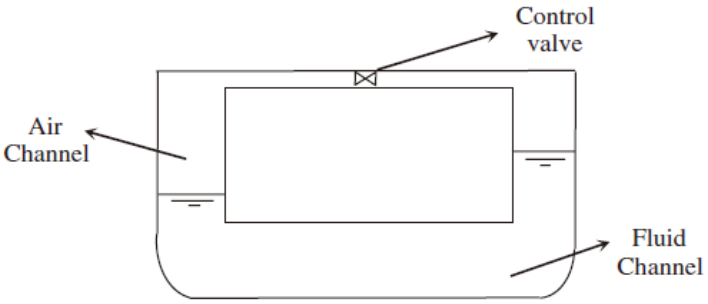

Figure 7. Passive U-shape tank

It was found that for ships with a small metacentric height operating in seas with a regular wave pattern, good results were obtained with a roll reduction of approximately 50%. However, in choppy seas with no regular pattern, the results were poor, frequently with no observed roll reduction at all (Bennett 1991).

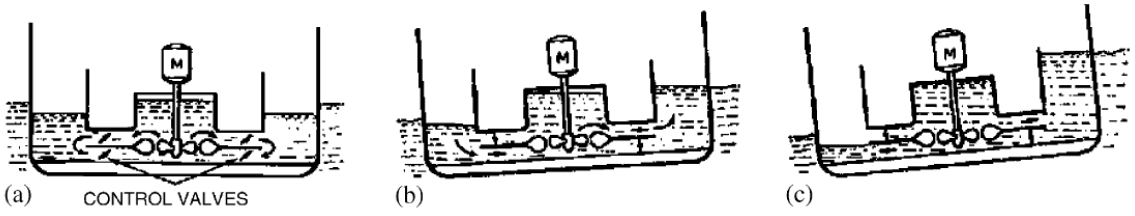

Figure 8. Activated U-shape tank

A logical development of the Frahm system was to pump the water from one leg of the U to the other, rather than relying on the ship's rolling motion exclusively for the transfer. By doing so, a limitation of the passive tanks with their dependence on resonance could be largely overcome. Such tanks are generally known as U-shape activated tanks or

simply ‘‘active tanks’’. A system was evolved by Bell and Walker (1966), which achieved more than the damping effect of a passive-type tank and also did not involve setting into motion a long column of fluid. Fig. 8 shows the arrangement of this system. It is seen that the impeller which rotates continuously drives fluid from the lower to the upper of the two ducts connecting the port and starboard tanks.

2.2.3 Free-flooding tank

In some installations, the horizontal leg of the U-tank was entirely removed and the bottoms of the tanks were opened to the sea, Figure 9 (left). One of the few cases of installation of free-flooding tanks was in 1931 and 1932 when tanks were retrofitted to six USN cruisers of the Pensacola and Northampton classes. The tanks had no air cross connection, despite initial misgivings the tanks were successful reducing the roll motion by 30–40% and increasing the roll period by 20%.

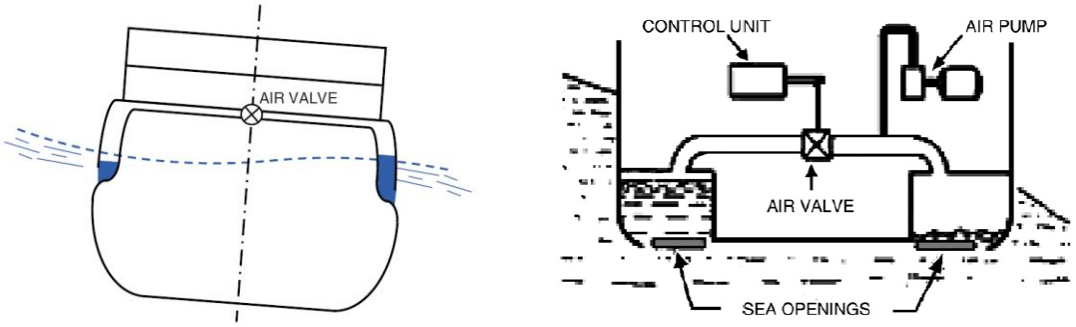

Figure 9. Free-flooding tank

In 1958 a more advanced version of free-flooding tanks were tested on a model in the Denny Model Ship Tank at Stevens Institute of Technology (Figure 9 right).

Results showed that this system could reduce roll by about 60% (Vasta 1961). The effectiveness of the free-flooding tanks falls off as the ship speed increases, because at higher speeds, water cannot get into the flooding port. The main advantage of free-flooding tanks is that they do not need a water crossover duct, and therefore do not require major modifications of the ship when installation is contemplated in an existing ship. Free-flooding tanks use seawater as working fluid and this can have considerable impact on the design in terms of corrosion, fouling and maintenance.

2.2.4 Summary of anti-roll tanks

Table 1. Summary of different anti-roll tanks

Type	Control	Roll reduction	Merit	Defect
Free surface tank	Passive	37.5%	Simple; cost efficient	Free liquid surface Difficult to control the water and adversely affects stability; Location
Rectangular tank with baffles	Passive	up to 80% in periodic waves; up to 50% in irregular waves	easily be adapted to another condition of loading changing the water depth	Location
Passive U-tank	Passive/ Passive air control	Approximately 50%	Good performance in seas with a regular wave pattern	Poor performance in choppy seas with no regular pattern; Water crossover duct
Activated U-tank	Activated	(Same as passive U tank)	-	Power consumption; Water crossover duct
Free-flooding tank	Activated	60%	No water crossover duct	Water cannot get into the flooding port at higher speeds.

2.3 Numerical methods

Recently studies have tried to perform numerical simulations of the complicated 3D motion of water in tanks together with the sloshing at the free surface, both for simple open tanks and U-tanks. A specific numerical study using a 2D finite element method for U-tube passive anti-rolling tanks was done by Zhong et al. (1998) who reported numerical analysis of sloshing in a road container with a MAC type method for tracing the free surface evolution. Many papers have reported on the sloshing phenomenon in a rigid rectangular tank and theoretical and experimental research has been carried out by means of the shallow water wave theory (Chern et al., 1999; boundary element methods by Liu and Huang, 1994; finite element methods, VOF method by Celebi and Akyildiz, 2002. Extensive comparative studies on sloshing loads has been made by Sames et al., 2002. Most of the methods reported were based upon finite difference, finite volume approaches or even shallow water equation solvers.

Another interesting solution was proposed by Souto Iglesias et al. (2004). They simulated the motion of water using the smoothed particle hydrodynamics method where the fluid is represented by a set of particles which follow the fluid motion and have the fluid quantities such as mass and momentum. Associated with each particle are its position, velocity, and mass. They validated their method by performing experiments on different kind of free-surface tanks such as rectangular tanks with and without baffles and on a C-tank, and showed very good agreement between the simulation and experimental results.

2.4 Key parameters of free surface tank

2.4.1 Tank dimensions

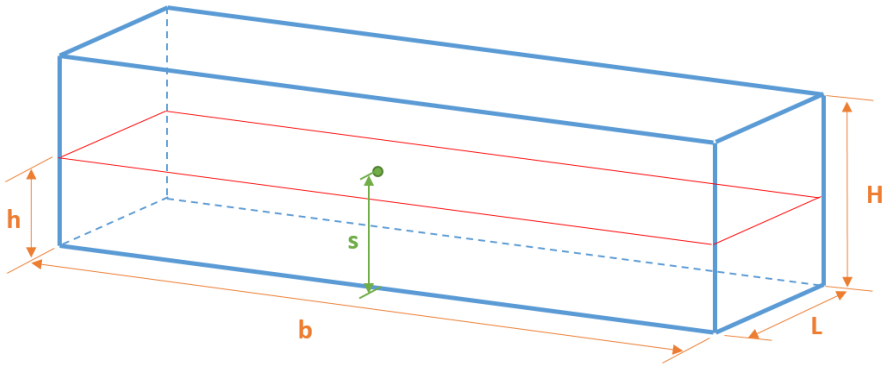

Figure 10. Definition of geometry and tank dimensions: Free surface tank (FST)

The following parameters are important when the tank moment and phase is to be determined:

- **Tank geometry/dimensions:** Defined by the width b, length L and height H.
- **Vertical position relative to the rotation axis, s/b:** Characterized by the vertical distance from the tank bottom to the ship's center of gravity, s. The factor s/b is often used to describe this parameter, where s is the vertical distance defined as positive when the tank bottom is above COG.
- **Tank filling, h:** Denoted by the non-dimensional number h/b where h is the fluid level in the tank.

  In practice, for shallow-liquid sloshing, tank filling rations $h/b \leq 0.05 - 0.1$. The reason for the lower range is that it is difficult to obtain good effect of the tank for lower fillings (large roll angles leads to a partly dry tank bottom). $0.05 - 0.1 \leq h/b \leq$

$0.2 - 0.25$ is so-called intermediate depths. Finite depth is a depth larger than the intermediate depth and corresponds to when $tanh(\pi h/l)$ is not close to 1. Finally, the deep-water approximation implies relatively large h/l so that $tanh(\pi h/l) \approx 1$.

2.4.2 Natural period

Natural frequencies or eigenfrequencies describe the modes in which a body or fluid can oscillate when excited. The modes are characteristic wave patterns as shown in Figure 4. The relationship of any period T and frequency ω is

$$T = \frac{2\pi}{\omega}$$

The natural sloshing frequencies and periods for a roll damping tank with arbitrary water depth are given by

$$\sigma_n = \sqrt{\frac{\pi \cdot i}{b} g \cdot tanh\left(\frac{\pi \cdot i}{b} \cdot h\right)} \quad (1)$$

$$T_n = 2\pi / \sqrt{\frac{\pi \cdot i}{b} g \cdot tanh\left(\frac{\pi \cdot i}{b} \cdot h\right)}, \; i = 1,2, \ldots \quad (2)$$

Where

- i is mode number;
- b is tank breadth;
- g is gravity constant;
- h is water depth;
- T1 represents the highest natural period since increasing i in the denominator of the fraction gives lower period values.

From the above equation, it can be clearly seen that the water depth h and the tank breadth b have great influence on the natural tank period. So, the performance of the given tank can be adjusted to different roll periods due to changing loading conditions, by simply regulating the water depth in the tank. The following figure 11 based on equation (2) illustrates that the natural period increases with increasing tank breadth b for a given filling level h. For a given breadth b the natural period will decrease for increasing h.

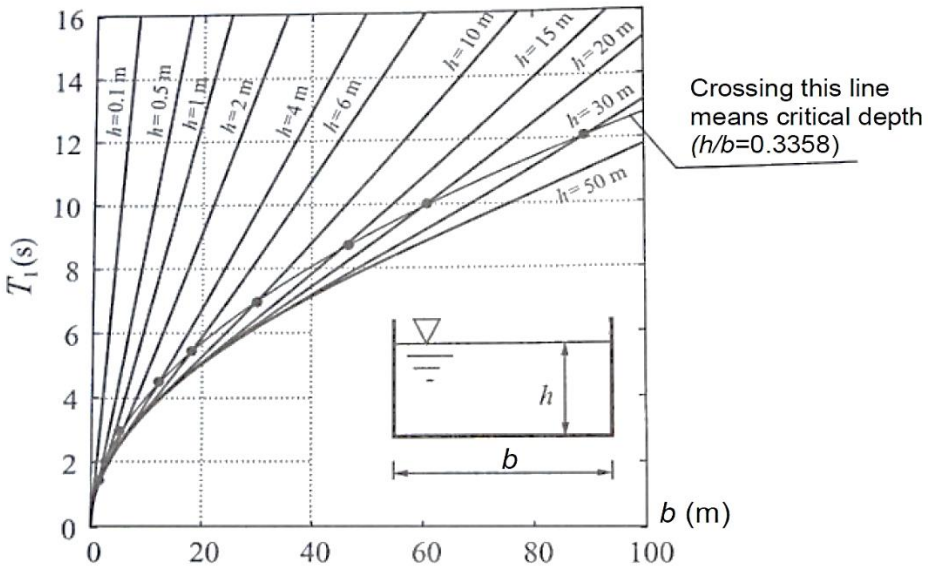

Figure 11. Natural sloshing period for a rectangular tank versus the tank breadth b for different filling levels (Faltinsen, 2009)

2.4.3 Hydrostatic and Dynamic pressure

The relationship of wave length and tank breadth is given as:

$$n\,\lambda = 2\,b \tag{3}$$

According to this relationship, the typical wave patterns for the natural periods can be drawn as in figure 12. For n = 1 for the first natural period in the upper part of the figure, the longest possible wave is given whereby only half of the wave can be seen within the tank. There is most of the water concentrated on one side of the tank which gives high dynamic and hydrostatic pressure forces resulting in a high moment. The first natural period gives therefore the highest damping moment when the tank is installed on a ship. In the following, the highest natural period is also referred to as the resonance period as excitation at this period leads to resonance.

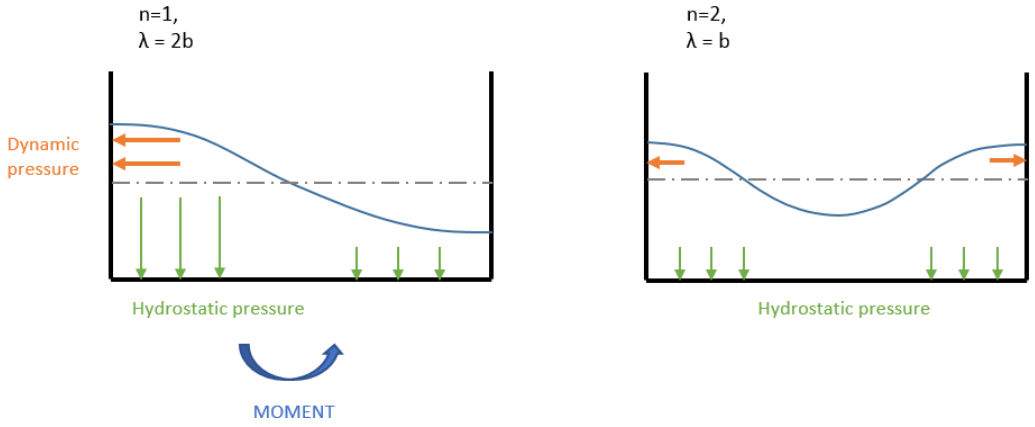

Figure 12. Pressure in a FST

For the second natural period on the right in figure 12, the forces stay in equilibrium and give no damping moment. There is one whole wave in the tank but with a lower amplitude than for the first, highest natural period. The lower the periods or higher the frequencies get, the more waves with an even lower amplitude will be in the tank as exemplified in the lower part of the figure.

2.4.4 Damping

Damping is given when the moment is negative to the velocity as illustrated in Figure 3. The tank is moving with a roll angle η_4:

$$\eta_4 = \eta_{4a} \cdot \sin(\omega t) \tag{4}$$

The measured moment is

$$M = M_a \cdot \sin(\omega t - \varphi) \tag{5}$$

with a phase shift φ between roll angle and moment. The moment can be split into

$$M = M_a \cdot A \cdot \sin(\omega t) + M_a \cdot B \cdot \cos(\omega t) \tag{6}$$

The first part after the equal sign of equation (6) represents a part of the excitation force which is needed to give a forced motion on the tank. The sine components are inertia and restoring forces as in the equation of motion (8) for roll which applies for a tank in combination with a ship:

$$m\ddot{\eta}_4 + c\dot{\eta}_4 + k\eta_4 = P_4 \tag{7}$$

$$-\omega^2 m\eta_{4a}\,sin\,(\omega t) + \omega c\,\eta_{4a}\,cos(\omega t) + k\,\eta_{4a}\,sin\,(\omega t) = P_{4a}\,sin(\omega t - \varphi) \tag{8}$$

In equation (8), inertia forces plus damping forces plus restoring forces equal to the excitation forces which can be phase shifted to the other terms. The factor B in the last

part of equation (6) finally is the damping component of the moment in the tank as this cosine term is in phase with the cosine term of the equation of motion (8) where this part represents the damping in the system. There is a 90° phase difference between the tank motions and the stabilizing moment because the cosine term of the moment is 90° phase shifted to the sine term in equation (4) for the tank motions. By adding a stabilizing moment to the unstable roll motion the roll motion will become well stabilized as on the last line of figure 13.

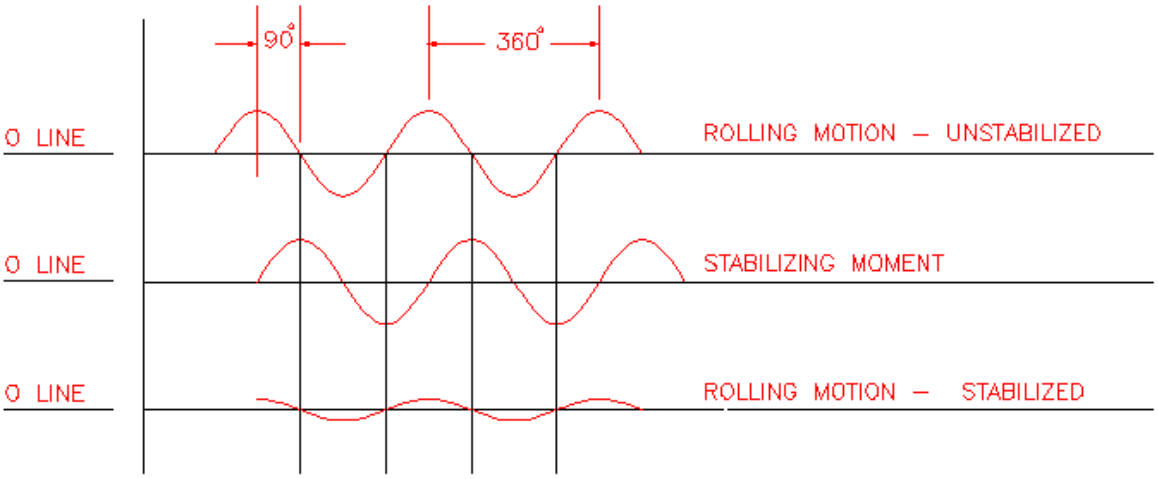

Figure 13. Achieving 90° phase difference for a stabilized motion (Winkler 2012)

A system will oscillate with the same period as the excitation force which can be a harmonic function as in equation (8). The amplitude of the displacement can be found by

$$a = P_a/k \cdot DLF \tag{9}$$

Here, Pa / k is the static displacement which will occur when the system is hidden with a load amplitude Pa. The dynamic load factor (DLF) can enlarge or reduce the displacement as the DLF is depending on the frequency ratio β and the damping ratio ξ. The frequency ratio β is defined as the ratio between the load frequency ω and the eigenfrequency ω_0:

$$\beta = \omega/\omega_0 \tag{10}$$

The damping ratio ξ is defined as the ratio between the damping coefficient c and the critical damping c_{cr}:

$$\xi = c/c_{cr} \tag{11}$$

For a damped system in forced oscillation as it is the case for a roll damping tank, the DLF becomes

$$DFL = 1/\sqrt{(1-\beta^2)^2 + (2\xi\beta)^2} \tag{12}$$

The dependency on both the frequency ratio β and the damping ratio ξ can be seen. Formula 12 can be plotted as in figure 14 where the DLF varies for different frequency ratios and for different damping ratios which are given in percent on the right hand side of the figure where the order of the numbers complies with the order of the lines. This figure points out that the response of a system will be very large when the load frequency equals the eigenfrequencies such that the frequency ratio equals one. This case is called resonance. For lower load frequencies than the eigenfrequencies, the DLF approaches one which means that here the displacement of the system will follow the slow excitation in phase. A so called static condition is reached. At the other end the graph approaches zero because the excitation frequency is too high for the mass of the

system to follow. For this reason it is an inertia dominated system in that range. A high load frequency gives then only small response amplitudes. As Larsen (2014) concluded, the damping of a system is only for the resonance range of importance.

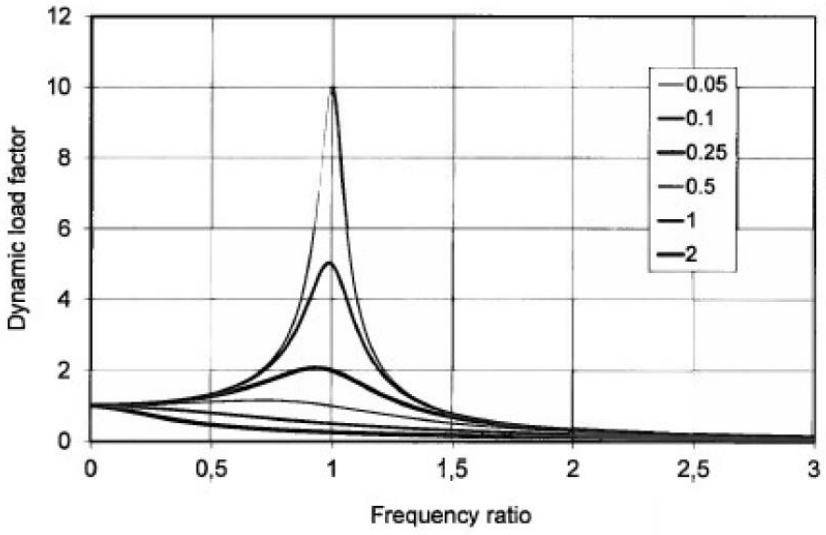

Figure 14. Dynamic load factor as function of the frequency ratio for given damping ratios

Corresponding to this issue, figure 15 exemplifies how large the phase shift between load and response will be for different frequency ratios and for various damping. For a frequency ratio smaller than one, load and response are almost in phase for low damping and the term "quasi static response" is used. At resonance the response is 90° phase shifted to the excitation. Thereafter both are opposite in phase for a frequency ratio greater than one.

The phase shift is depending on the load frequency but not on the load´s amplitude. The phase shift is also depending on the damping in figure 15 as well as the response amplitude in figure 14.

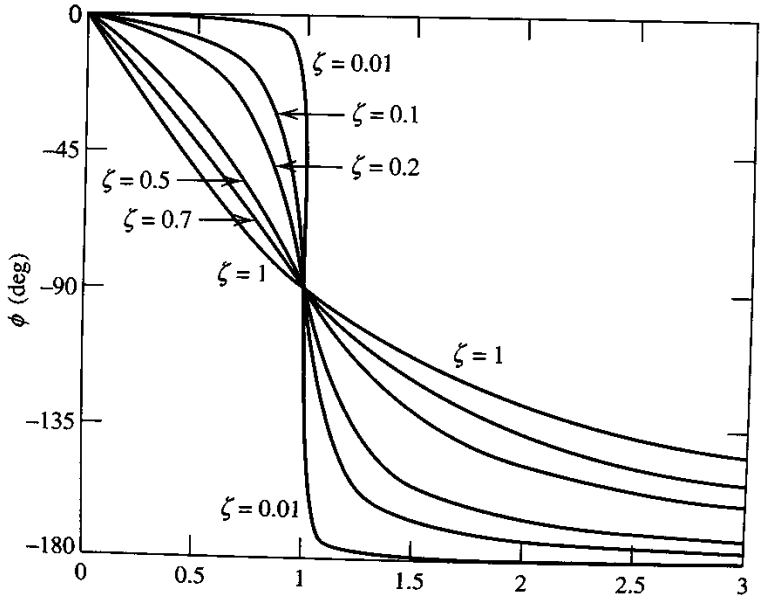

Figure 15: Phase angle between load and response as function of the frequency ratio for given damping ratios (Palm 2007)

3 METHODS

3.1 Governing equations

The Navier-Stokes Equations describe the behavior of a viscous (usually Newtonian) fluid. This considerably more general model introduces nonlinearities rendering a closed-form solution for all but the simplest cases impossible. Unfortunately sloshing is not one of these.

In marine field, we normally neglect the energy part which assumes that the temperature in our case is constant.

The motion of a fluid can be described by a set of partial differential equations expressing conservation of mass, momentum and energy per unit volume of the fluid. The Navier Stokes equations for three dimensional incompressible fluid flow can be written in conservation form as follows

$$\nabla \cdot \vec{v} = 0 \tag{13}$$

$$\frac{\partial \vec{v}}{\partial t} + \nabla \cdot (\vec{v}\vec{v}^{\,T}) = -\frac{1}{\rho}\nabla p + \nu(\nabla \cdot \nabla)\vec{v} - g\vec{e}_3 \tag{14}$$

where

- $\vec{v}$ is the velocity field vector;
- p is the pressure;
- ρ is the mass density;
- ν is the kinematic viscosity;
- g is the acceleration of gravity;
- $\vec{e_3}$ is the unit vector pointing upwards;
- ∇ is the gradient operator;
- ∇· is the divergence operator;
- ∇·∇ is the Laplace-operator;

3.2 VOF Model

Volume Of Fluid (VOF) is a simple multiphase model. It is suited to simulating flows of several immiscible fluids on numerical grids capable of resolving the interface between the phases of the mixture, as shown below. In such cases, there is no need for extra modeling of inter-phase interaction, and the model assumption that all phases share velocity, pressure, and temperature fields becomes a discretization error.

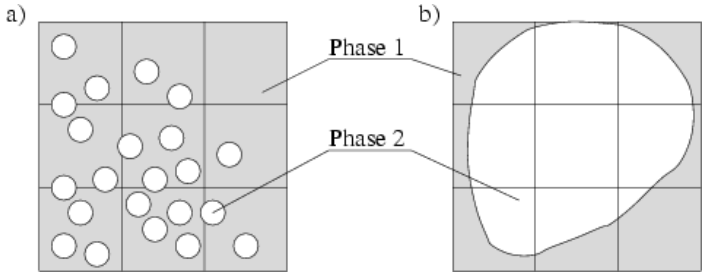

Figure 16: Illustration of unsuitable grids (left) and suitable grid (right) for two-phase flows using the VOF model

Due to its numerical efficiency, the model is suited for simulations of flows where each phase constitutes a large structure, with a relatively small total contact area between phases. A good example of this type of flow is sloshing flow in a water tank, where the free surface always remains smooth. If the tank movement becomes pronounced, this results in breaking waves, large numbers of air bubbles in the water, and water droplets in the air. The method would then require a fine mesh (at least three cells across each droplet/bubble) to produce small modeling errors.

Basic VOF Model Equations

The VOF model description assumes that all immiscible fluid phases present in a control volume share velocity, pressure, and temperature fields. Therefore, the same set of basic governing equations describing momentum, mass, and energy transport in a single-phase flow is solved. The equations are solved for an equivalent fluid whose physical properties are calculated as functions of the physical properties of its constituent phases and their volume fractions.

The equations are:

$$\rho = \sum_i \rho_i \alpha_i \tag{15}$$

$$\mu = \sum_i \mu_i \alpha_i \tag{16}$$

$$c_p = \sum_i \frac{(c_p)_i \rho_i}{\rho} \alpha_i \tag{17}$$

where:

$a_i = v_i/v$ is the volume fraction and ρ_i , μ_i and $(c_p)_i$ are the density, molecular viscosity and specific heat of the i th phase.

The conservation equation that describes the transport of volume fractions a_i is:

$$\frac{d}{dt}\int_V \alpha_i dV + \int_S \alpha_i (\boldsymbol{v} - \boldsymbol{v}_g) \cdot d\boldsymbol{a} = \int_V \left(s_{\alpha_i} - \frac{\alpha_i}{\rho_i}\frac{D\rho_i}{Dt} \right) dV \tag{18}$$

Where Sa_i is the source or sink of the i th phase, and $D\rho_i/Dt$ is the material or Lagrangian derivative of the phase densities ρ_i.

If there is a large time variation of phase volume fractions a_i , there is a large time variation of the mixture density ρ which features in the continuity equation, Eqn. (18). Since this unsteady term cannot be linearized in terms of pressure and velocity, it acts as a large source term which can be "unpleasant" for a numerical treatment within a segregated solution algorithm. Therefore, Eqn. (18) is rearranged in the following, non-conservative form:

$$\int_A (\boldsymbol{v} - \boldsymbol{v}_g) \cdot d\mathbf{a} = \sum_i \int_V \left(s_{\alpha_i} - \frac{\alpha_i}{\rho_i}\frac{D\rho_i}{Dt} \right) dV \tag{19}$$

In the case when phases have constant densities and have no sources, the continuity equation reduces to $\nabla \cdot \boldsymbol{v} = 0$.

3.3 Turbulence modelling

There is no consensus apparent whether and when sloshing flow should be modelled as turbulent or laminar. Previous studies hace shown that turbulence model is more widely used. Rhee (2005) observed significant variations between laminar and turbulent flow models in the test cases and concluded that turbulence effects should be taken into account in a CFD model for this particular case. Similar effects have been observed in the sensitivity study by Godderidge et al. (2006). Thus, we assume the flow in our cases to be turbulent. A breif introduction on different turbulence models is shown below.

3.3.1 Standard K- Epsilon

A K-Epsilon turbulence model is a two-equation model in which transport equations are solved for the turbulent kinetic energy k and its dissipation rate ε .

Turbulent dissipation is the rate at which velocity fluctuations dissipate. This is the default k–ε model. Coefficients are empirically derived; valid for fully turbulent flows only. In the standard k-e model, the eddy viscosity is determined from a single turbulence length scale, so the calculated turbulent diffusion is that which occurs only at the specified scale, whereas in reality all scales of motion will contribute to the turbulent diffusion. The k-e model uses the gradient diffusion hypothesis to relate the Reynolds stresses to the mean velocity gradients and the turbulent viscosity. Performs poorly for complex flows involving severe pressure gradient, separation, strong streamline curvature. The most disturbing weakness is lack of sensitivity to adverse pressure gradients; another shortcoming is numerical stiffness when equations are integrated through the viscous sublayer which are treated with damping functions that have stability issues

Pros: Robust. Widely used despite the known limitations of the model. Easy to implement. Computationally cheap. Valid for fully turbulent flows only. Suitable for initial iterations, initial screening of alternative designs, and parametric studies (Menter 1993).

Cons: Performs poorly for complex flows involving severe pressure gradient, separation, strong streamline curvature. Most disturbing weakness is lack of sensitivity to adverse pressure gradients; another shortcoming is numerical stiffness when equations are integrated through the viscous sublayer which are treated with damping functions that have stability issues (F.R.Menter, Two-Equation Eddy-Viscosity Turbulence Models for Engineering Applications 1994).

3.3.2 Standard K-Omega

A two-transport-equation model solving for kinetic energy k and turbulent frequency ω. This is the default k–ω model. This model allows for a more accurate near wall treatment with an automatic switch from a wall function to a low-Reynolds number formulation based on grid spacing. Demonstrates superior performance for wall-bounded and low Reynolds number flows. Shows potential for predicting transition. Options account for transitional, free shear, and compressible flows. The k-e model uses the gradient diffusion hypothesis to relate the Reynolds stresses to the mean velocity gradients and the turbulent viscosity. Solves one equation for turbulent kinetic energy k and a second equation for the specific turbulent dissipation rate (or turbulent frequency) w. This model performs significantly better under adverse pressure gradient conditions. The model does not employ damping functions and has straightforward Dirichlet boundary conditions, which leads to significant advantages in numerical stability. This model underpredicts the amount of separation for severe adverse pressure gradient flows.

Pros: Superior performance for wall-bounded boundary layer, free shear, and low Reynolds number flows. Suitable for complex boundary layer flows under adverse pressure gradient and separation (external aerodynamics and turbomachinery). Can be used for transitional flows (though tends to predict early transition).

Cons: Separation is typically predicted to be excessive and early. Requires mesh resolution near the wall.

3.3.3 SST K-Omega

Shear Stress Transport (SST) is a variant of the standard k–ω model. Combines the original Wilcox k-w model for use near walls and the standard k–ε model away from walls using a blending function, and the eddy viscosity formulation is modified to account for the transport effects of the principle turbulent shear stress.Also limits turbulent viscosity to guarantee that τT~k. The transition and shearing options are borrowed from standard k–ω. No option to include compressibility.

Pros: Offers similar benefits as standard k–ω. The SST model accounts for the transport of turbulent shear stress and gives highly accurate predictions of the onset and the amount of flow separation under adverse pressure gradients. SST is recommended for high accuracy boundary layer simulations.

Cons: Dependency on wall distance makes this less suitable for free shear flows compared to standard k-w. Requires mesh resolution near the wall.

A Reynolds Stress model may be more appropriate for flows with sudden changes in strain rate or rotating flows while the SST model may be more appropriate for separated flows.

3.3.4 RSM

RSM(Reynolds-stress model): Use the same idea of flucturated flow but doesn't accept the assumption of isotropic flow. The turbulence stresses are modelled directly. Hence, 6 aditional unknowns are solved by 6 additional transport equations.

1. Better performance in complex flow regimes, especially in strongly curved streams

2. Improved stability as the asymptotic solution attracts all initial conditions (Charles G Speziale 1991).

The main drawback of a Reynolds stress model is the introduction of six additional transport equations for the turbulence stress terms. In addition, convergence problems are identified when using the Reynolds Stress Model by Speziale et al. (1991).

4 CFD SIMULATION

CFD simulations are performed by a commericial numerical software STAR-CCM+.

The physics of the sloshing problem are considered in order to identify the key modelling aspects. The correct application of CFD and how it can be used to model sloshing is considered.

A space and time discretisation independence study is carried out to ascertain the applicability of the results. Subsequently, the effect of including either a K- Epsilon or K - Omega turbulence model as opposed to forcing laminar flow is examined.

4.1 Computational model

The Free surface tank model discussed in this paper is scaled from a full size tank on an OSV (Offshore supply vessel). Table below gives the main dimensions of the vessel.

Table 2. Main dimensions of the Vessel

Parameter	Value [m]
Lpp	75.5
Breadth	21
Draught	6.8
Vertical center of gravity,VCG	7.6

Generally speaking, the liquid inside free surface tank should have a weight which accounts to approximately 2-4% of the total ship displacement.This affect the tank dimensions to a certain extent.

The tank breath is designed as large as possible in order to provide more damping moment. Based on industrial experience, it is recommended that the designed tank length should follow:

$$L = 3 + 3\% \times Lpp \tag{20}$$

This is due to the ship hull structure factor. If the tank is designed too long, it may occupy two bulkheads or even more which will affect the integrity of the ship hull.

Therefore, a recommended anti-roll tank for this particular OSV has following dimensions:

Table 3. Full scale tank dimensions

Parameter	Value [m]
Tank width	20
Tank length	5
Tank height	3
Vertical position of tank bottom	7.6

The full size tank is scaled to a model size tank by a scale factor 1:20. The model size tank is therefore used in both numerical calculations and model tests.

4.1.1 Geometry description

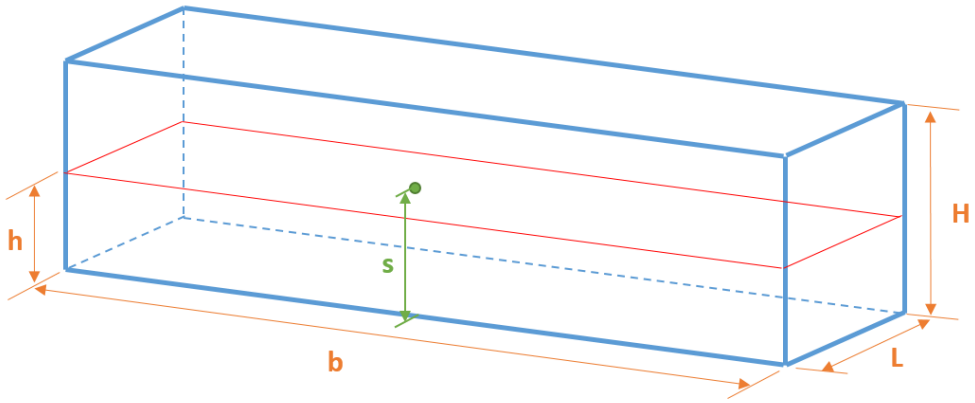

Figure 17: Definition of geometry and tank dimensions: Free surface tank

Table 4. Model scale tank dimensions

Dimension		Value [mm]
Tank width	b	1000
Tank length	L	250
Tank height	H	150
Water level	h	50, 75, 100
Vertical position of tank bottom from rotation center	s	0
Fluid density		997.561 [kg/m3]
Dynamic Viscosity		8.8871E-4[Pa-s]

Table below shows the relation between water level in the tank model and the theoretical natural period.

Table 5. Natural periods of differnt filling tanks

Filling percentage	Water level h[cm]	Natural period [s]	Natural frequency
33.3%	5.0	2.86	0.35
50%	7.5	2.33	0.43
66.6%	10.0	2.02	0.50

4.1.2 Tank motion

The tank motion is defined as a 1-DOF sinusoidal motion with the rotation center in the middle of the tank bottom.

This paper will discuss three different rotation amplitudes: 3deg, 4.5deg, 6deg. And the rotation periods includes from 1 second to maximum 10 seconds.

Motion frequency:

$$\omega = \frac{2\pi}{T} \tag{21}$$

Motion displacement:

$$x = A \cdot sin(\omega t) \tag{22}$$

Angular velocity:

$$\dot{x} = A \cdot \omega \cdot cos(\omega t) \tag{23}$$

4.2 Grid (Mesh)

A grid (or mesh, the terms are often used interchangeably) is used to represent the problem in computational fluid dynamics usually as a set of finite volume elements. The grid design process is centered around the following trade-offs.

1. Spacing. The grid needs to be sufficiently fine so as to sustain conservation of mass and momentum at an acceptable level. However, reducing grid size will increase the computational cost and memory requirements. The rate of increase depends on the type of solution algorithm used.
2. Resolution. Grid spacing needs to be sufficiently small to resolve the flow in all regions of the computational domain. This is especially important when using a turbulence model, where the position of the first near-wall grid point can have a significant influence on the CFD output quality. This is discussed by (Wilcox 1998) in considerable detail. When the grid is too coarse, local flow features are smeared and, especially when considering a sloshing flow, pressure spikes are not resolved with sufficient detail.
3. Geometry. Although not an issue in the current study, the grid must provide a sufficiently accurate representation of the geometry used. This becomes very important when there are small changes (e.g. ripples) on a surface, or a body has particular details influencing the flow.

As the grid represents the problem in computational space, one should always ascertain that any CFD result is independent of the grid used. This has been considered by the Maritime CFD best practice guidelines (Consultants 2003).

In this report, the tank geometry is meshed by Trimmer model using a base size 0.005m. In order to get better results, volumetric control in Z direction is introduced. The relative Z size is 0.0025m which is 50% of the other two directions.

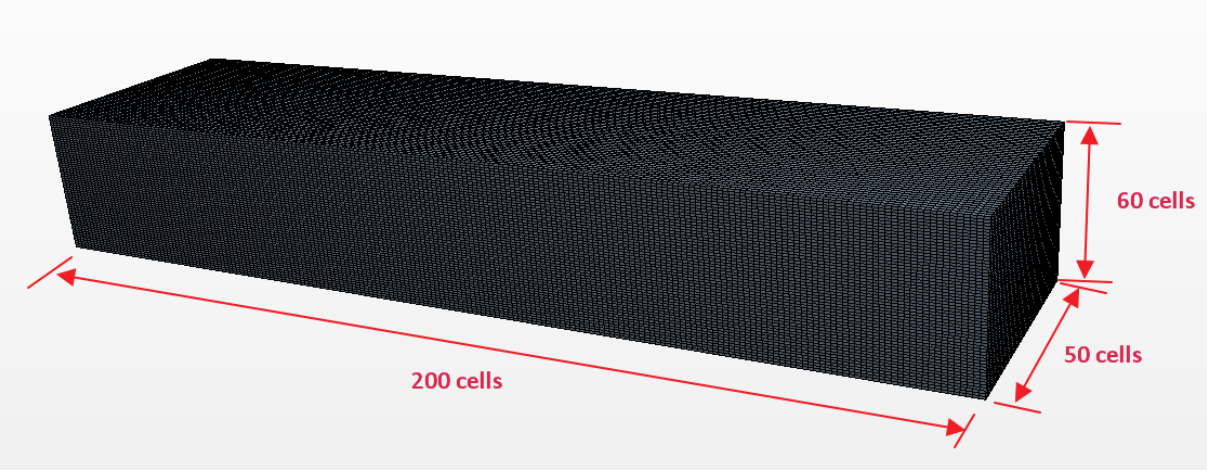

Figure 18: Tank mesh

4.3 Temporal discretization scheme

Star CCM+ offers two different time discretisation schemes, a first order and second order backward Euler scheme. The first order scheme approximates the time derivatives in integral form,

$$\frac{d}{dt}(\rho\chi\phi V)_0 = \frac{(\rho\chi\phi V)_0^{n+1} - (\rho\chi\phi V)_0^{n}}{\Delta t} \tag{24}$$

While this scheme is robust, it does induce numerical diffusion. Therefore, a second order approximation of the time derivative, given as

$$\frac{d}{dt}(\rho\chi\phi V)_0 = \frac{\left\{(\alpha^2-1)[(\rho\chi\phi V)_0^{n+1} - (\rho\chi\phi V)_0^{n}] + [(\rho\chi\phi V)_0^{n-1} - (\rho\chi\phi V)_0^{n}]\right\}}{\alpha(\alpha-1)\Delta t^{n+1}} \tag{25}$$

And

$$\alpha = 1 + \frac{\Delta t^{n+1}}{\Delta t^{n}}$$

$$\Delta t^{n+1} = t^{n+1} - t^{n}$$

$$\Delta t^{n} = t^{n} - t^{n-1}$$

The second order discretisation is conservative. However it may give nonphysical solutions when the flow experiences severe changes in the time domain. An advantage of the second order model is the extrapolation of an initial guess for the current timestep i based on previous timesteps. As fewer iterations are required to determine the new solution, computational times are significantly reduced. The current investigation will assess the difference between the two time marching schemes.

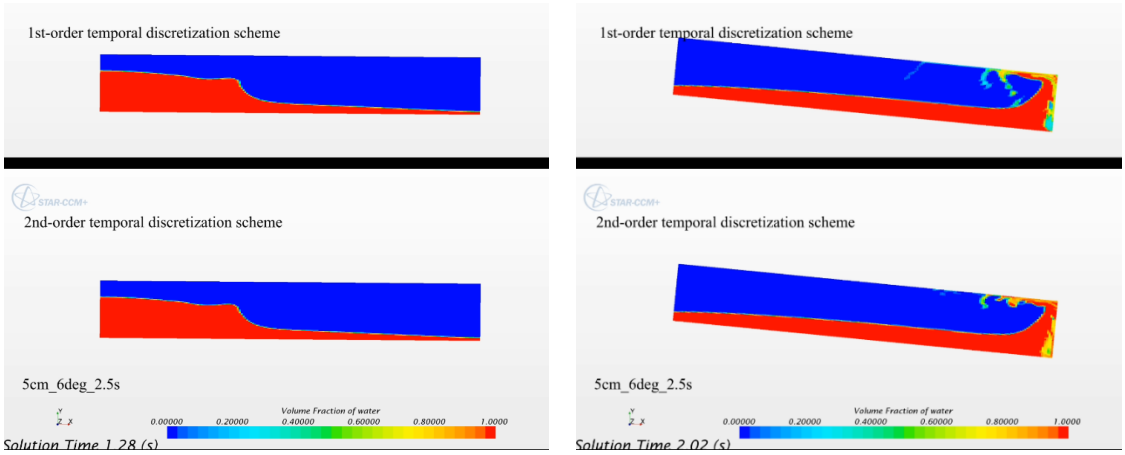

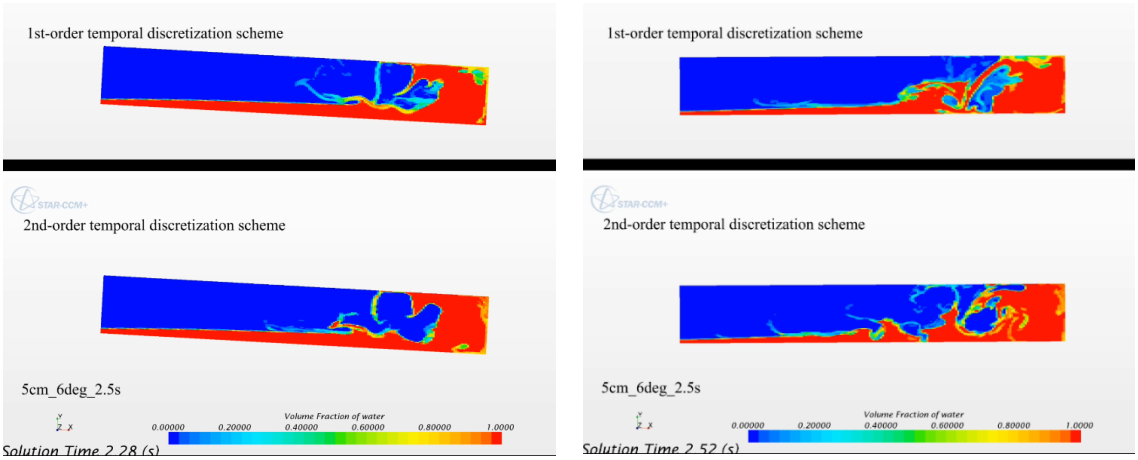

Figure 19. Temporal discretization scheme comparison 1

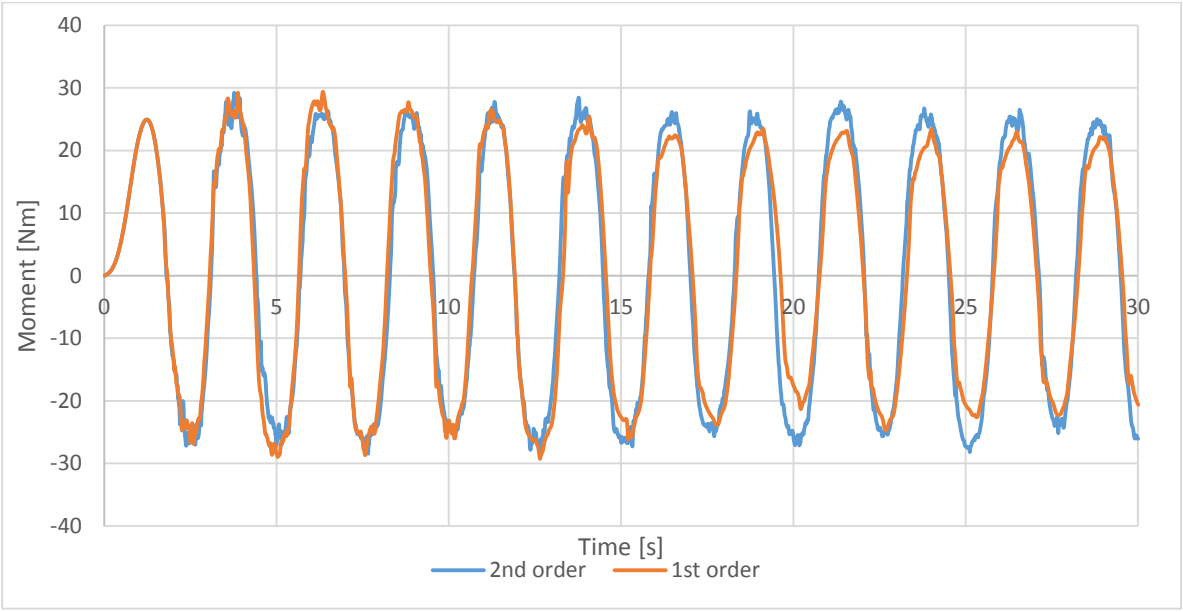

Figure 20. Temporal discretization scheme comparison 2

From the comparisons above, it can be easily found that there are great differences between the 1st-order and 2nd-order schemes when simulating a severe sloshing. Moment in Figure 20 shows some differences as well. It is difficult to make the decision to choose which. In this case, model tests are needed as a reference. Further discussion can be found in Model test part.

4.4 Time step control

As the velocity of the flow varies throughout the simulation, it is useful to adjust the timestep according to the flow velocity. This is governed using the Courant number, which is the rate of flow speed with which numerical disturbances propagate. The Courant number at node i is defined by (Hirsch 1988) for finite volume CFD as

$$C_N = u_i \frac{\Delta t}{\Delta x_i} \tag{26}$$

where ui is the flow velocity, t the time step and xi the grid spacing at node i. As flow velocity varies throughout the flow field, so will the Courant number.

Typically, it is recommended that $C_N \leq 1.0$ to maintain a stable solution if the flow field is not known a priori (John D Anderson 1995). If the grid spacing Δx were to be halved, the Courant number may be kept constant only by halving the time step as well. This

illustrates the interaction between grid size and time discretisation, underlining the importance of considering the time step size when generating the grid.

Systematic time step variations for sloshing flows have been carried out by Rhee (2005) uses a timestep of 0.001 sec. In order to find a suitable time step for the case, here we investigate three different time steps and make a comparison.

Here we compare three different time steps 0.005s, 0.001s and 0.0005s. Tank filling percentage is 33%; excitation amplitude is 4.5 degree; mesh size is 0.005m as predefined. Figure 21 shows the maximum courant number of each time step during a complete simulation.

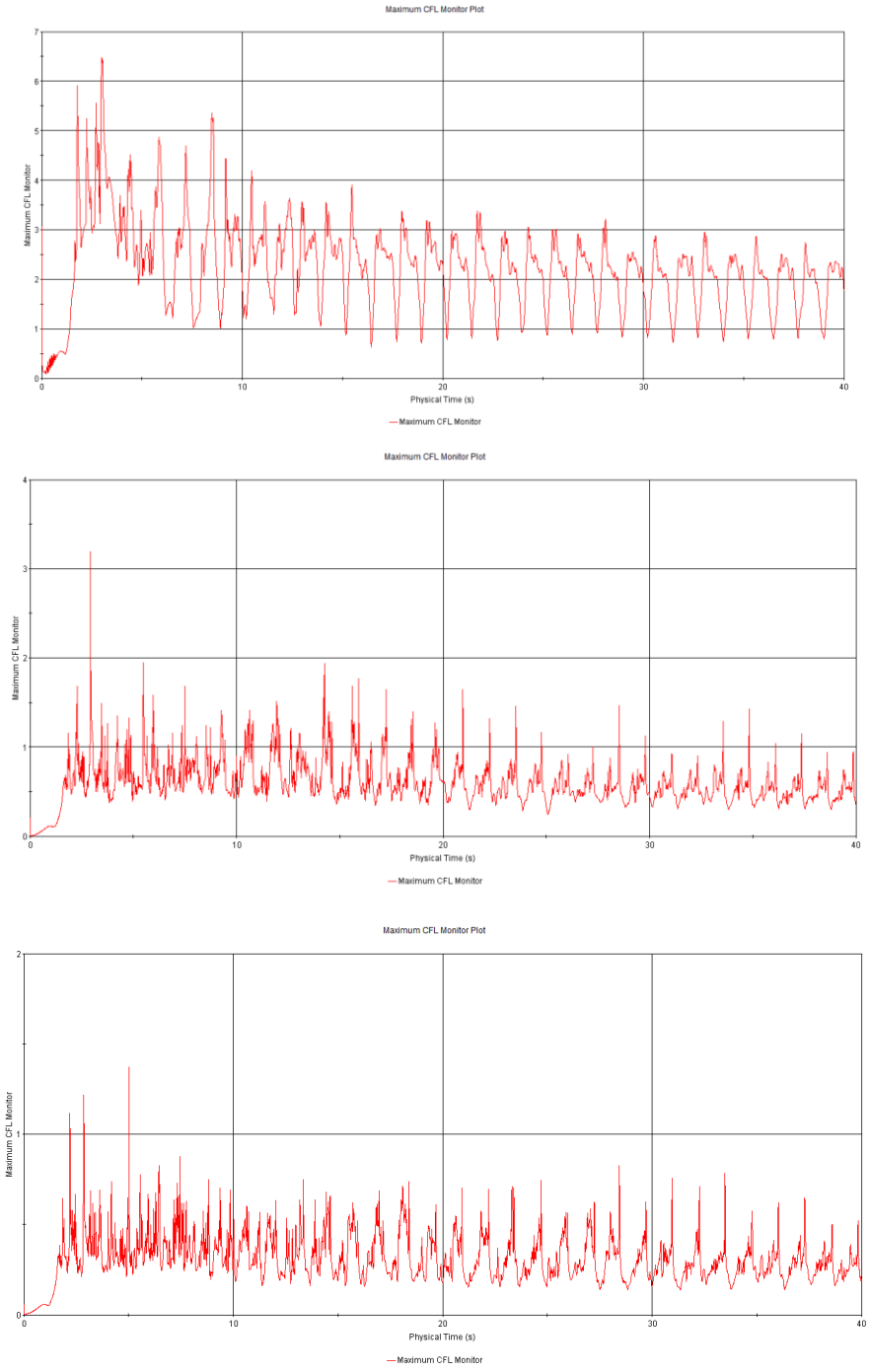

Figure 21. Courant Number comparison

Table 6 summerize the courant numer of three simulations. Figure 22 illustrate the damping moment of each case. We can find significant increase on moment amplitude from time step 0.005s to time step 0.001s. While there is not such a big moment difference between time step 0.001s to time step 0.0005s. Both moment amplitude and phase are stable, which means that the result is converged. Therefore, it is sufficient to sue the criterion which courant number is 1.0.

Table 6. Time steps and Courant Number

Time step	CFL
0.005	< 3
0.001	≈ 1
0.0005	≈ 0.5

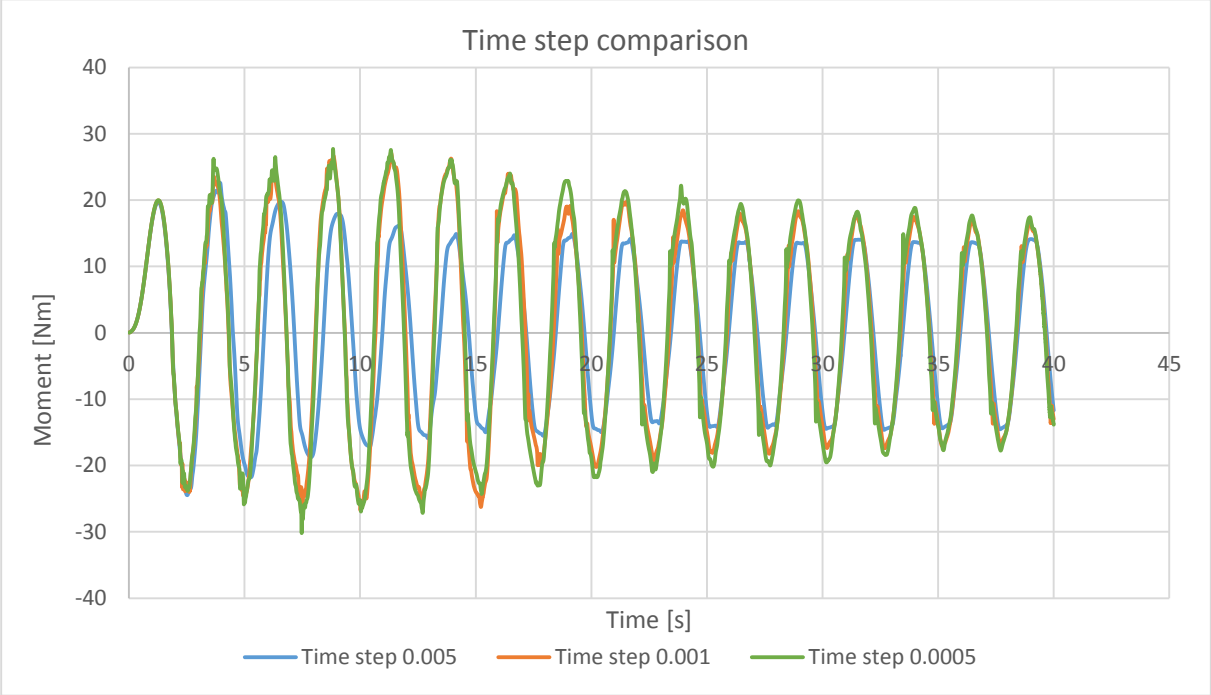

Figure 22. Time steps comparison

4.5 Turbulence modelling

The successful numerical solution depends on sufficient grid resolution to capture all flow features. Turbulence takes place at often very small spatial and time scales. In order to capture the effects of turbulence using the governing equations in their present form, grids with extremely high resolution and very small time steps would be required.

In this paper, two turbulence models (K-Epsilon and K-Omega) are compared and discussed. As explained in chapter 3.3, K-Epsilon turbulence model is a two-equation model in which transport equations are solved for the turbulent kinetic energy k and its dissipation rate ε . While K-Omega turbulence model uses turbulent frequency ω instead of dissipation rate ε.

Basically, a K- Epsilon model is robust, and widely used despite the known limitations of the model. Compared to other turbulence models, it is easy to implement and computationally cheap. Besides, it is suitable for initial iterations, initial screening of alternative designs, and parametric studies.

K-Omega model has superior performance for wall-bounded boundary layer, free shear, and low Reynolds number flows. It is suitable for complex boundary layer flows under adverse pressure gradient and separation (external aerodynamics and turbomachinery). It also can be used for transitional flows (though tends to predict early transition).

Figures below compare these two models in greater details. Here we compare three different excitation periods 4s, 3s and 2s.

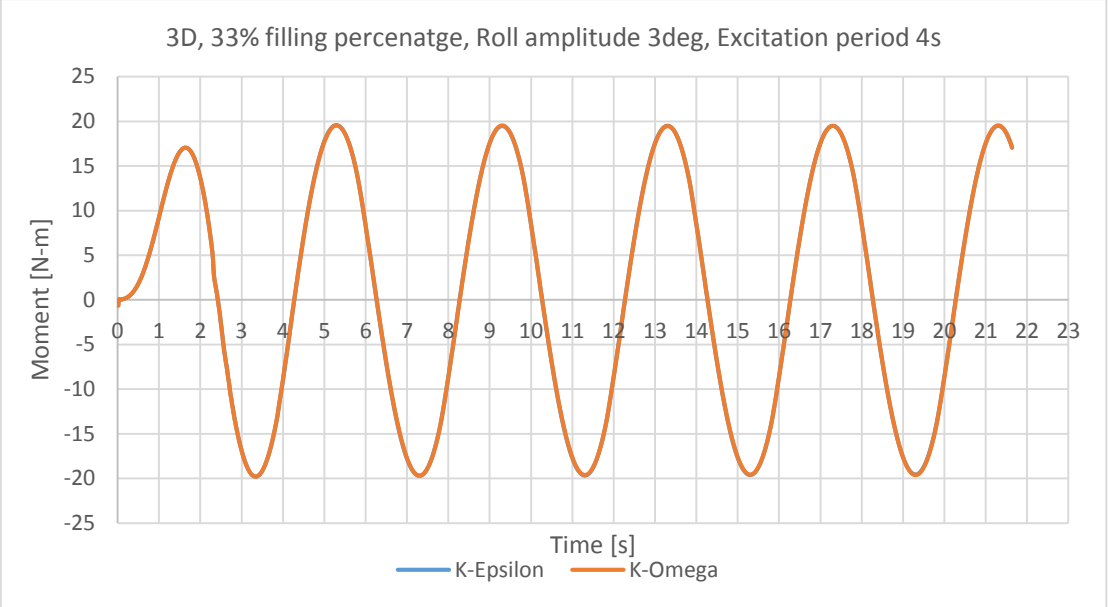

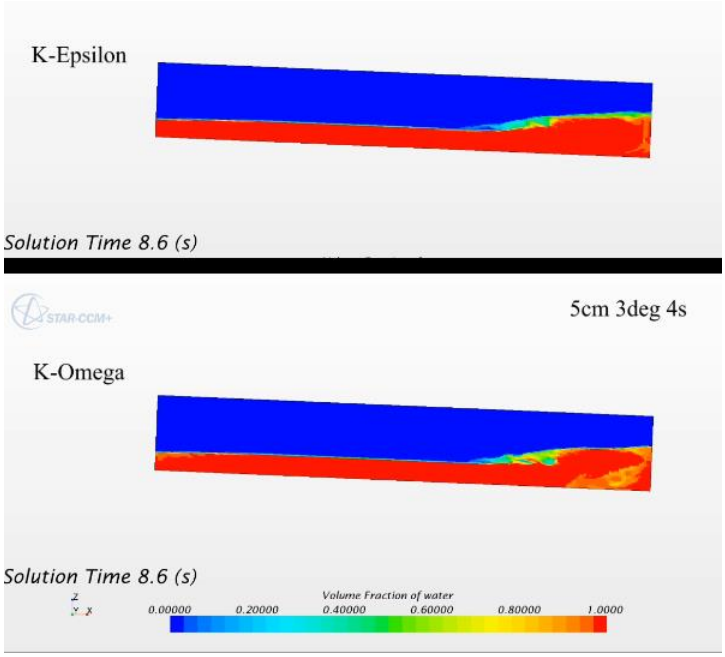

Figure 23. Turbulence modelling at 4s

When the excitation period is 4s, there is nearly no difference between K-Epsilon and K-Omega models on the moment curves. However, if we look carefully at the liquid inside the tank, we may say that K-Omega provides more excessive details in water-air interface and interaction between water and gas as shown in Figure 23.

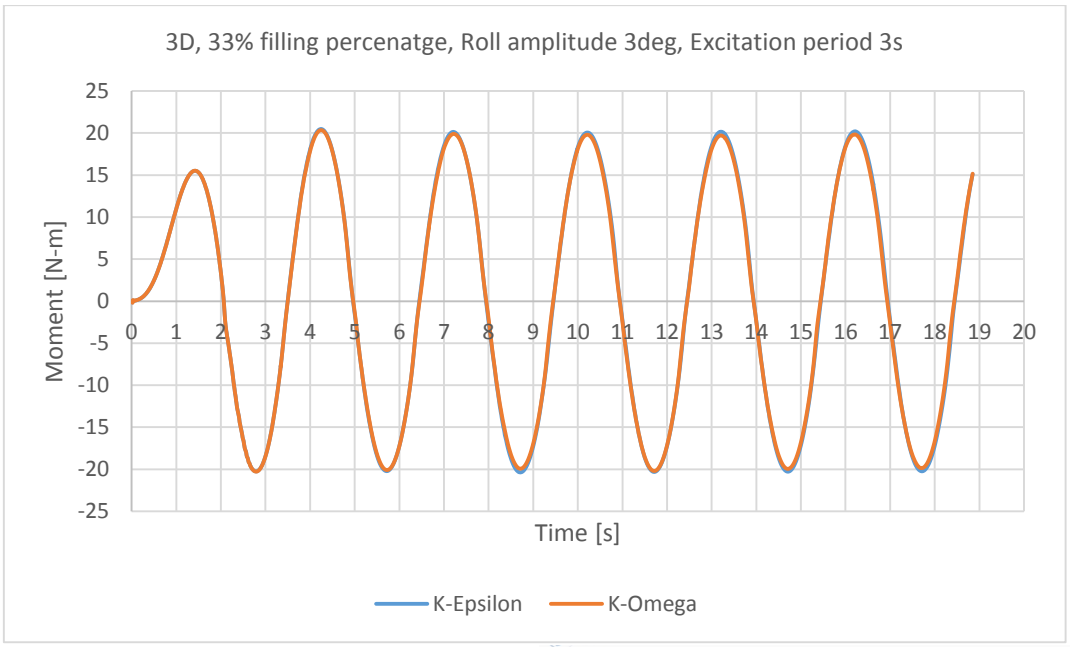

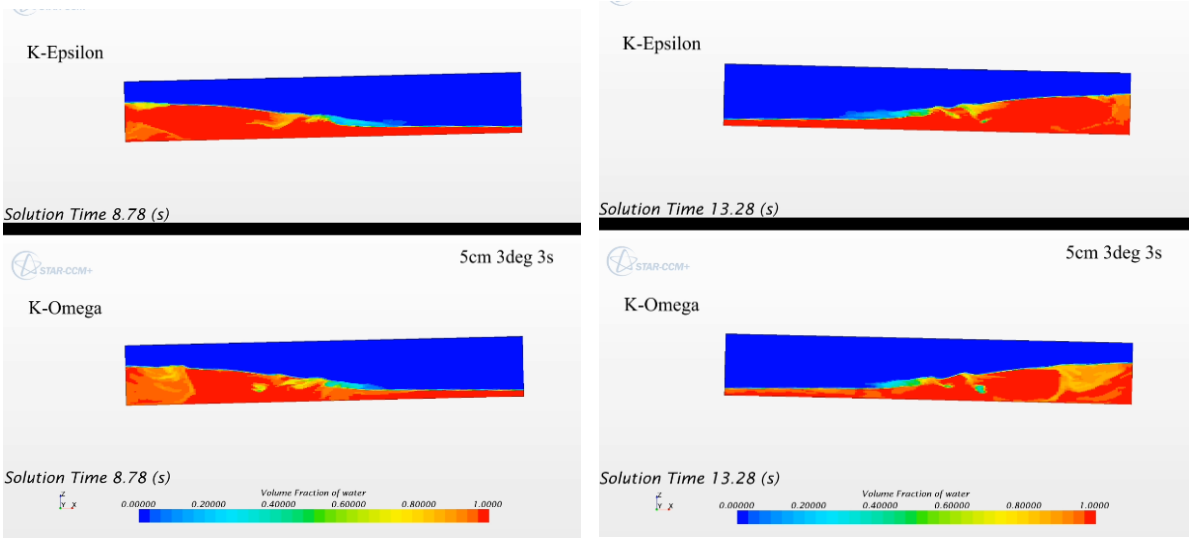

Figure 24. Turbulence modelling at 3s

If we reduce the excitation period to 3s, we may find a slight moment defference between K-Epsilon and K-Omega models. Therefore, we pick up two moments 8.78s and 13.28s when the difference is maximum. From the figures above, it can be found that the difference mostly due to the accuracy of predictions from two models. Similar to 2s, K-Omega provides more excessive details in water-air interface and interaction between water and gas in this case. This results in slightly less damping moment.

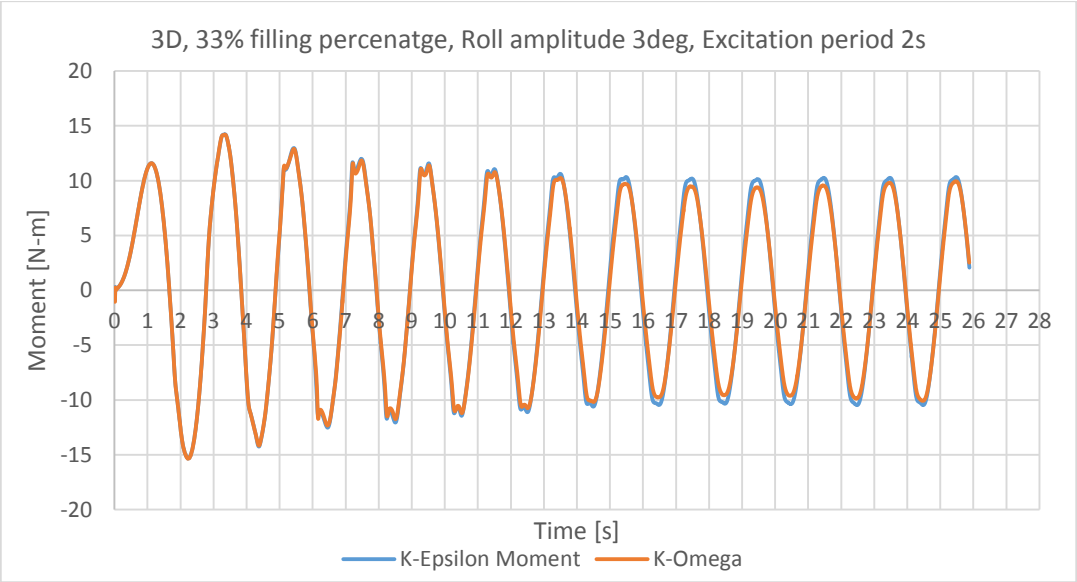

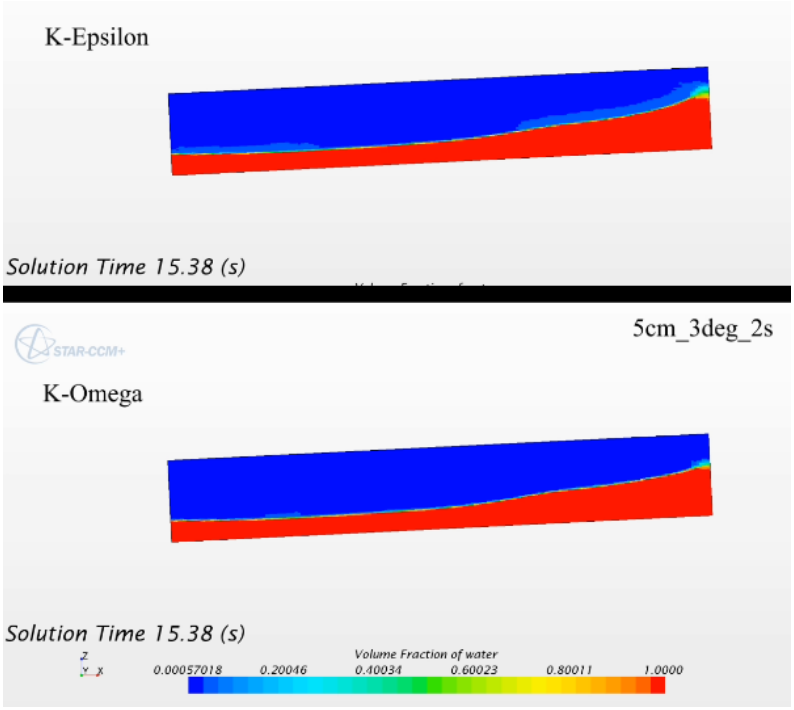

Figure 25. Turbulence modelling at 2s

If we keep on reducing the excitation period to 2s, obvious moment difference can be found in the curve. We pick up the moment 15.38s when obvious difference occurs. Different from previous cases, this time the difference occurs when the liquid hit the side wall. At the same time, turbulence flow and liquid seperation appears close to the side wall . All of these result in a less damping moment for K-Omega model.

In all the three cases, different turbulence models may affect the amplitude of damping moment to some extent, while it doesn't affect the moment phase at all. One thing should also be noticed is that in our cases, the liquid inside the tank is water and we neglect the compressibility of liquid and gas. If one simulate for instance LNG and consider the compressibility, different turbulence models should be carfully treated and fully discussed.

4.6 2D vs 3D model

Generally speaking, turbulence is a three-dimensional time-dependent phenomenon, therefore the simulations should use 3D model. However, a 2D model is computionally cheap compared to a 3D model when using same dimensions. Therefore, it is of interest to investigate the differences beteen 2D and 3D simulations.

The grids/meshes of 2D and 3D model are compared in the following table. Notice that the calculating environment is Windows 8.1 x64, Intel(R) Core(TM) i7-3635QM CPU @ 2.40GHz 2.40GHz, 8G RAM.

Table 7. 2D and 3D comparison

	cells	Interior Faces	Vertices	Computional time
2D	12000	23740	12261	20 mins for 10 s
3D	127296	376096	171609	233 mins for 10s
Ratio	1:10.6	1:15.8	1:14	12:1

Next, we will compare 2D and 3D simulations when excitation period is 2s, 2.5s, 3s, 4s, 5s, respectively. In order to make sure that 2D simulations are accurate enough, we use a smaller time step 0.001s.

When the excitation period is relatively small for instance 2.5s as shown in Figure 26, some differences appears between 2D and 3D simulations. An obvious reason is that 2D simulation neglect the vortex in tank length direction. Besides, it does not include the effect of the tank side walls. However, these two aspects may affect the result only when the flow inside the tank is fully turbulent. When we increase the excitation period to 3s, 4s and 5s, it can be found that the differences between 2D and 3D simulations become smaller and smaller.

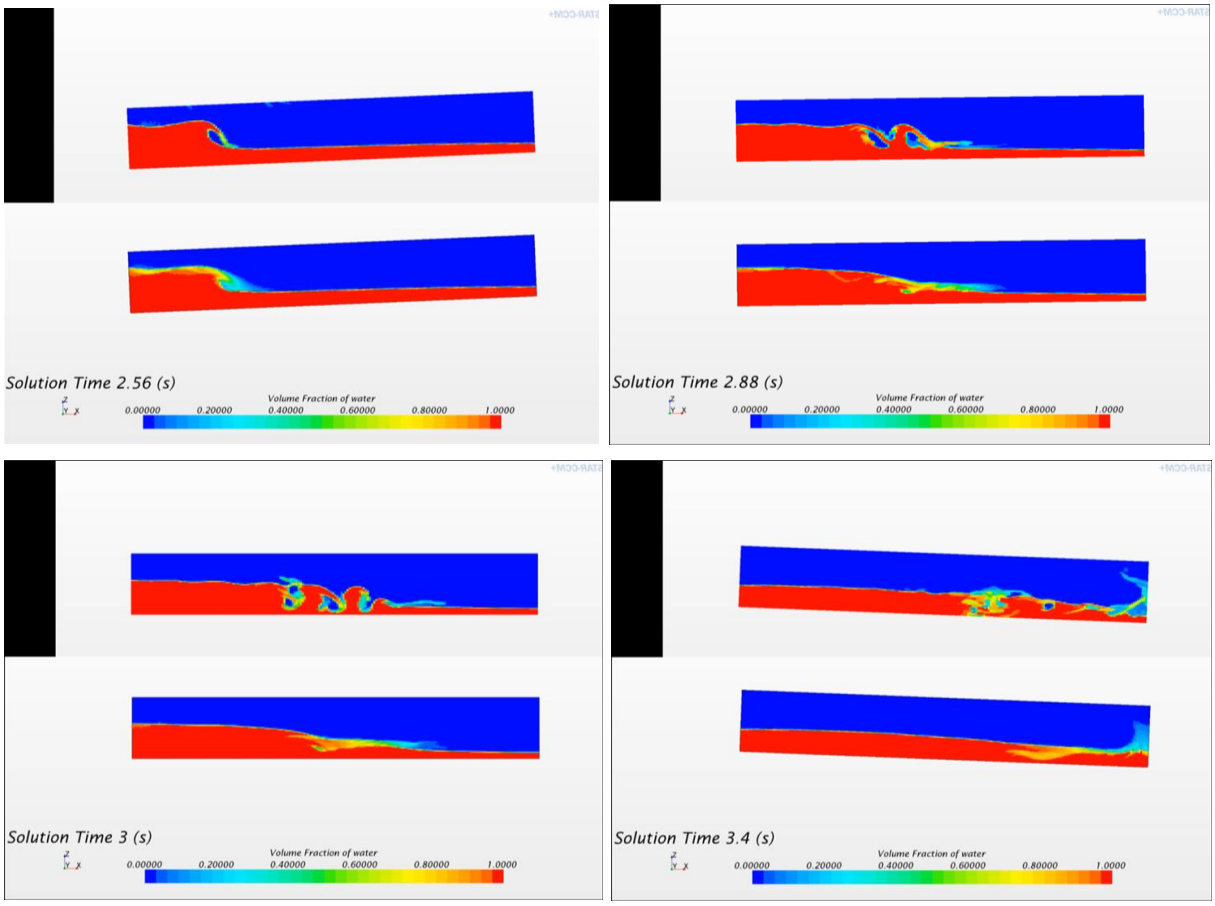

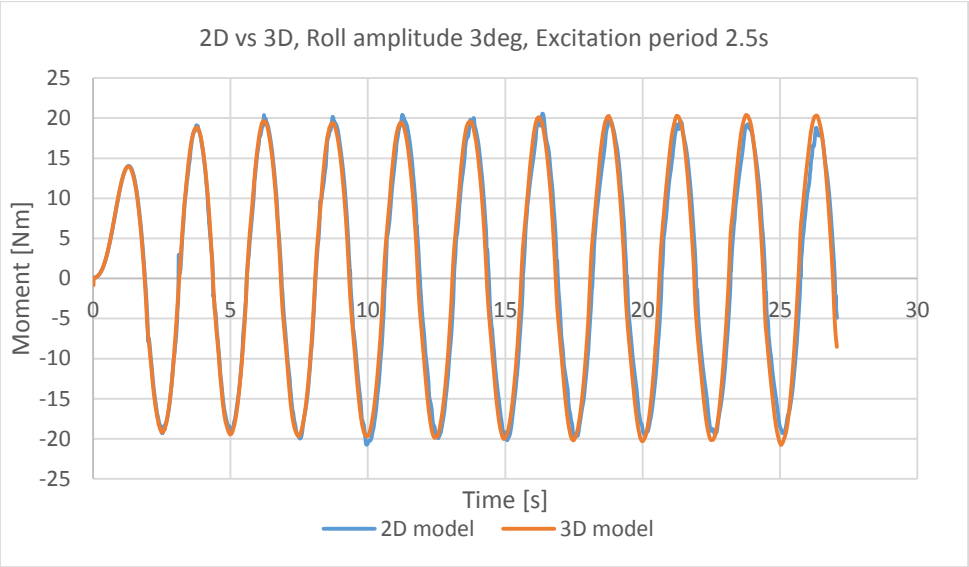

Figure 26. 2D vs 3D at excitation period 2.5s

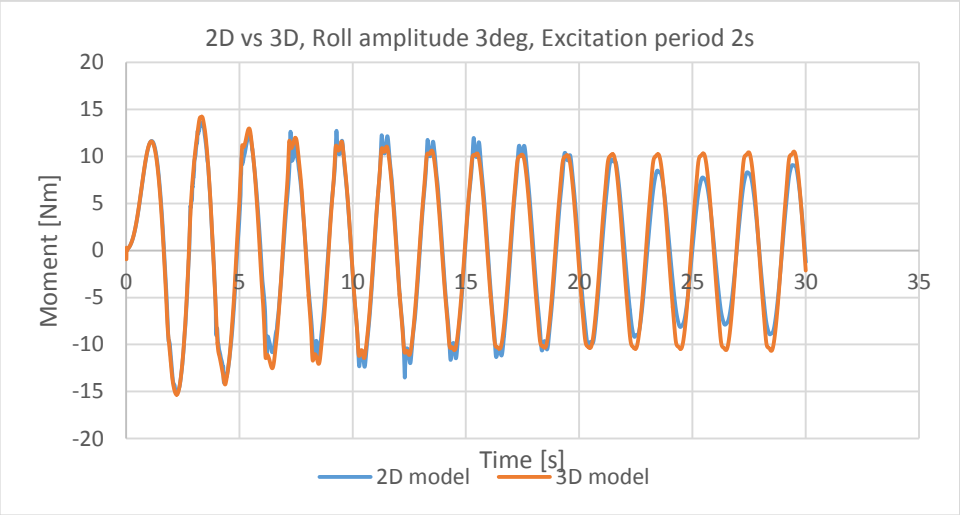

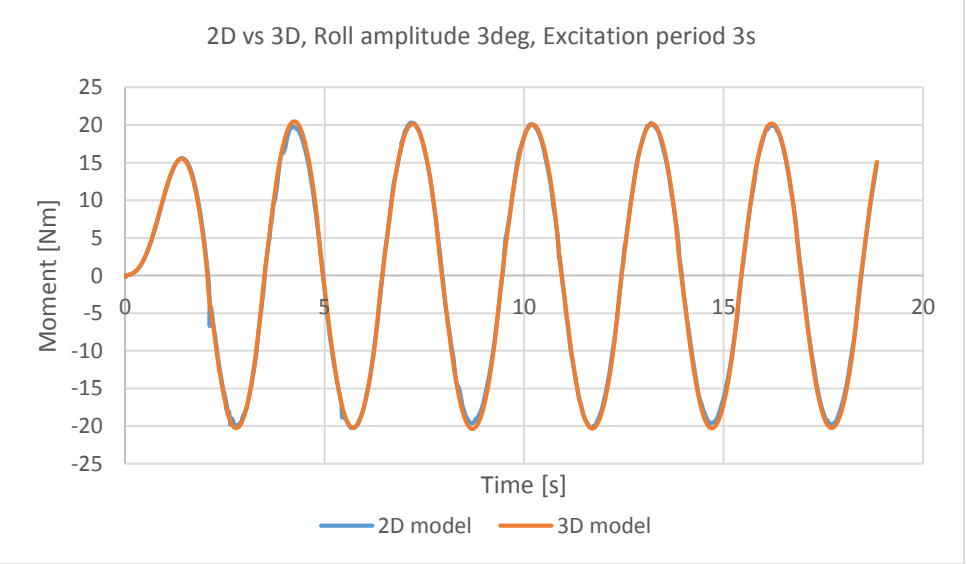

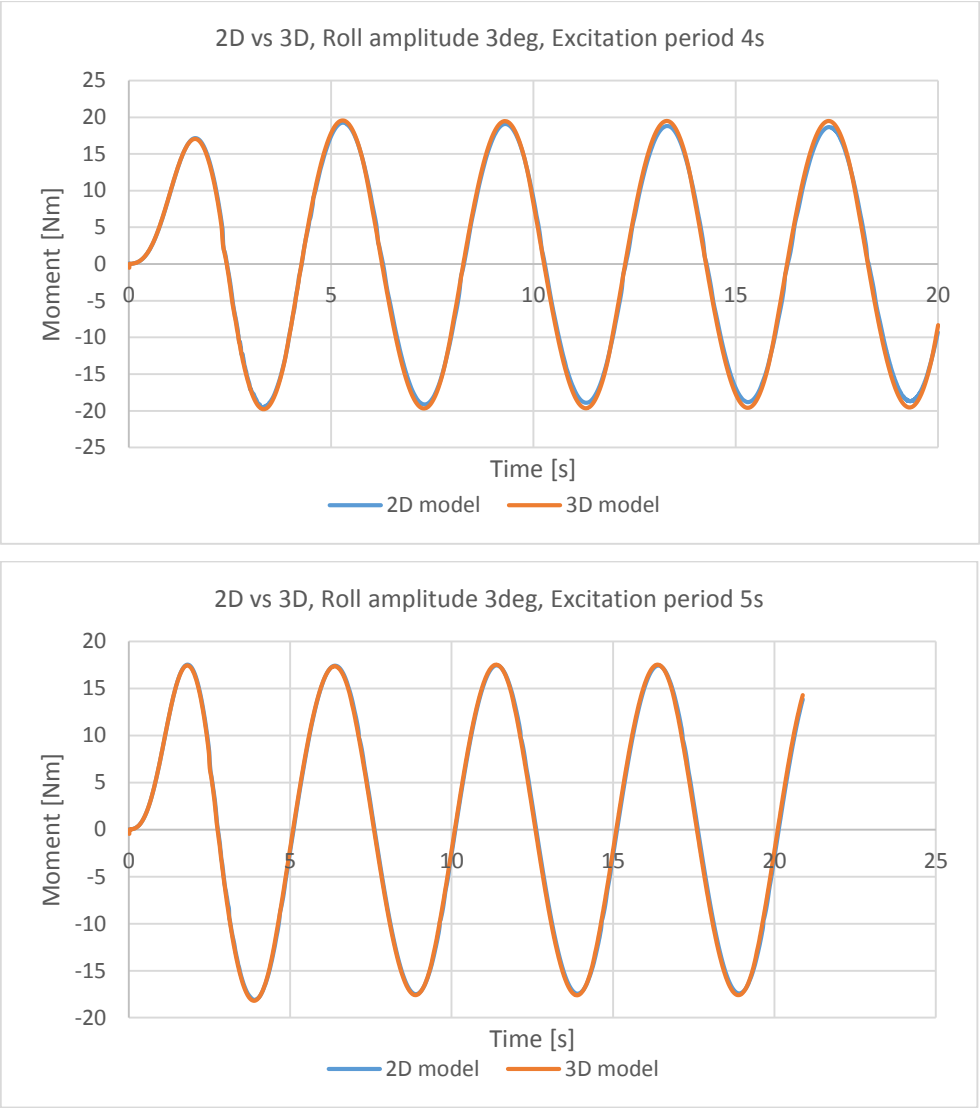

Figure 27. 2D vs 3D at different excitation periods

Based on previous discussion, the moment differences between 2D and 3D simulations are rather small. Therefore, we may accept 2D simulations only in our specific cases. Though turbulence is a three-dimensional time-dependent phenomenon, we may use 2D simulations to initial iterations, initial screening of alternative designs, and parametric studies because it is easy to implement and computationally cheap.

However, when the excitation period is very small and the sloshing inside is severe, 3D simulation is recommended and it is more reliable than a 2D simulation.

5 TANK PERFORMANCE DISCUSSION

5.1 Moment and phase

This part will discuss how to get the moment and phase from the results we received from simulations.

One can get the moment data after running a simulation in Star CCM+. As an initial analysis, one need to select the time region when the system reach steady status. One possible following step is to use Matlab Curving fitting tool to find out the expression of this curve and gain the mathematical equation. Then one can get the moment amplitude and phase lag at one excitation period. Repeat the procedure over and over again. The moment curve and phase curve can be achieved.

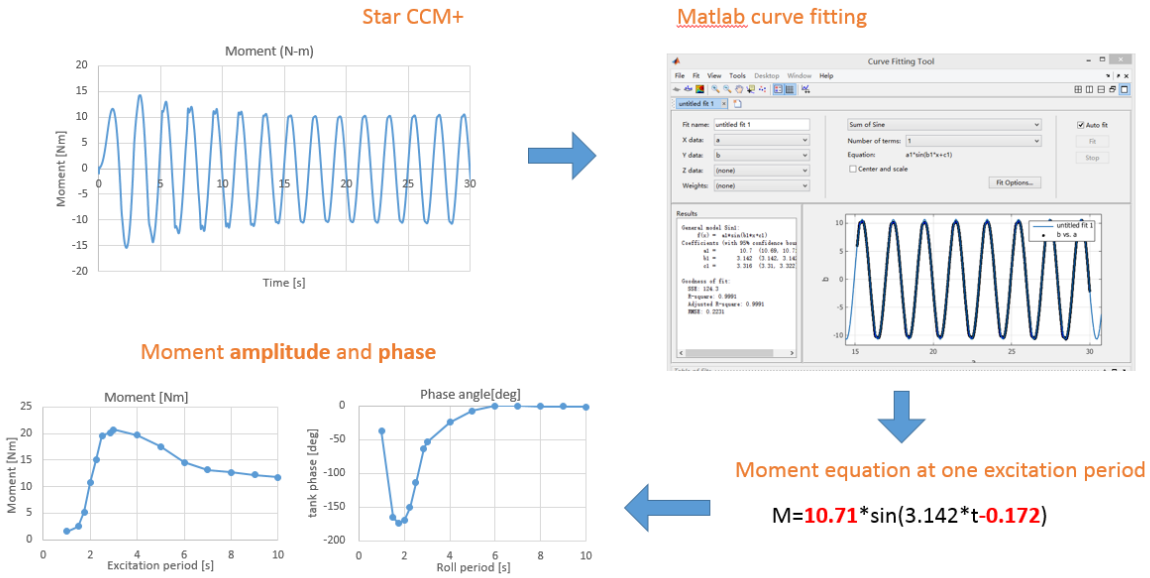

Figure 28. Data post-processing

5.2 Natural period

In chapter 2.4.2, we have already calculated the highest natural periods of the anti-roll tank. Table 5 gives the highest natural periods of different filling tanks. But are they the same with the realistic natural periods?

Since we already get the time domain results of the tank damping moment, we may therefore use Fast Fourier Transform(FFT) to find out the frequency domain. This process is implemented in 20-sim. Then the excitation frequency and natural frequency can be found directly.

Here, we select 33% filling percentage and 3deg excitation amplitude as an example to discuss.

Excitation period: 1s

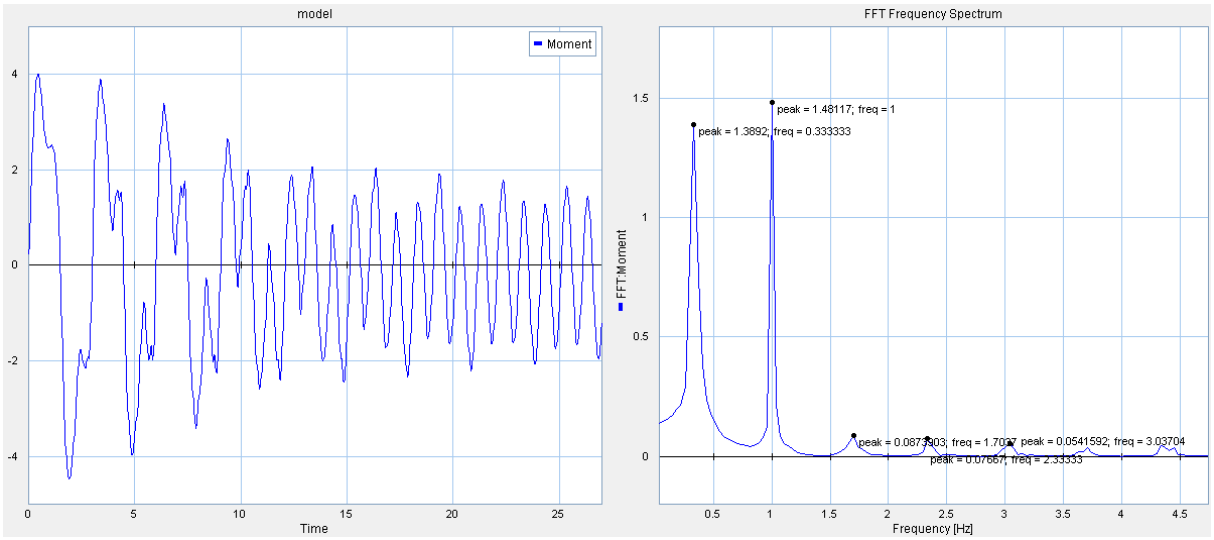

Excitation period: 1.2s

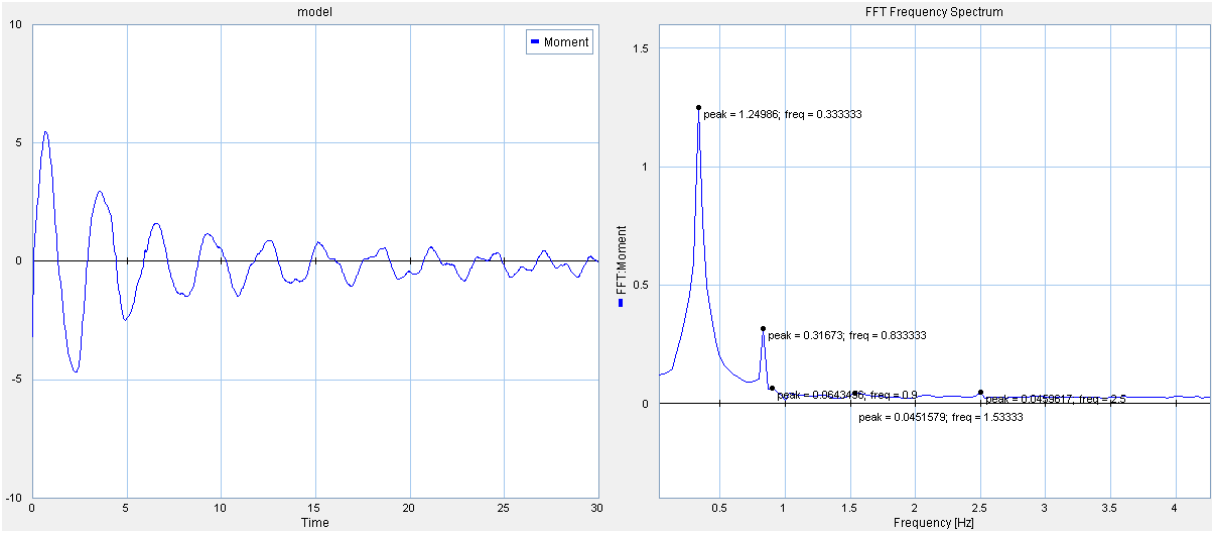

Excitation period: 1.5s

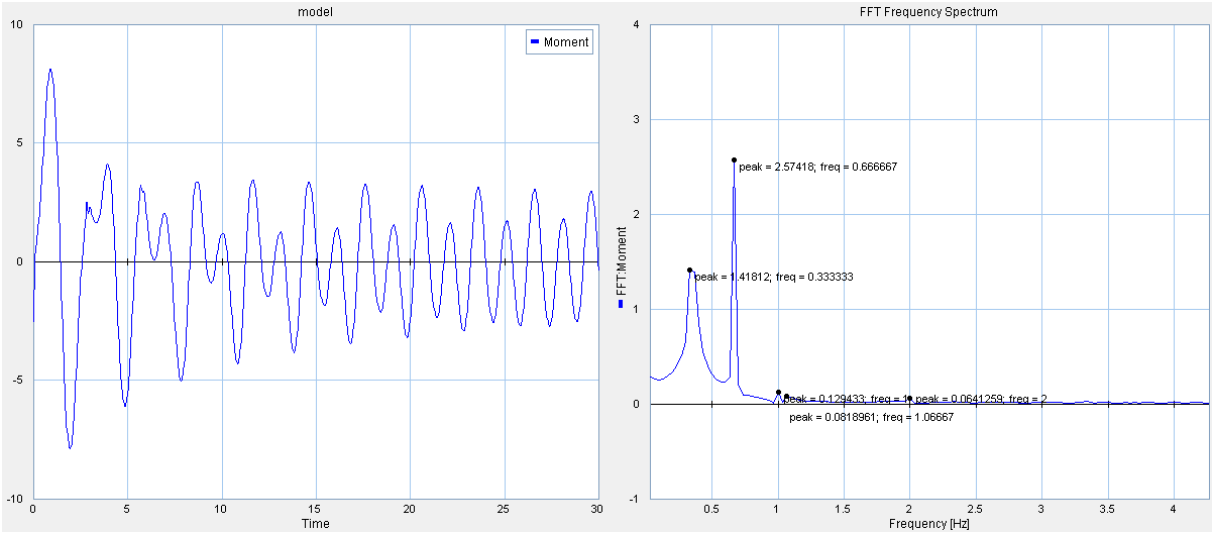

Excitation period: 1.75s

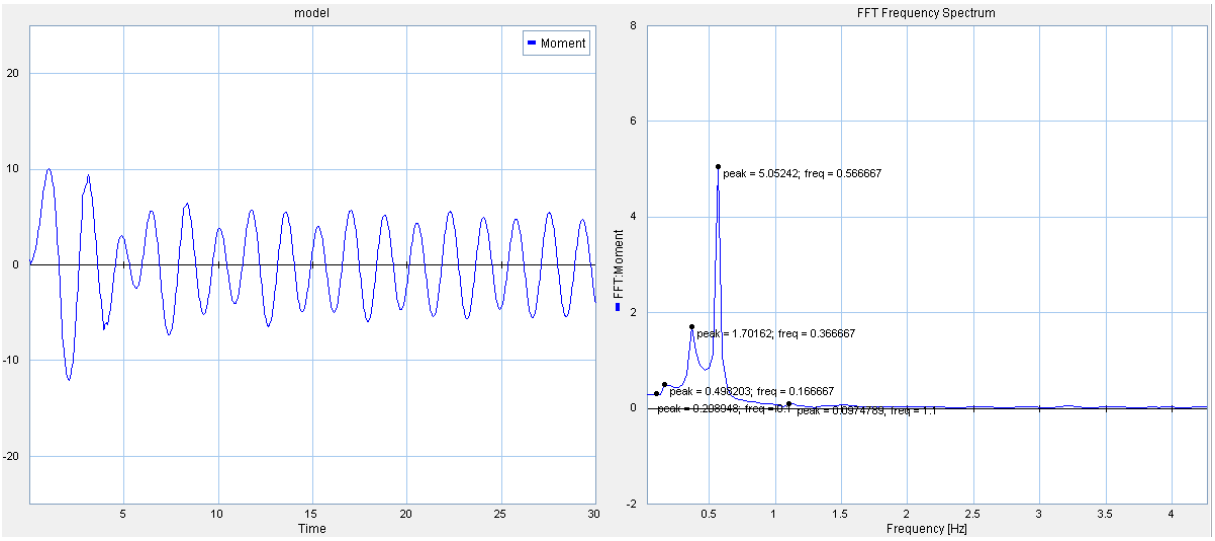

Excitation period: 2.0s

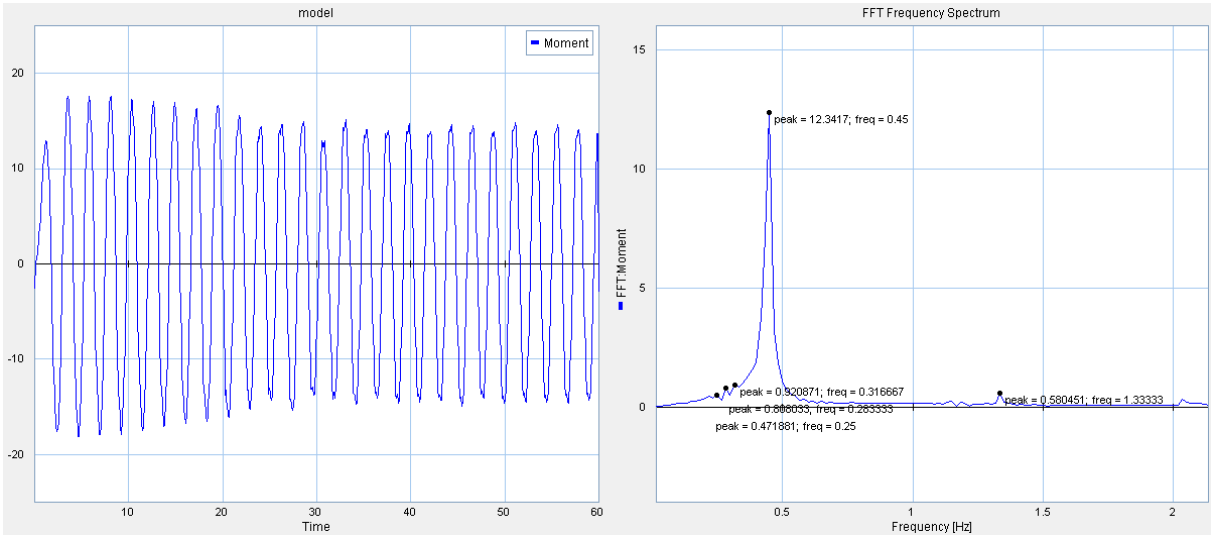

Excitation period: 2.5s

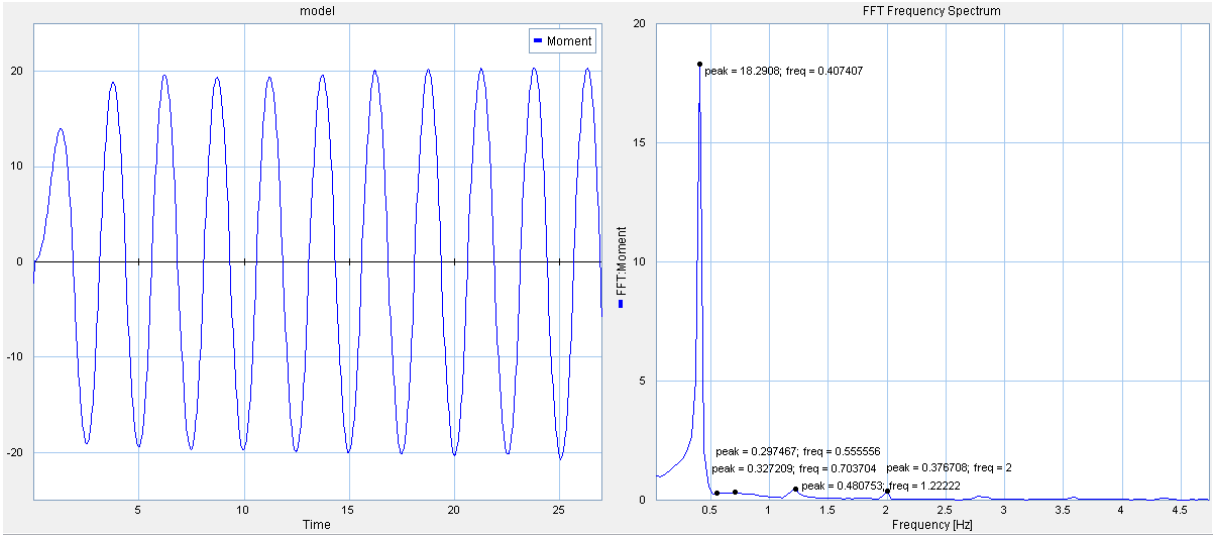

Excitation period: 3.0s

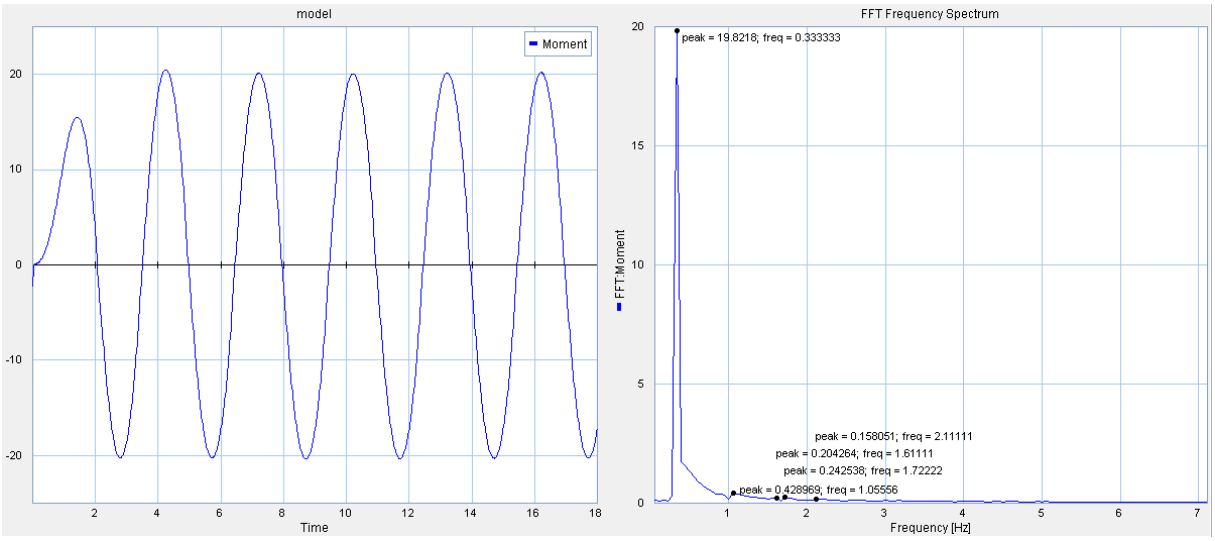

Excitation period: 4.0s

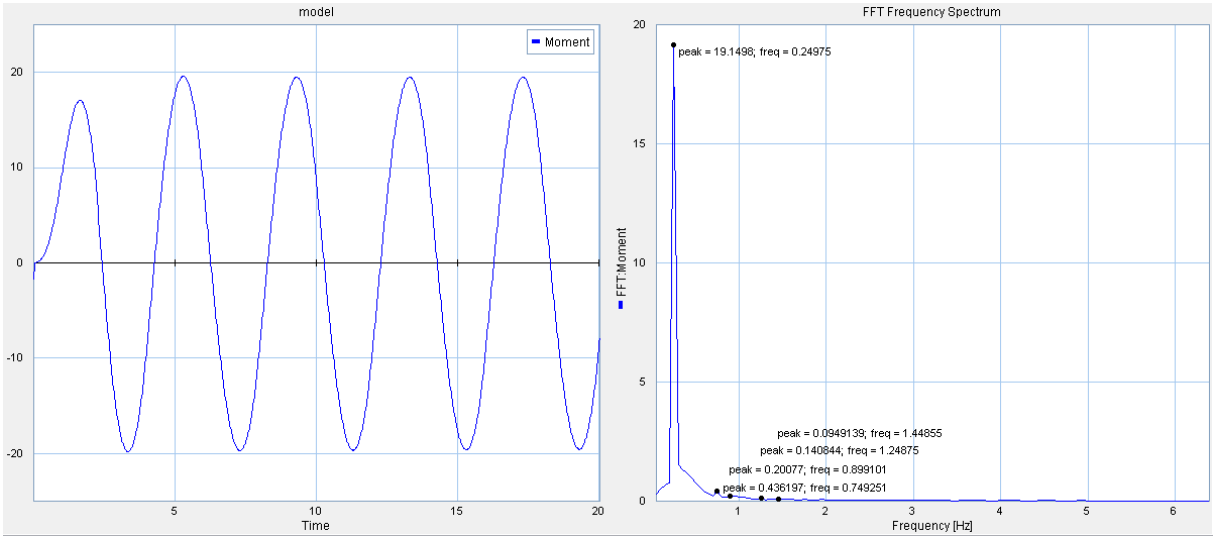

Excitation period: 5.0s

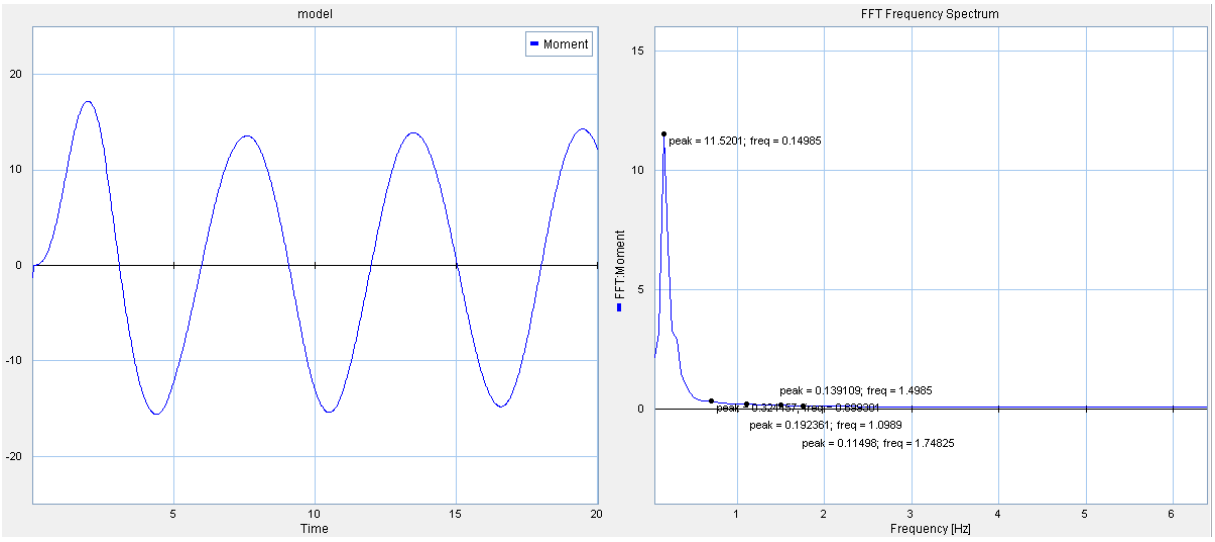

Excitation period: 6.0s

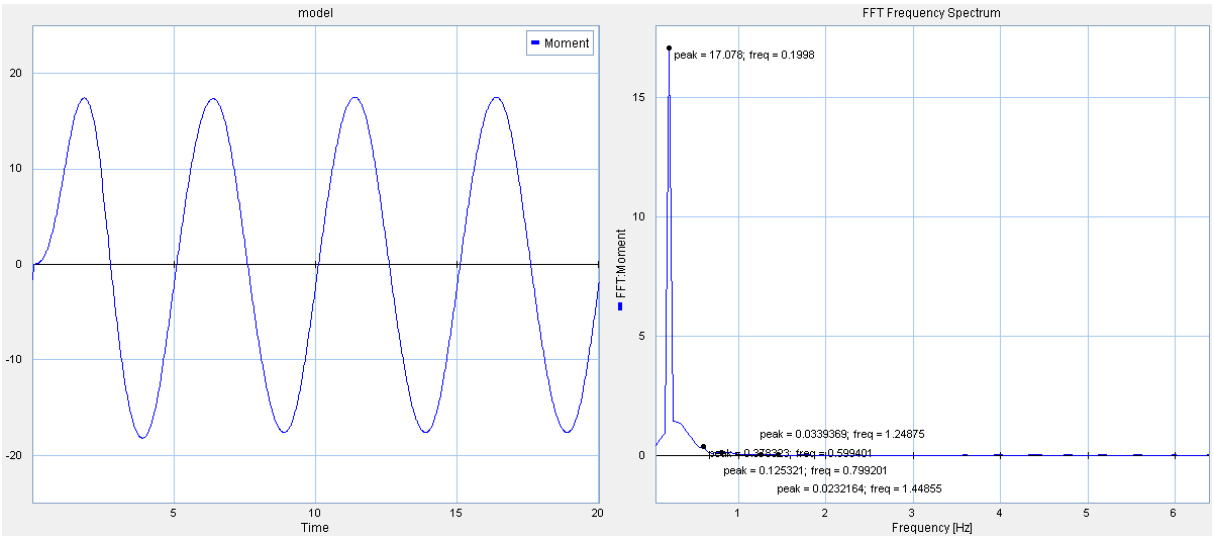

Excitation period: 7.0s

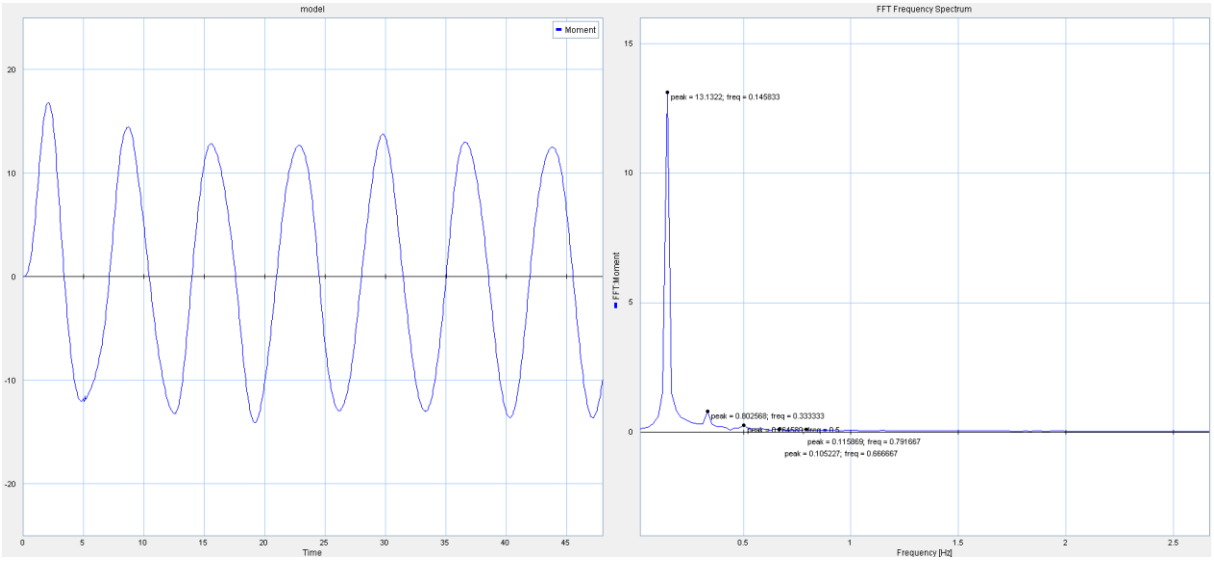

Excitation period: 8.0s

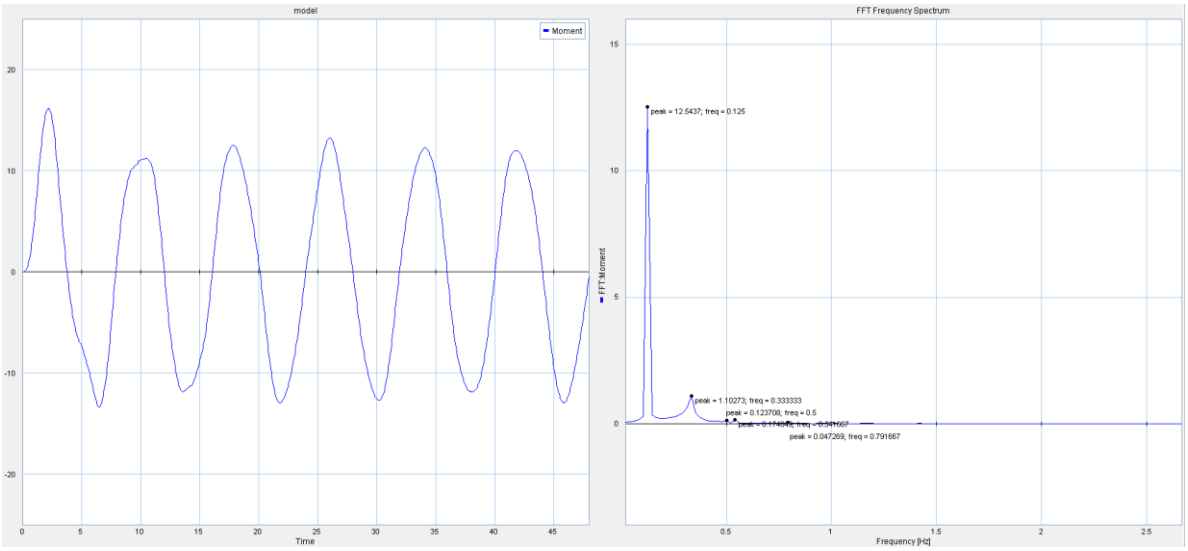

Excitation period: 9.0s

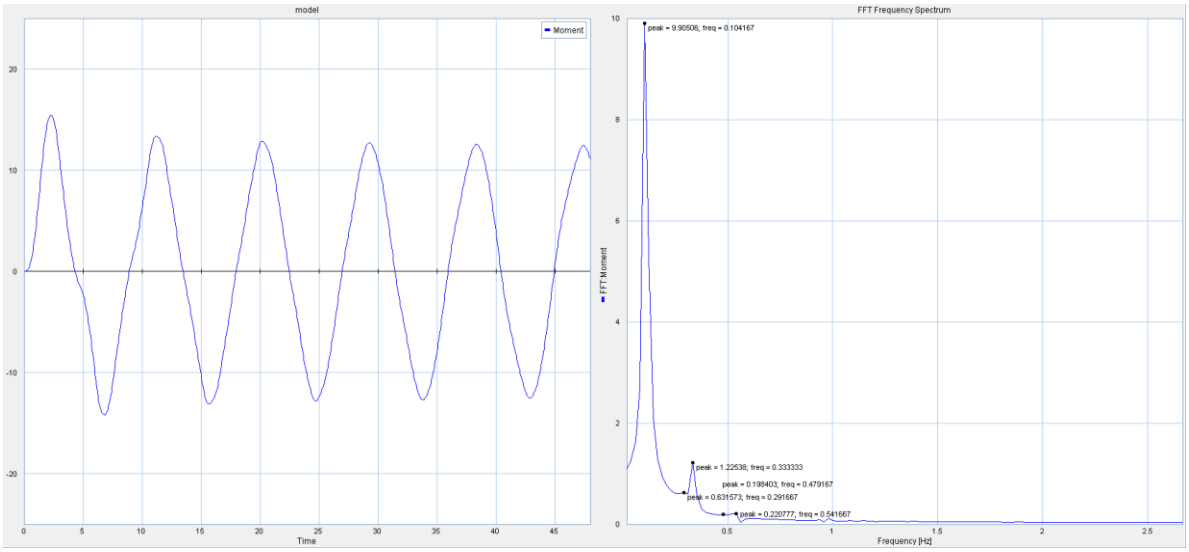

Excitation period: 10.0s

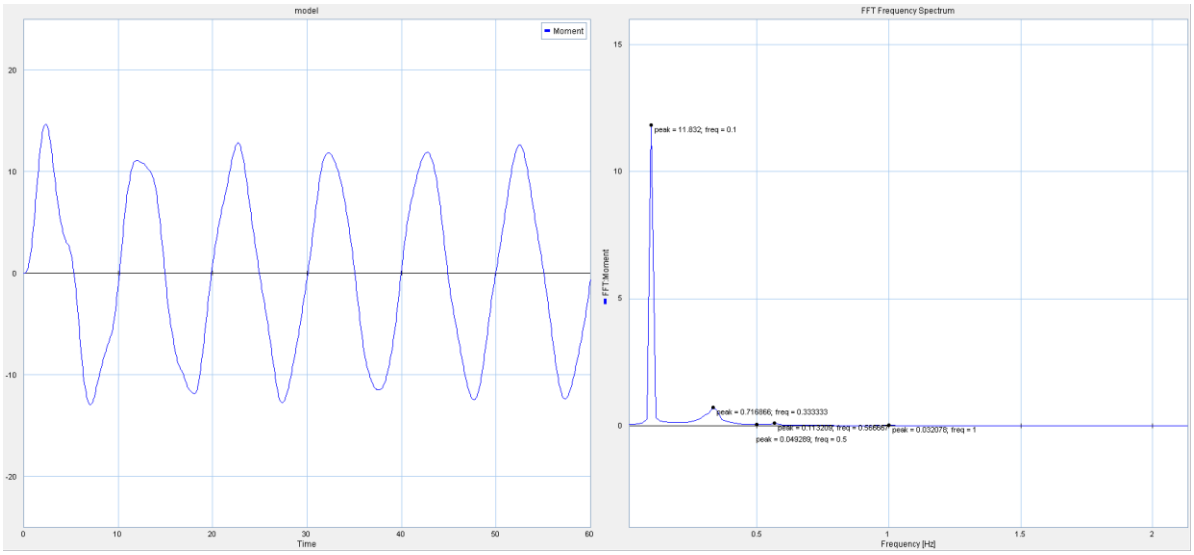

Figure 29. Time domain and frequency domain

As the excitation period varies from 1.0s to 1.75s, two dominated frequencies can be found in the frequency domain figure. One equals to the excitation frequency, and the other remains a stable value, which should be the natural frequency of the system. In this case, the natural frequency of the tank is 0.33. Besides, comparing the peak values of these two frequencies, we can find that the function/effect of the natural frequency reduces with the increase of excitation period. This also implies that the system transfers from stiffness dominated region to damping dominated region.

When the excitation period reaches 2.0s, only one dominated frequency (excitation frequency) can be found in the domain. It indicates that the system is dominated by external excitation and enters in the damping dominate region. When excitation period is 3.0s, which equals to the natural period, the peak of the frequency reaches the highest value among all the excitation periods. This is where the resonance happens. Comparing 3.0s with adjacent periods, we can also find that the peak value of 2.5s and 4.0s are close to the peak value of 3.0s. This phenomenon is so called frequency locking(or "lock-in").

If we increase the excitation period to 7.0s and even higher, the natural frequency appears again in the frequency domain. This is because the excitation period is far from the natural frequency. The system enters into inertial dominated region.

Figure 29 shows the distribution of these three regions. Basically, the designers wish their ART located in the damping dominated region so that they can achieve better performance. This is also why some people name it "damping tank". In order to maximize the performance, the designate tank is supposed to have a -90 deg phase angle. In this case, the amplitude of the moment is approximately 20 Nm which is close to the maximum amplitude.

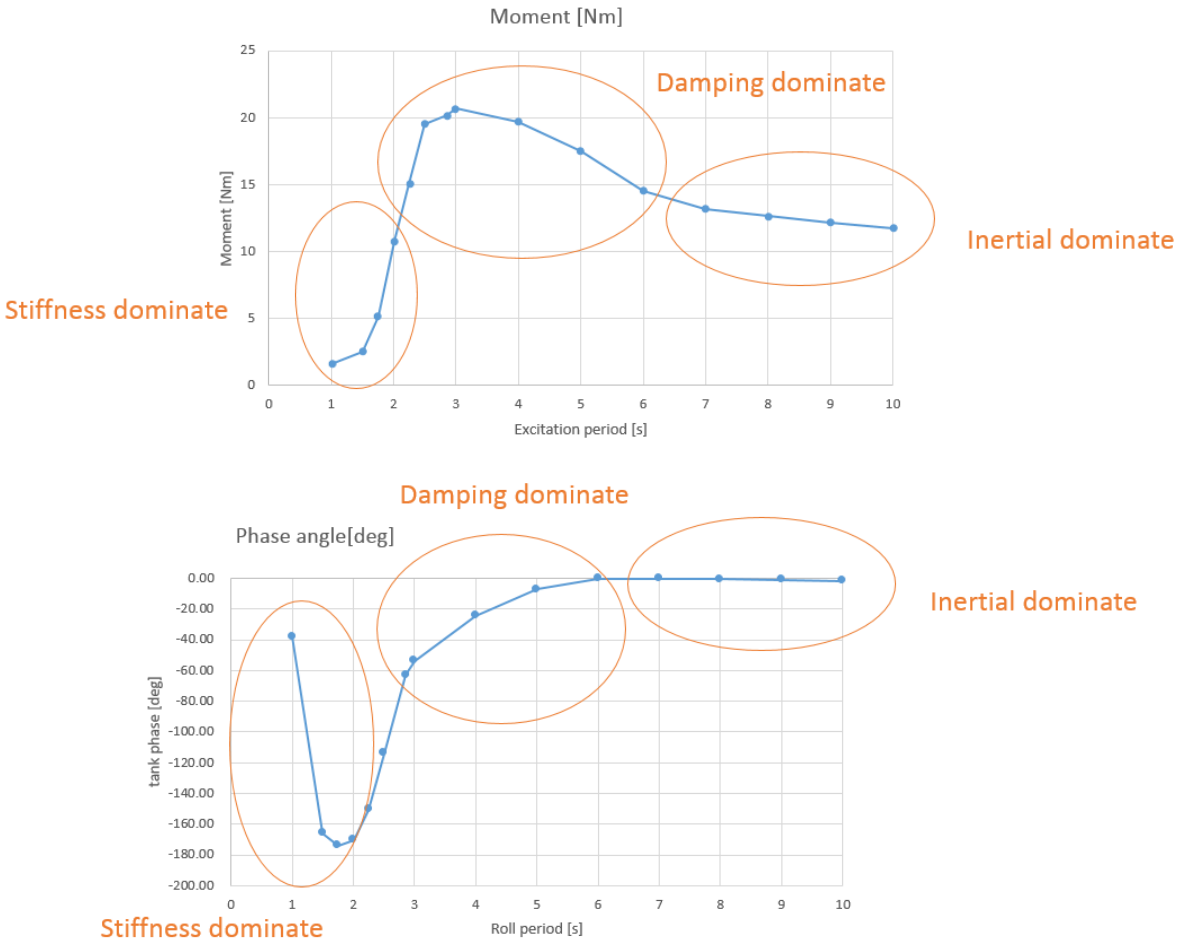

Figure 30. Different dominated regions

Using similar idea, natural frequencies of the other two filling percentage are found as shown in Table 8. It can be found that the natural frequencies from simulations are slightly smaller than those calculated by formula.

Table 8. Natural frequency comparison

Filling percentage	Water level h[cm]	Highest natural period	Natural frequency	Natural frequency from simulation
33.3%	5.0	2.86	0.35	0.33
50%	7.5	2.33	0.43	0.41
66.6%	10.0	2.02	0.50	0.49

5.3 Excitation Amplitude

This chapter will investigate the performance of the FST at different excitation amplitudes.

In figure 31, the moment is expressed as moment per unit roll to make the values comparable with other amplitudes of roll. The total moment can be found by multiplying with the amplitude of roll motion. The amplitude of the moment can also be read out of the time series.

When multiplying each curve by its roll amplitude it is clear that the black curve multiplied by six gives higher values than the blue curve multiplied by two. A higher roll amplitude represented by the black curve gives therefore higher damping moments. Another aspect can be seen from the graph: The distances between the single curves are not equal. The damping moment increases not linear with the roll amplitude.

The lower graph in figure 32 shows the phase of the moment relative to the rig motion in degrees over the roll periods. For the first period of four seconds and for the large periods towards the end, there is nearly no phase difference because either the water is too inert to follow the rig motions or it can easily follow the motions at large periods. The phase of the moment can be read out of the recorded time series after the measured forces are multiplied by the lever arm to the centre of gravity.

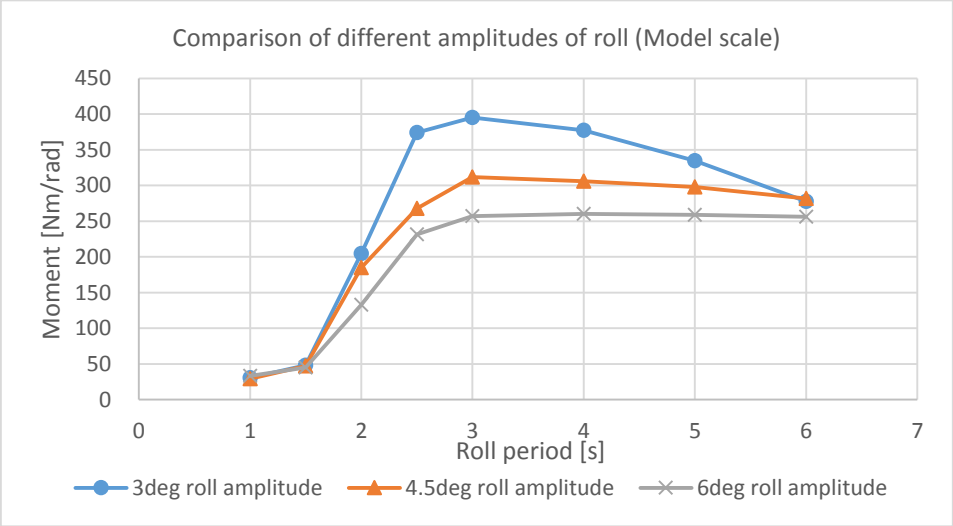

Figure 31. Moment comparison of different excitation amplitudes (Model scale)

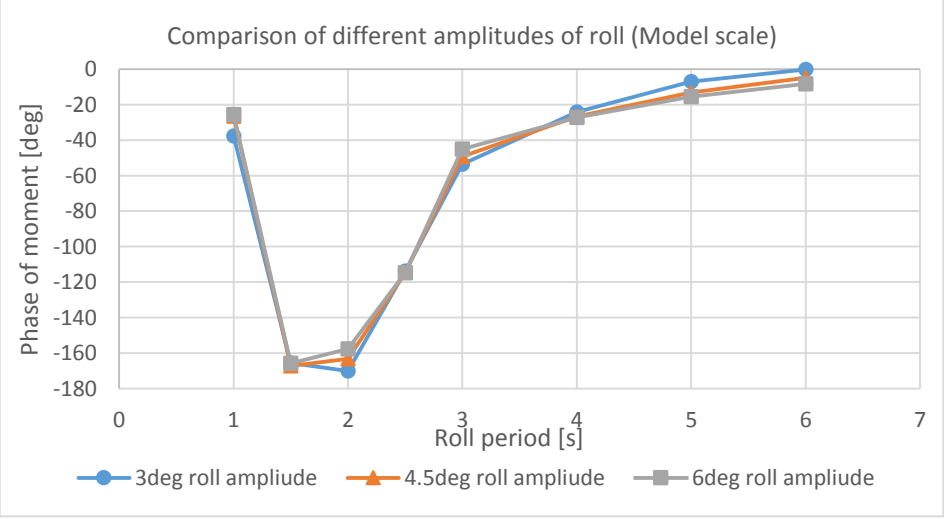

Figure 32. Phase comparison of different excitation amplitudes (Model scale)

We simply transfer the CFD simulations from model-scale to full-scale by using following equations:

Scale factor:

$$\lambda=20$$

Roll Period:

$$T_{full-scale} = \sqrt{\lambda} \cdot T_{model} \tag{27}$$

Bending Moment:

$$M_{full-scale} = \lambda^4 \cdot M_{model} \tag{28}$$

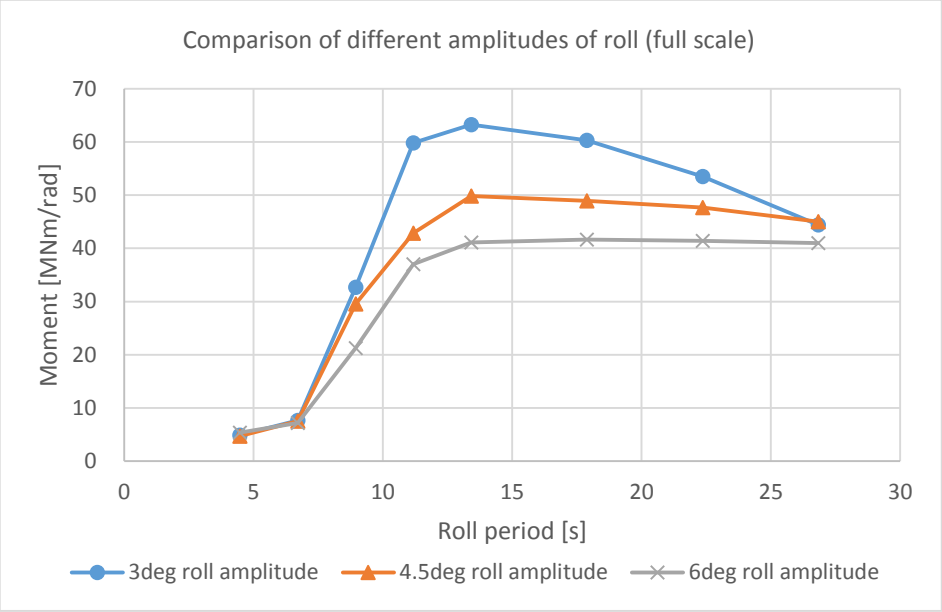

Figure 33. Moment comparison of different excitation amplitudes (Full scale)

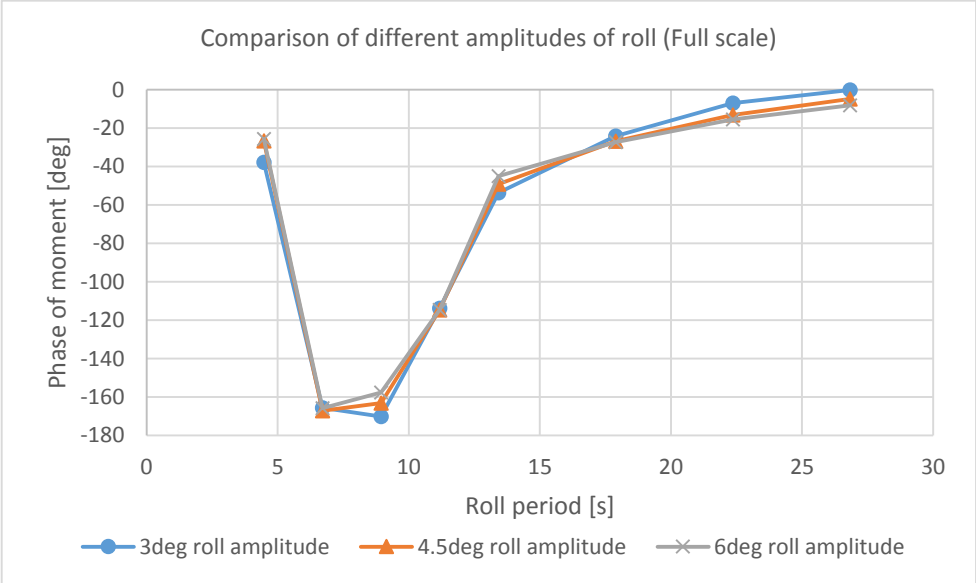

Figure 34. Phase comparison of different excitation amplitudes (Full scale)

5.4 Filling level/percentage

The main dimensions of a ART are defined in design phase. Therfore, change the filling percentage becomes the only way to ajust the natural frequency of the tank. In this part, we will discuss three different filling levels: 5cm, 7.5cm and 10cm, corresponding to 33%, 50% and 66% filling percentage.

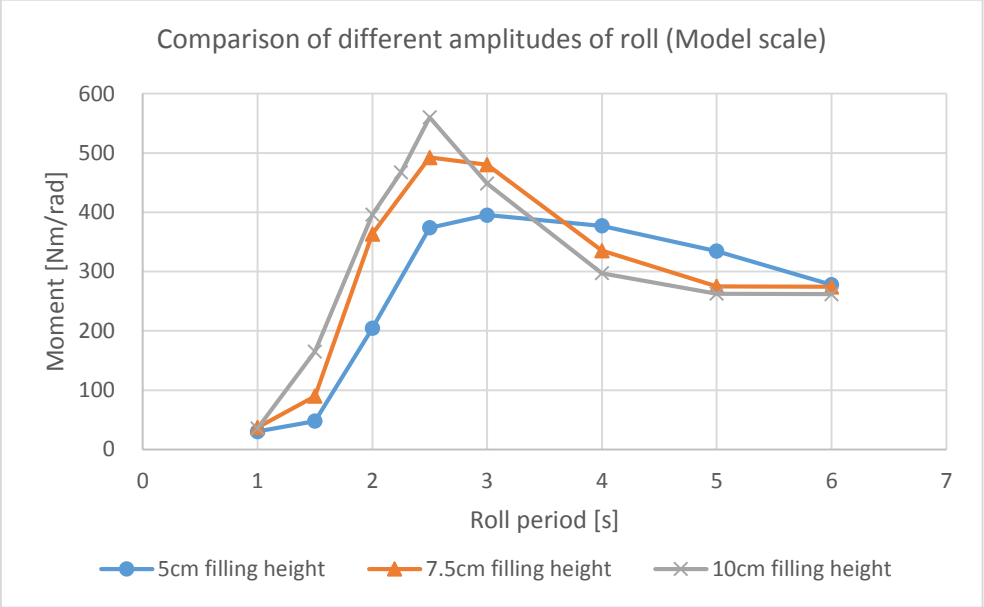

Figure 35. Moment comparison of different filling levels (Model scale)

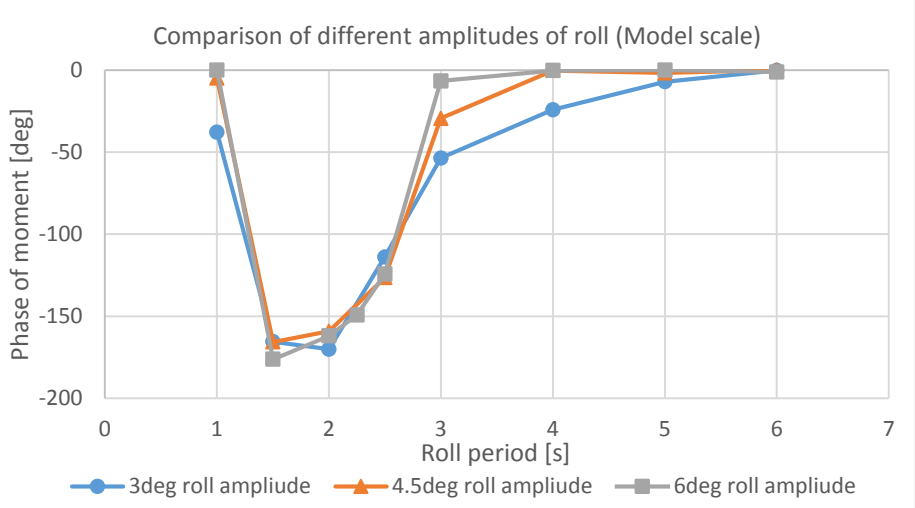

Figure 36. Phase comparison of different filling levels (Model scale)

Normally, higher filling level means more liquid inside the tank which will provide more static forece thus create more damping moment. This phenomenon can be found from 1s to 2.5s in Figure 35.

The natural period of the tank reduces as the filling level increases. It can be found that higher filling level create higher peak moment.

When the sytem enters in inertial dominated region, the tank with more liquid generates less moment. More liquid inside the tank means more mass, which creates more inertial impact. Therefore, it is more difficult to excite the liquid motion. Besides, the system with more mass enters in inertial dominated region much more early than those with less mass. This can also be found in the phase curve.

When the phase close to 0 (after 3.0s), the system enters in interial dominated region. Besides, it indicates the resonance occurs when the phase angle close to -90deg.

Then we transfer the model scale result to full scale result as shown in Figure 36. Considering the resonance period of the vessel is around 13s (Figure 37), we can found the tank performance at 50% filling is much better that it with 33% filling. The optimal filling level for this particular tank is between 50% and 66%.

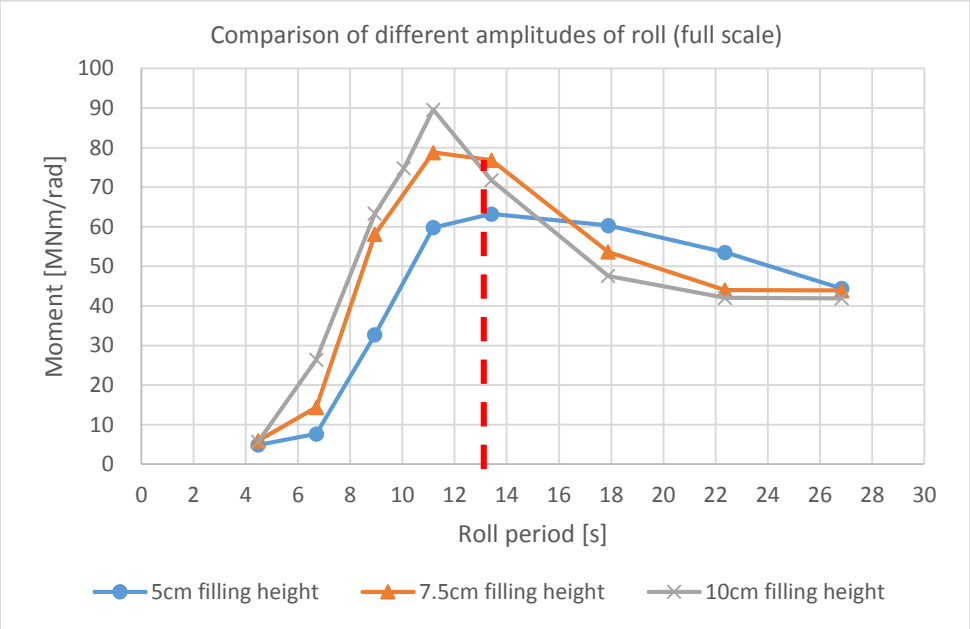

Figure 37. Moment comparison of different filling levels (Full scale)

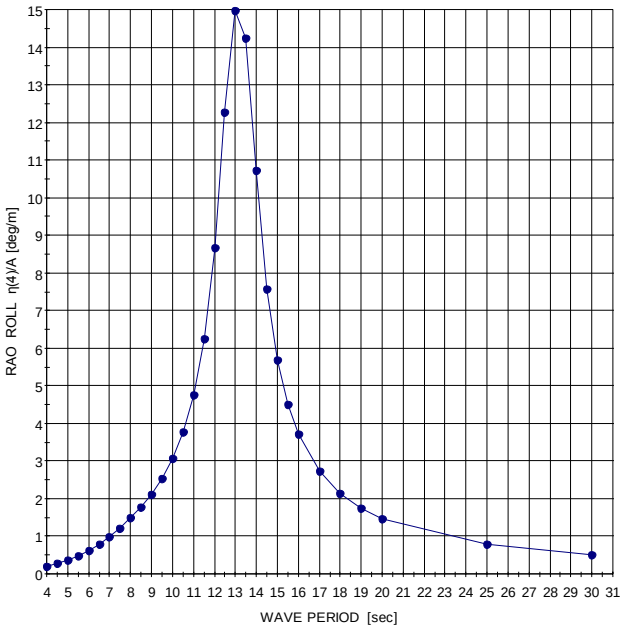

Figure 38. Roll RAO of the OSV

5.5 Cover Panel Effect

This part will discuss the influence of the cover panel. The predefined tank height is 15cm. In order to make a comparion, a second tank with a doubled height 30cm is introduced. Figure 39 show the snap shots at different moment.

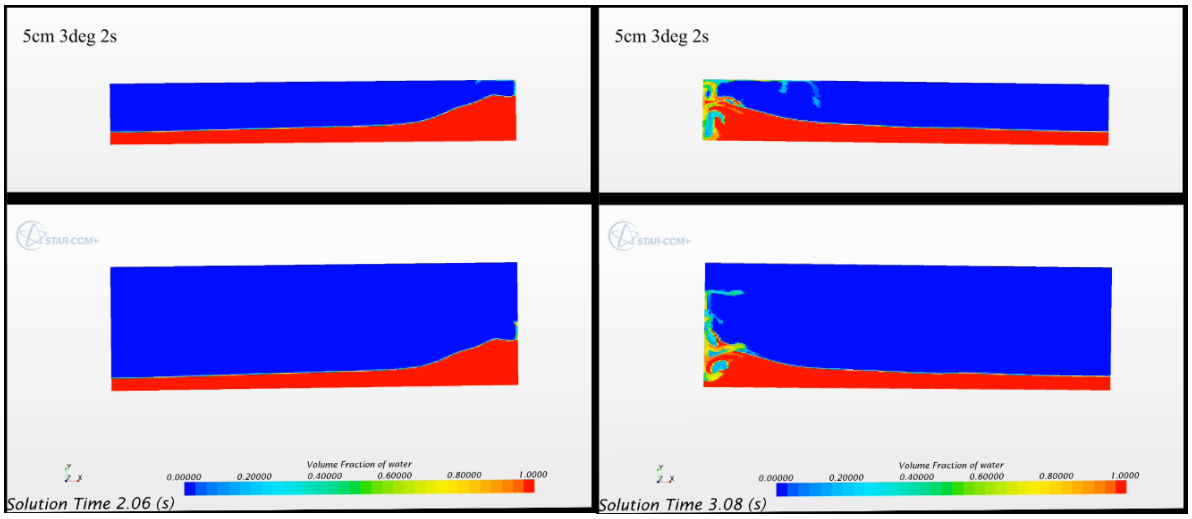
5cm 3deg 2s
Volume Fraction of water
0.00000 0.20000 0.40000 0.60000 0.80000 1.0000
Solution Time 2.06 (s)
5cm 3deg 2s
Volume Fraction of water
0.00000 0.20000 0.40000 0.60000 0.80000 1.0000
Solution Time 3.08 (s)

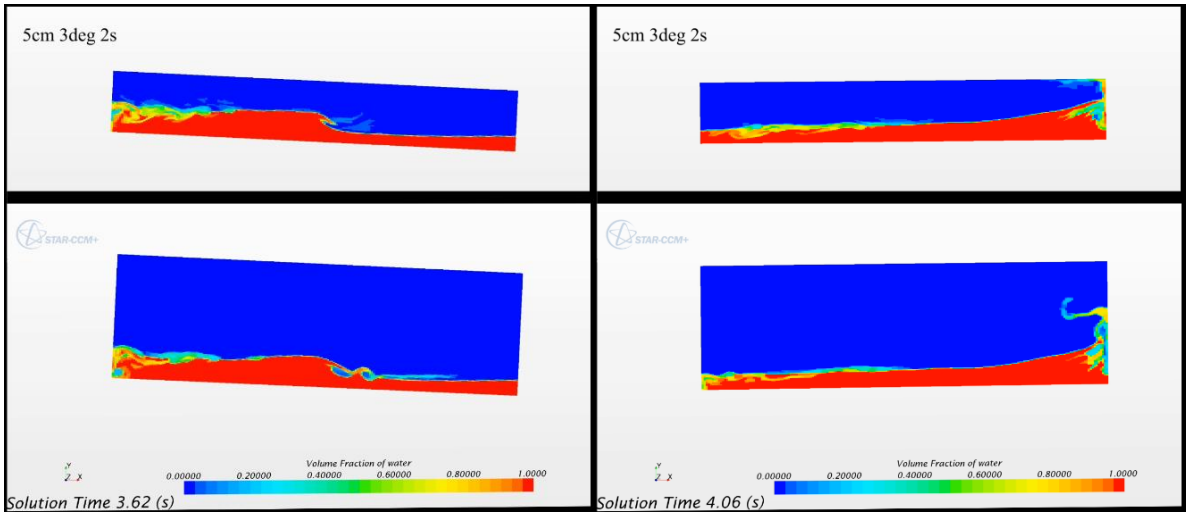
5cm 3deg 2s
Volume Fraction of water
0.00000 0.20000 0.40000 0.60000 0.80000 1.0000
Solution Time 3.62 (s)
5cm 3deg 2s
Volume Fraction of water
0.00000 0.20000 0.40000 0.60000 0.80000 1.0000
Solution Time 4.06 (s)

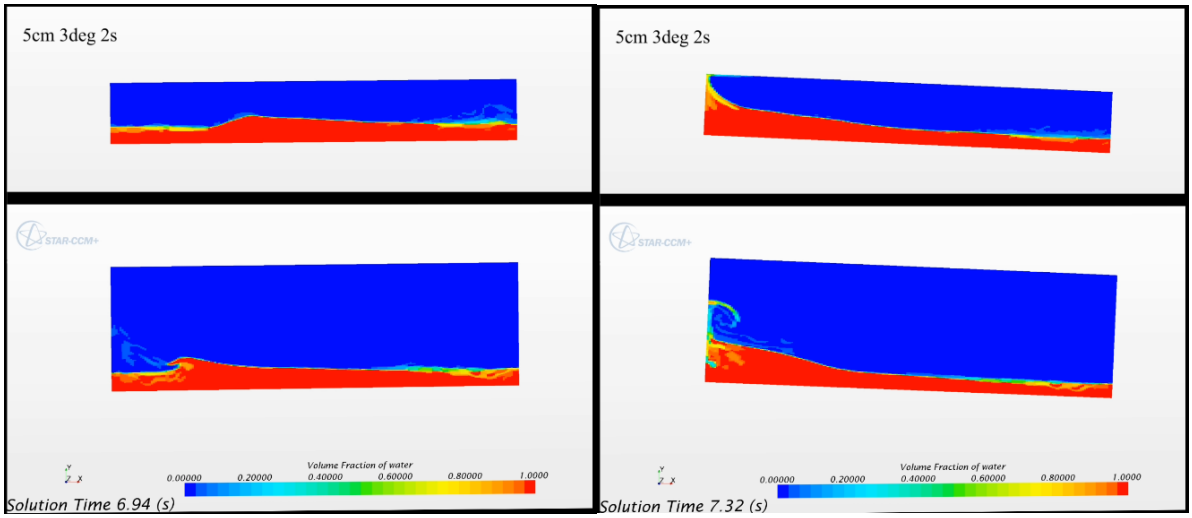
5cm 3deg 2s
Volume Fraction of water
0.00000 0.20000 0.40000 0.60000 0.80000 1.0000
Solution Time 6.94 (s)
5cm 3deg 2s
Volume Fraction of water
0.00000 0.20000 0.40000 0.60000 0.80000 1.0000
Solution Time 7.32 (s)

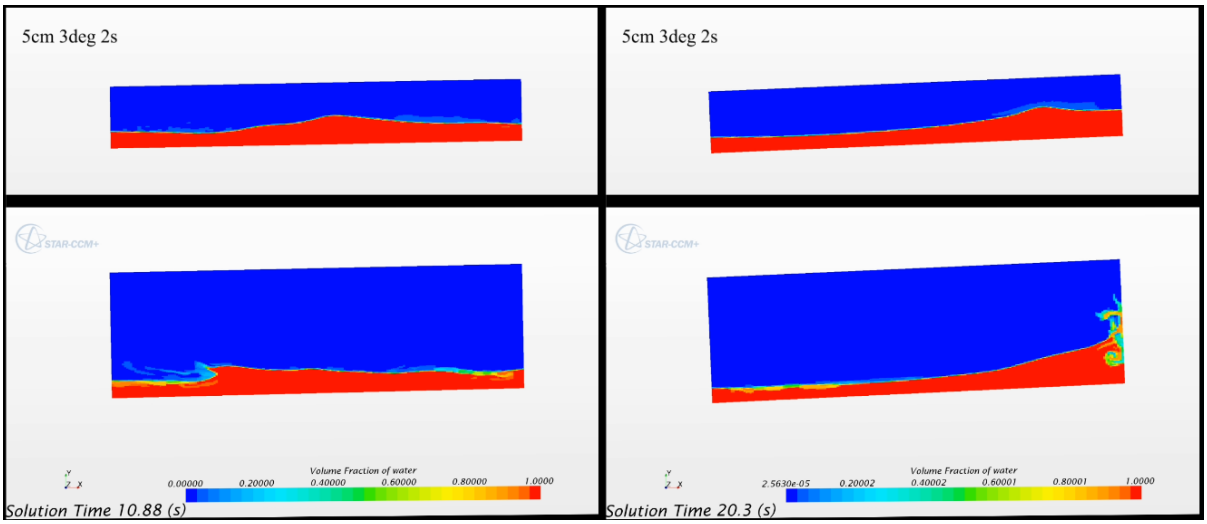

Figure 39. Snapshots of cover effect

From the figures above, we can find that the cover panel has influence when the water hits side walls which will result in a less damping moment. Futhermore, the water drops falling down from the cover panel affect the flow below. This results in the phase different as shown in solution time 5.84s, 6.94s.

As time goes on, the cover effect increase more. The wave pattern inside the tank is different. At time 10.88s and 20.3s, we can see that the wave in the limited height tank becomes a combined wave instead of hydraulic jump and travalling wave.

Figure 40 gives the damping moment of these two tanks. It is suggested that using a finite tank height to do pure sloshing study is better since it may negelect the cover panel effect and the system can reach steady state in a shorter time.

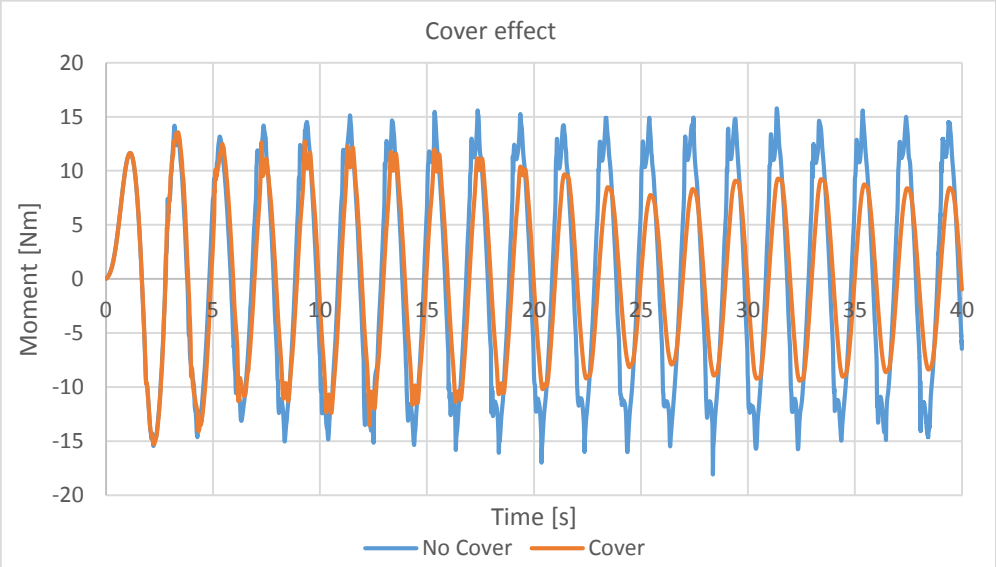

Figure 40. Cover effect

6 EXPERIMENT AND VALIDATION

Numerical method provides complete analysis and solutions to the ART problem. However, it is difficult to convince the accuracy of the results. It is therefore necessary to do validation by using experiment data. Two ways of test validation are provided in this thesis. One validation comes from ShipX database, which is established by MARINTEK in 2014. The other is the model test performed by the author at Aalesund University College. Next will give an introduction of these validations.

6.1 Experimental data from ShipX

6.1.1 Tank design in ShipX

MARINTEK uses the ShipX Vessel Responses (VERES) programme to include the effect of motion control systems on the ship motions. Different types of tanks can be handled. Either model test data from a given tank or data from systematically performed tests stored in a database can be taken as input for designing a tank using the VERES programme.

The user manual written by Fathi (2014) (Fathi 2014) gives a guidance on how a rough design of a free surface roll damping tank is determined according to the sea performance of the actual ship. First, the ship motion transfer function is found in VERES which is defined by the given vessel geometry and the loading condition. Mass and position of the tank are already included but the free surface effects are of course not incorporated because the original ship performance shall be treated. It should be noticed that the sea state where the ship shall operate is an important factor in the transfer function, as larger waves will lead to larger roll amplitudes of the vessel. By plotting the transfer function one can find the natural roll period of the ship.

Second, tank geometry and maximum filling height are specified. Additional options as damping grids can be chosen. The programme then calculates which filling level is optimal for each roll period. An important assumption is made in this programme: It is assumed that the roll damping increases linear with increasing roll amplitude, also at resonance.

Third, by knowing now the natural roll period of the ship the optimal filling level can be read out of a plot from the second step. Finally, the modified ship transfer function with included roll reduction can be plotted. If the achieved damping should not be sufficient, a longer tank as well as a higher location of the tank would increase the effect of the roll damping moment. Sometimes, a second tank is installed. Such operating vessels have often bilge keels in addition as initial configuration. Some of these ships cannot operate with the tank when the GM-requirements are not fulfilled. Bilge keels need to be included in the ship motion calculations.

6.1.2 Tank database

The data in the VERES database are collected from literature, as well as systematic model tests in MARINTEK's roll simulator. In the model tests, a roll amplitude of 0.07 radians (4 deg) is applied in the roll simulator.

Tank filling:

$$0.04 \leq h/b \leq 0.10$$

Vertical positions:

$$-0.2 \leq s/b \leq 0.40$$

6.1.3 Data comparison

The model in ShipX is a full-scale OSV which defined in chapter 4.1. So the tank installed on this vessel is full scale as well. Therefore, we will compare the data from CFD simulations and experimental data from ShipX in full scale size.

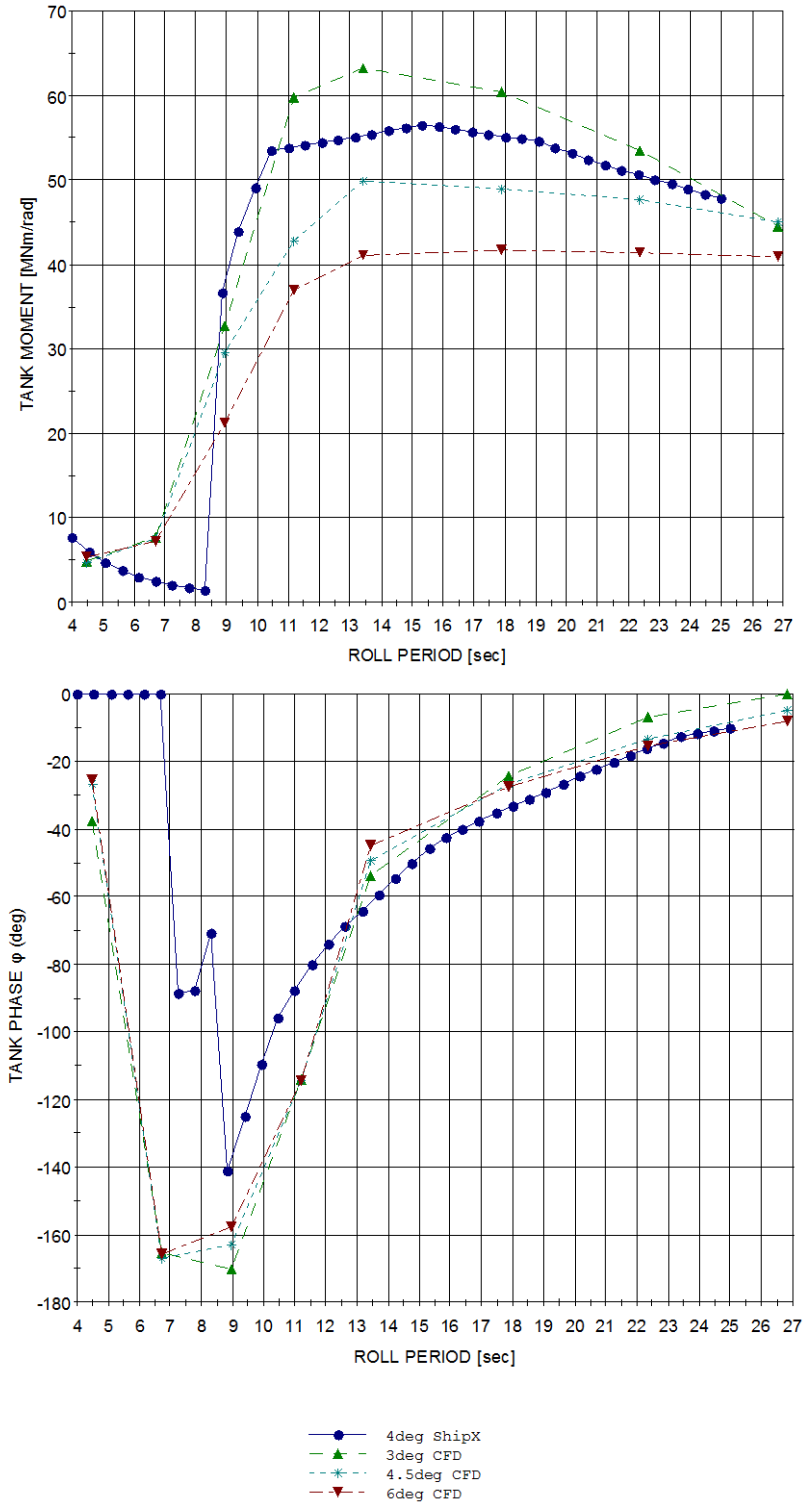

Figure 41. Comparison between simulations and database in ShipX

The moment plotted in Figure40 is in MNm/radians in order to make the values comparable with other amplitudes of roll. It should be noticed that the model tests in ShipX only provides a roll amplitude of 0.007 radians (4deg). While the CFD simulations

have three different roll amplitudes: 3deg, 4.5deg and 6deg. The trend of the curves maintain consistency especially in damping and inertial dominated regions. In high frequency (small excitation periods) region, the results do not match perfectly.

Further comparisons are performed in following figures. Moment and phase at different filling levels are compared separately.

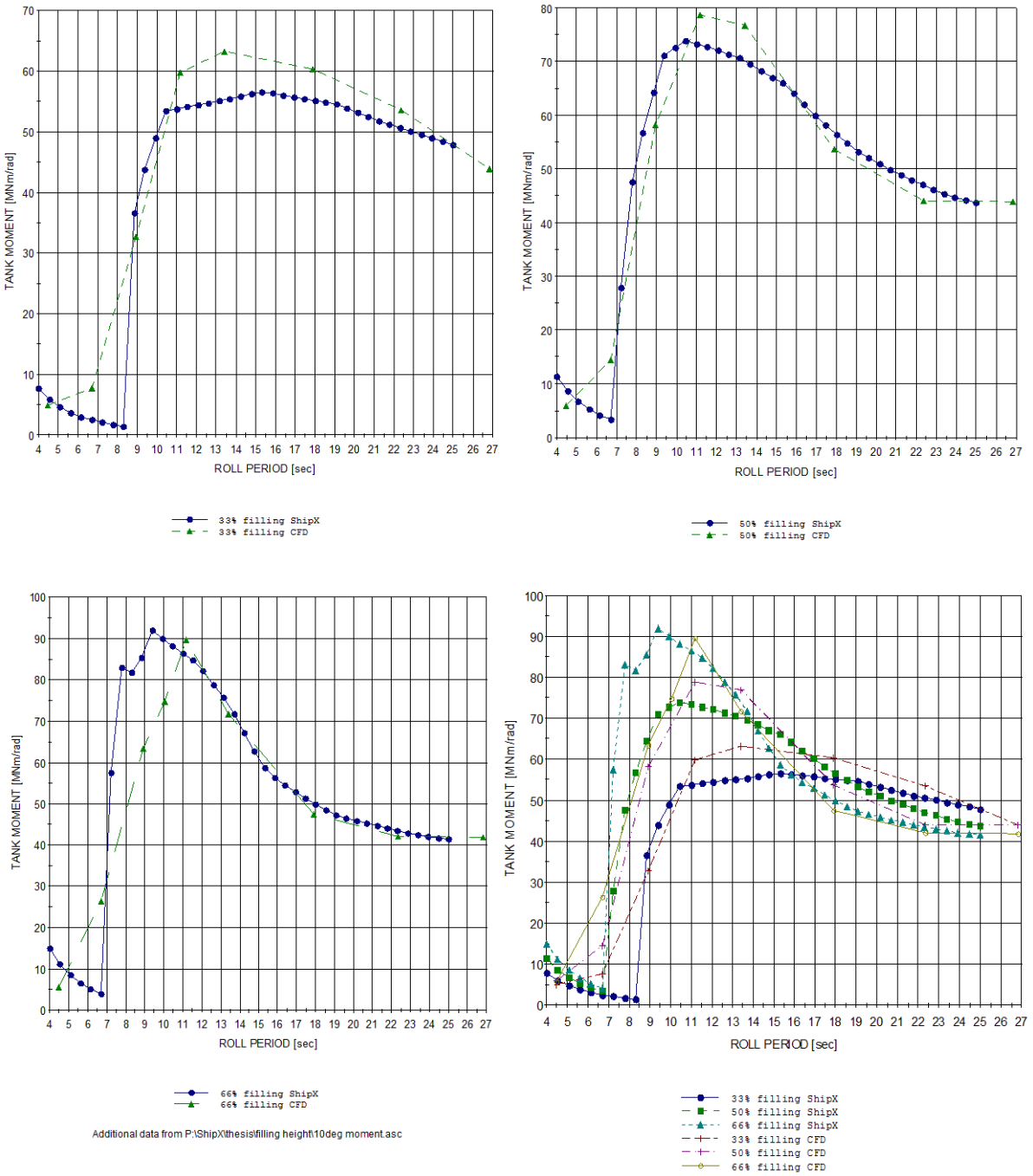

Figure 42. Moment comparison at different filling percentages between simulations and database in ShipX

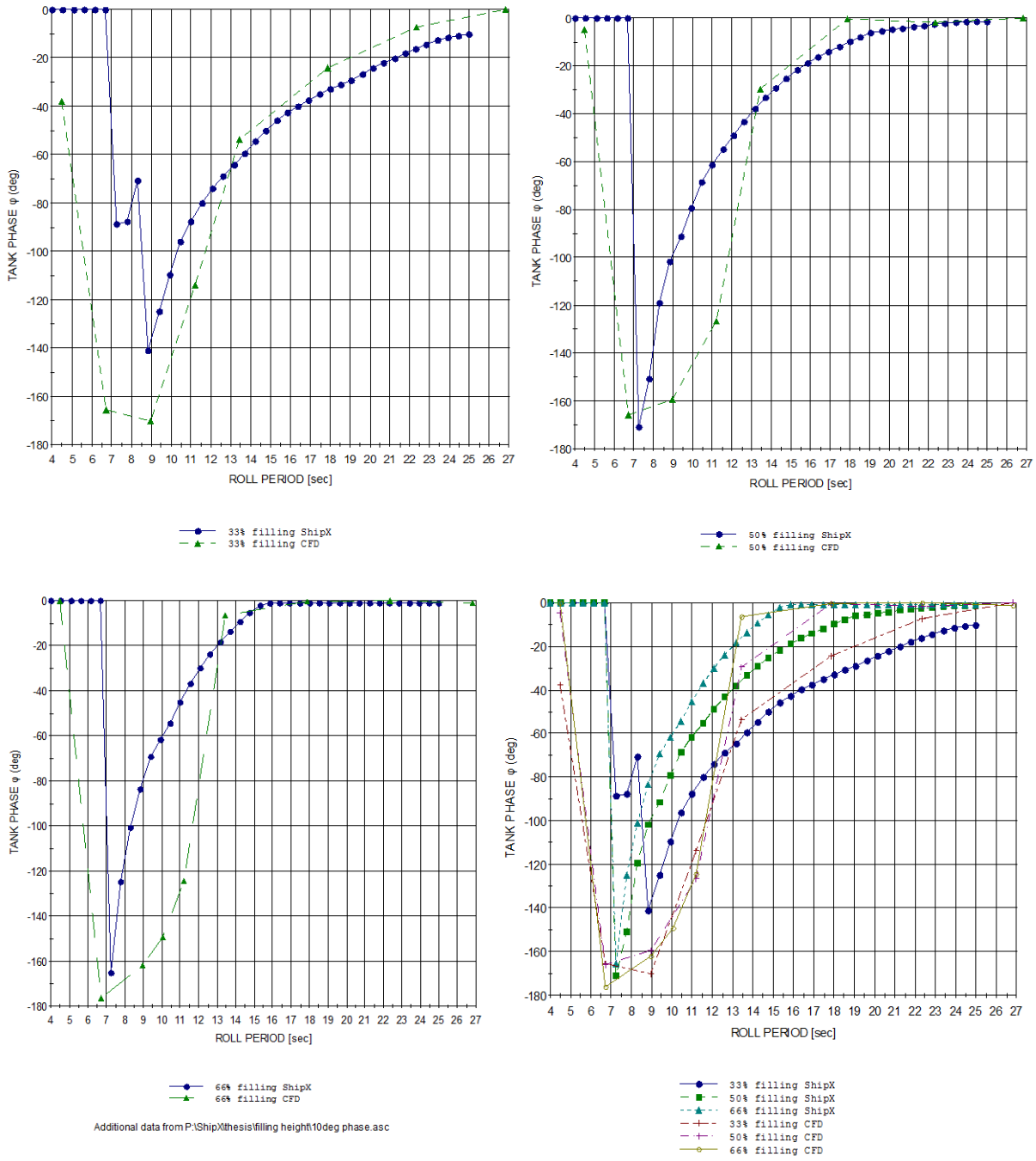

Figure 43. Phase comparison at different filling percentages between simulations and database in ShipX

All comparisons give similar result. The trend of the moment curves maintain consistency especially in damping and inertial dominated regions.

While the phase curves from the experiments and simulations maintain consistency in inertial dominated region. In the damping dominated region, the phases from simulations are normally larger than those from experiments. Besides, it shows some difference in high frequency (small excitation periods) region.

6.2 Model Test set up and plan

Model tests are designed and performed at Aalesund University College, Aalesund, Norway. This chapter will introduce the overall design of the tank platform and test plans.

6.2.1 Model Tank Design

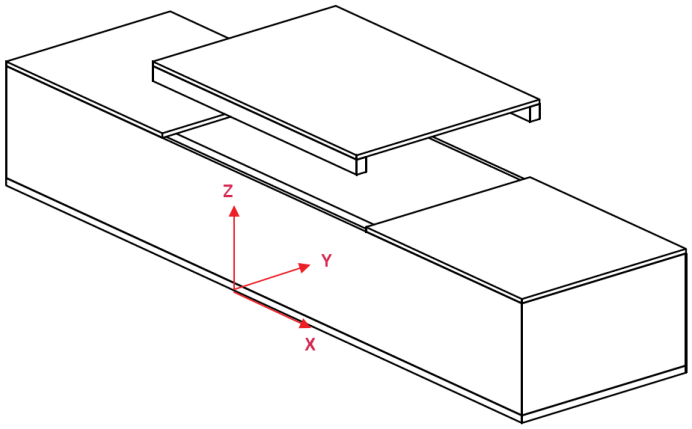

Figure 44. Tank design

The retangular tank was made of plexiglass with the same dimensions as in the CFD simulations. The thickness of the tank side wall is 6mm and 10mm for bottom. An additional cover is needed to make sure that the liquid inside won't splash out. Detailed drawing can be found in Appendix A.

6.2.2 Platform Set Up

The designed tank platform contains three parts: foundation structure, tank carrier and link-motor part as shown in Figure 45. Details can be found in the Appendix 3D models.

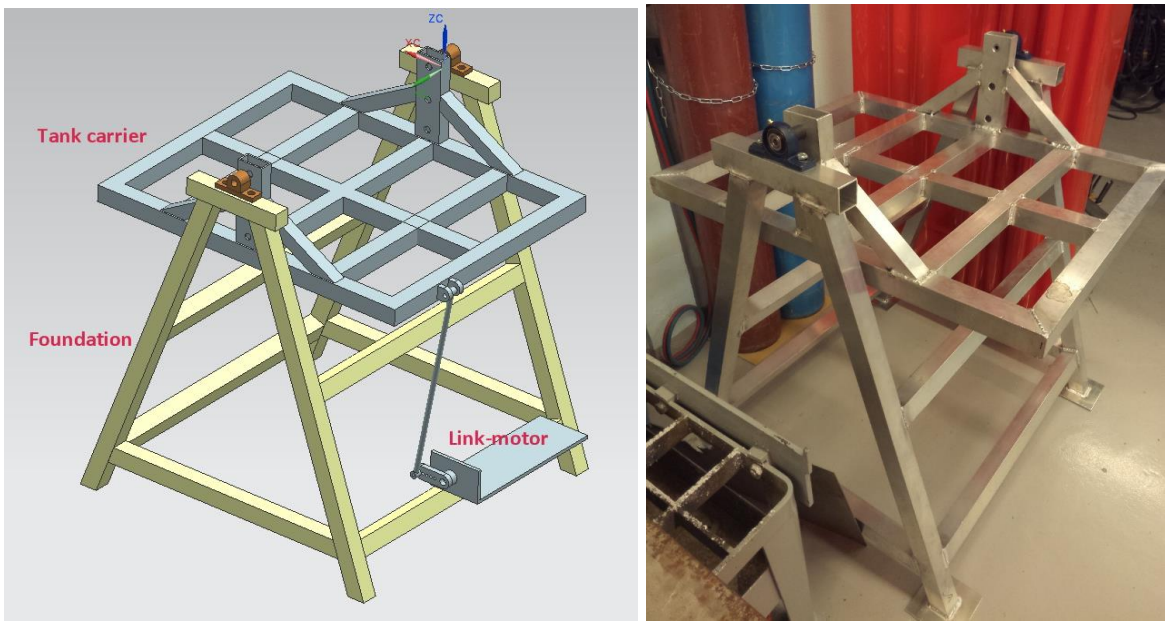

Figure 45. Platform design and physical model

Physical model was manufactured at Aalesund University College as shown in Figure 46.

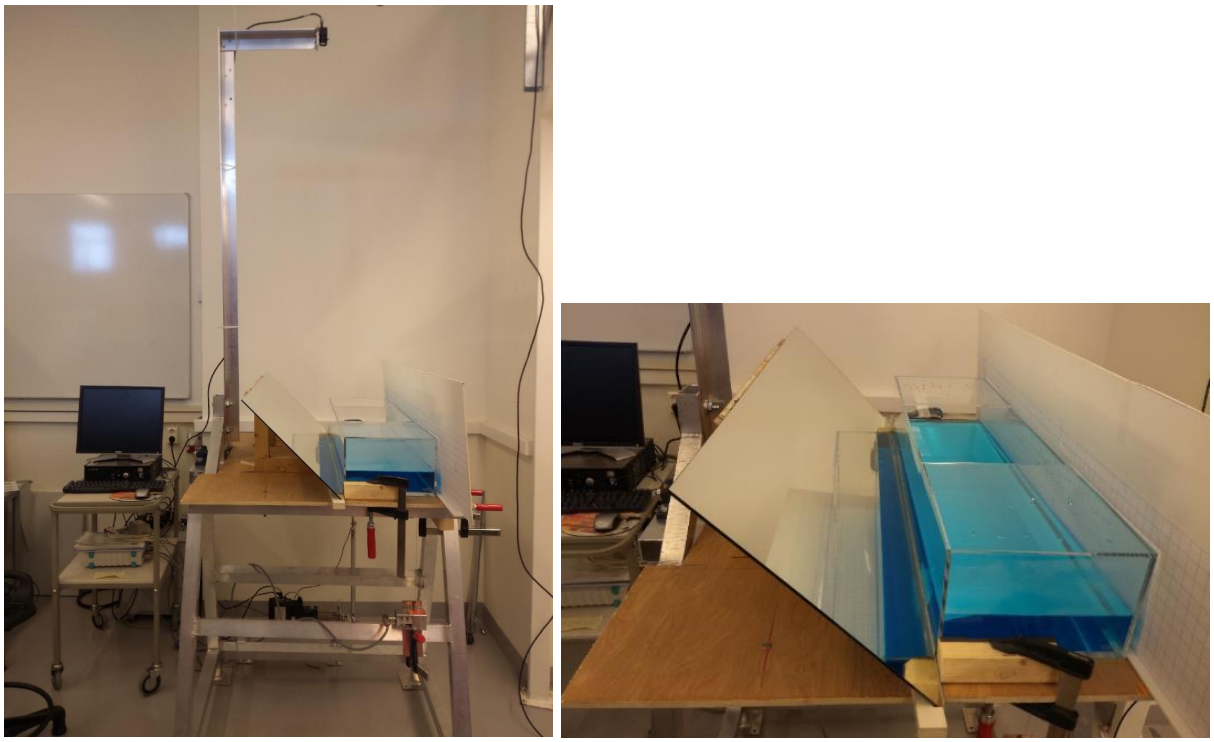

Figure 46. Model Platform overview

Table 9. Main conponents on the phatform

Component	**Description**
Motor	AC-servo JVL MAC800 X1; Driver: Mactalk
Gear box	Gear ratio 1:50
Sensors	Full bridge strain sensor X1 Half bridge angle sensor X1
Data logging system	Hardware: Spider 8; Software: Catman
Camera	CS-Mount 6.2mm f/1.8 Non-Distortion Fixed Lens X2 Driver: StCamSWare Arrangement: One fixed camera; the other moving with the tank.
Mirror	1.2m*0.4m

Table 9 lists the main component installed on the platform. The motor used in the tests is an AC-servo motor: JVL MAC800, which controlled by integrated software Mactalk. The uniform rotation of the motor is then transferred to a roll motion of the tank carrier by using a crank link. It is essential to make sure that the motion of the tank carrier is the correct motion we expected. The whole platform has been simulated in NX with a constant motor speed. A snap shot can be found in Figure 47. The motion of the point is plotted in Figure 48.

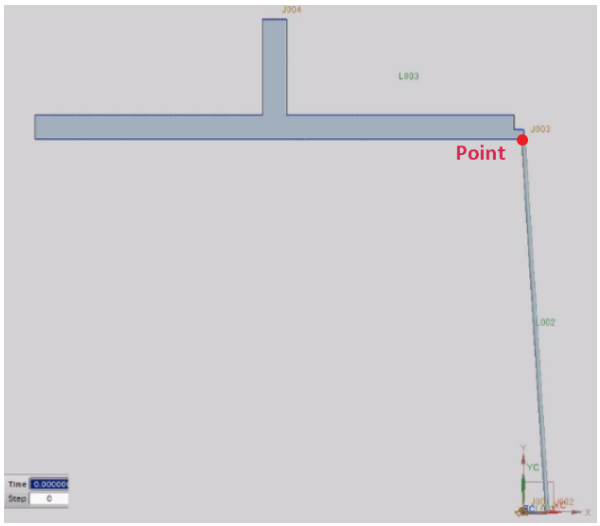

Figure 47. Simulation view in NX

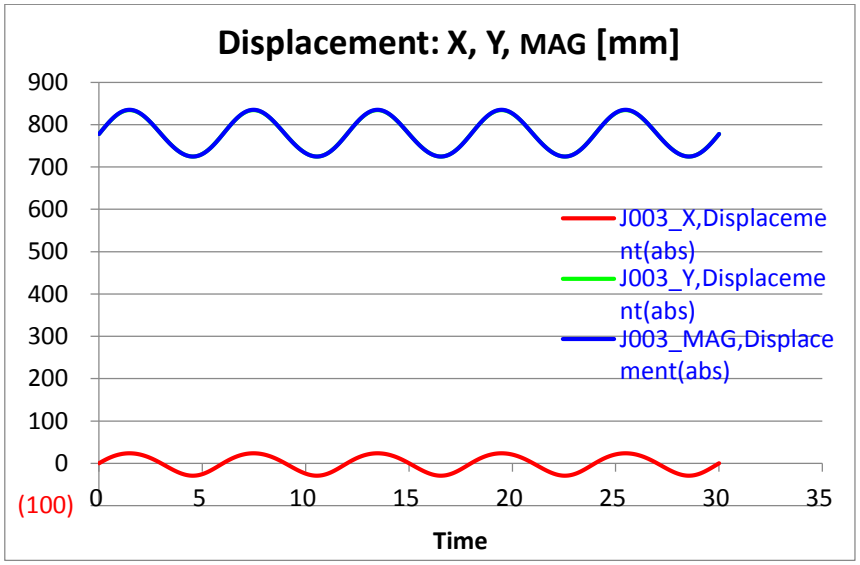

Figure 48. Tank motion result from simulation

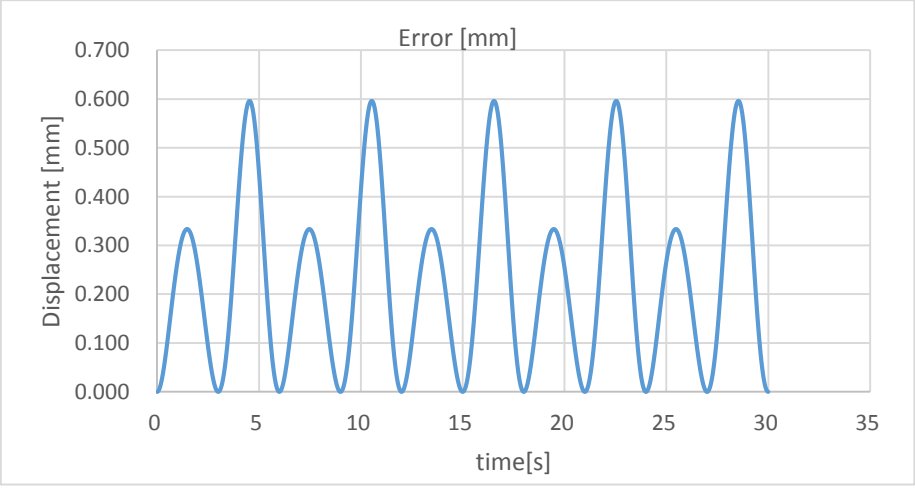

Figure 49. Tank motion error from simulation

In Figure 49, the difference between the displacement in Y direction and magnitude displacement is less than 0.6mm. Compared to the magnitude displacement, the error only account for 1% which is acceptable in our case.

The platform is designed to have the capacity to test different types of tanks including FST, U shape tank, C shape tank and cylinder tank. The maximum tank size should be less than 0.7m in length and 1.5m in breadth.

Table 10. Phatform test capacity

Maximum Tank size	Tank length $L \leq 0.7$m
Rotation center	0cm; $\pm$10cm; $\pm$20cm; 30cm
Excitation amplitude	3deg; 4.5deg; 6deg; 7.5deg; 9deg
Excitation period	Minimum 1s

6.2.3 Test Preparation and Plans

Before doing the experiment, the strain transducers on the platform should be calibrated first. This is carried out by measuring their output while applying a certain force on them. The angle transducers are calibrated by measuring the highest and lowest point. After finishing each test, the platform and the transducers are requied to be set at zero position for doing the following tests.

Due to some reasons, currently the platform can only test the anplitude of 6 degree. Therefore, in this paper we would perform the tests with the excitation amplitude of 6 degree. Detaled text plan can be found in table 11. Notice that the tests without water are also required at each excitation periods.

Table 11. Test plan

Test number	Amplitude	Excitation Period [s]	Motor Input	With/Without liquid
001	6 deg	1	3000	both
002	6 deg	1.25	2400	both
003	6 deg	1.5	2000	both
004	6 deg	1.75	1714	both
005	6 deg	1.8	1667	both
006	6 deg	1.9	1579	both
007	6 deg	2	1500	both
008	6 deg	2.5	1200	both
009	6 deg	3	1000	both
010	6 deg	4	750	both
011	6 deg	5	600	both
012	6 deg	6	500	both

One thing should be noticed is that the Motor input is the value where we put in the Mactalk software. In this case, we have already transferred the excitation period to the motor rotation speed and mutiplied by the gear box ratio 50.

6.2.4 Data post-processing

After finishing all the tests, we can get the moment data both from the tests without liquid and the tests with liquid. The basic idea is to substract the moment without liquid from the moment with liquid. In this way, the liquid moment can be achieved. Then we can do the similar procedure to get the moment amplitude and phase lag from these data.

7 DISCUSSION

7.1 Comparison between model tests and simulations

This part compares the data from simulation with those from model tests. Discussions of model tests and simulations will be conducted here.

The following series of snap shots give a good comparisn between the model test and numerical simulation when the excitation period is 6s.

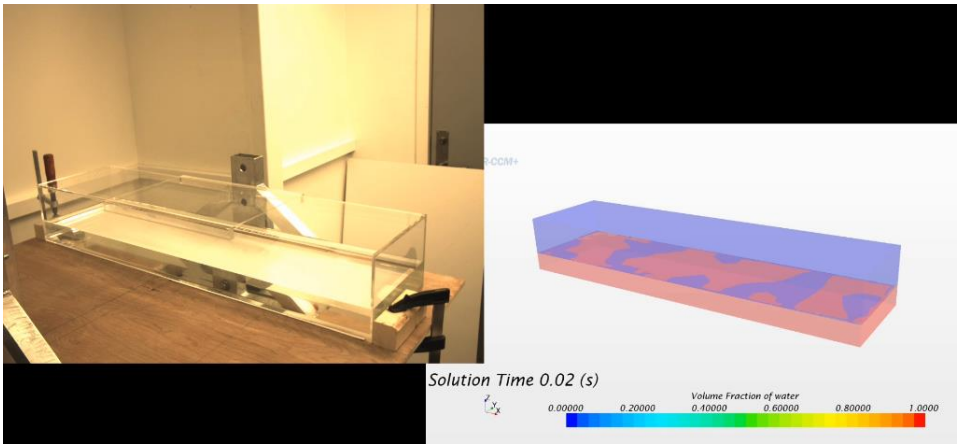

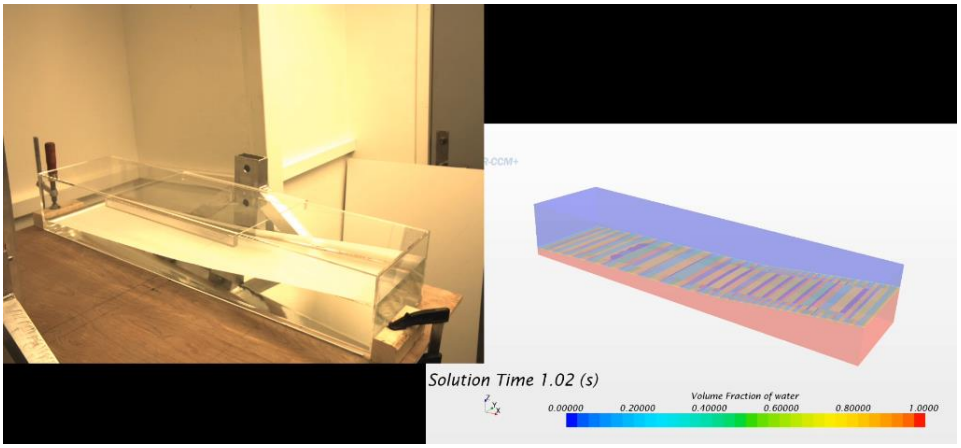

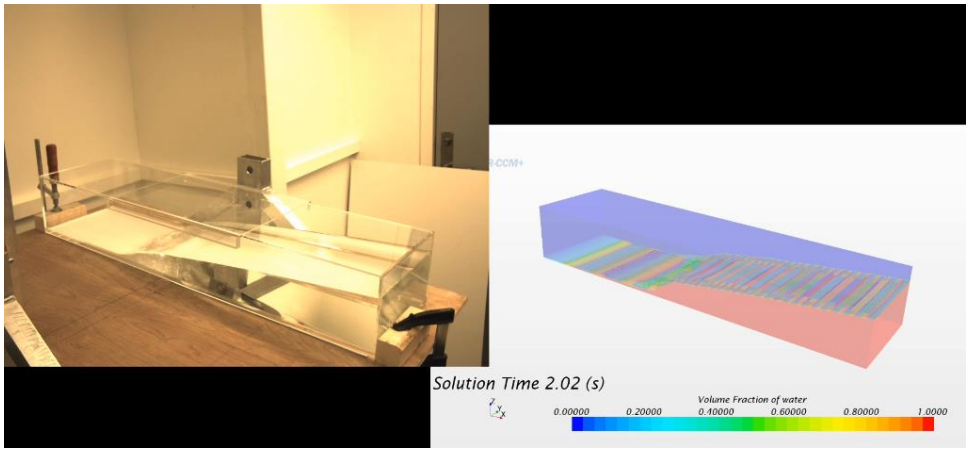

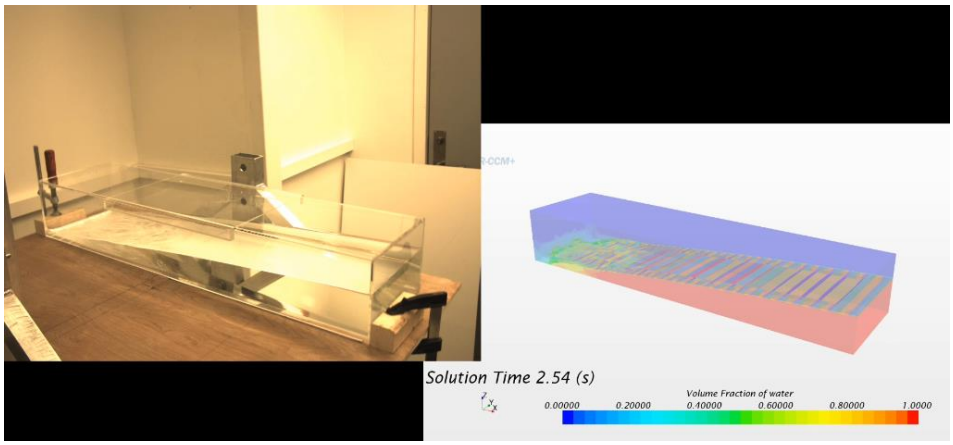
Solution Time 2.54 (s)
Volume Fraction of water
0.00000 0.20000 0.40000 0.60000 0.80000 1.0000

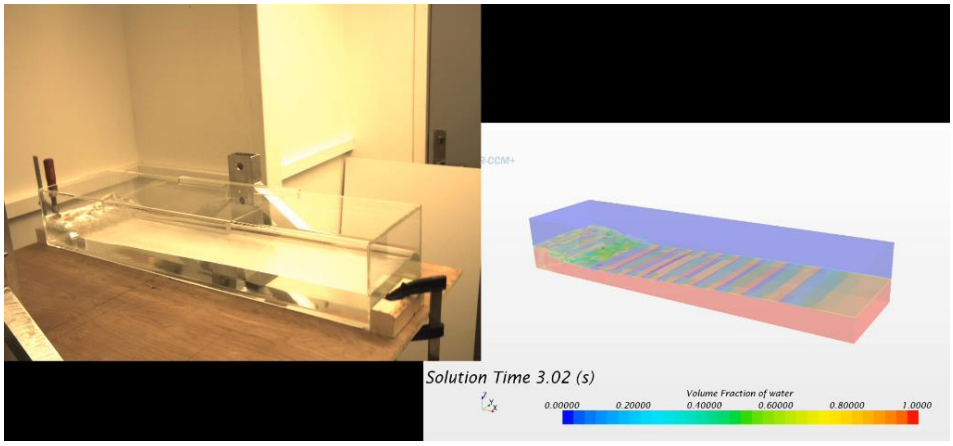
Solution Time 3.02 (s)
Volume Fraction of water
0.00000 0.20000 0.40000 0.60000 0.80000 1.0000

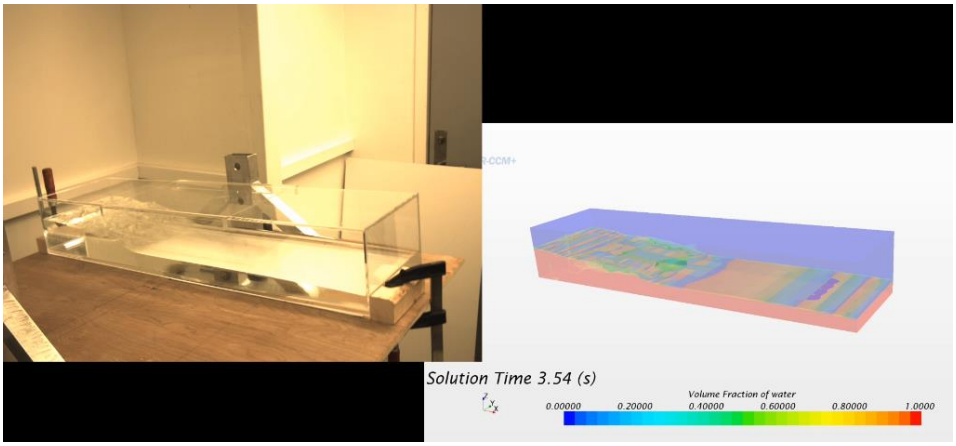
Solution Time 3.54 (s)
Volume Fraction of water
0.00000 0.20000 0.40000 0.60000 0.80000 1.0000

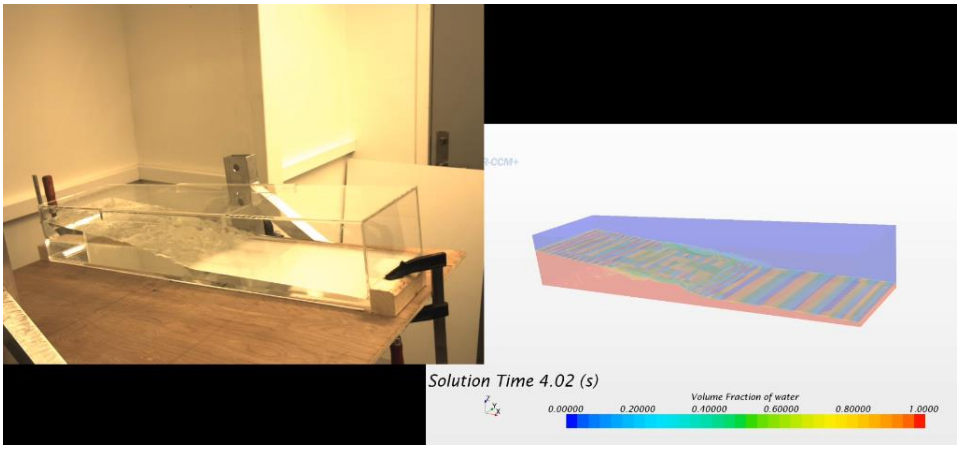
Solution Time 4.02 (s)
Volume Fraction of water
0.00000 0.20000 0.40000 0.60000 0.80000 1.0000

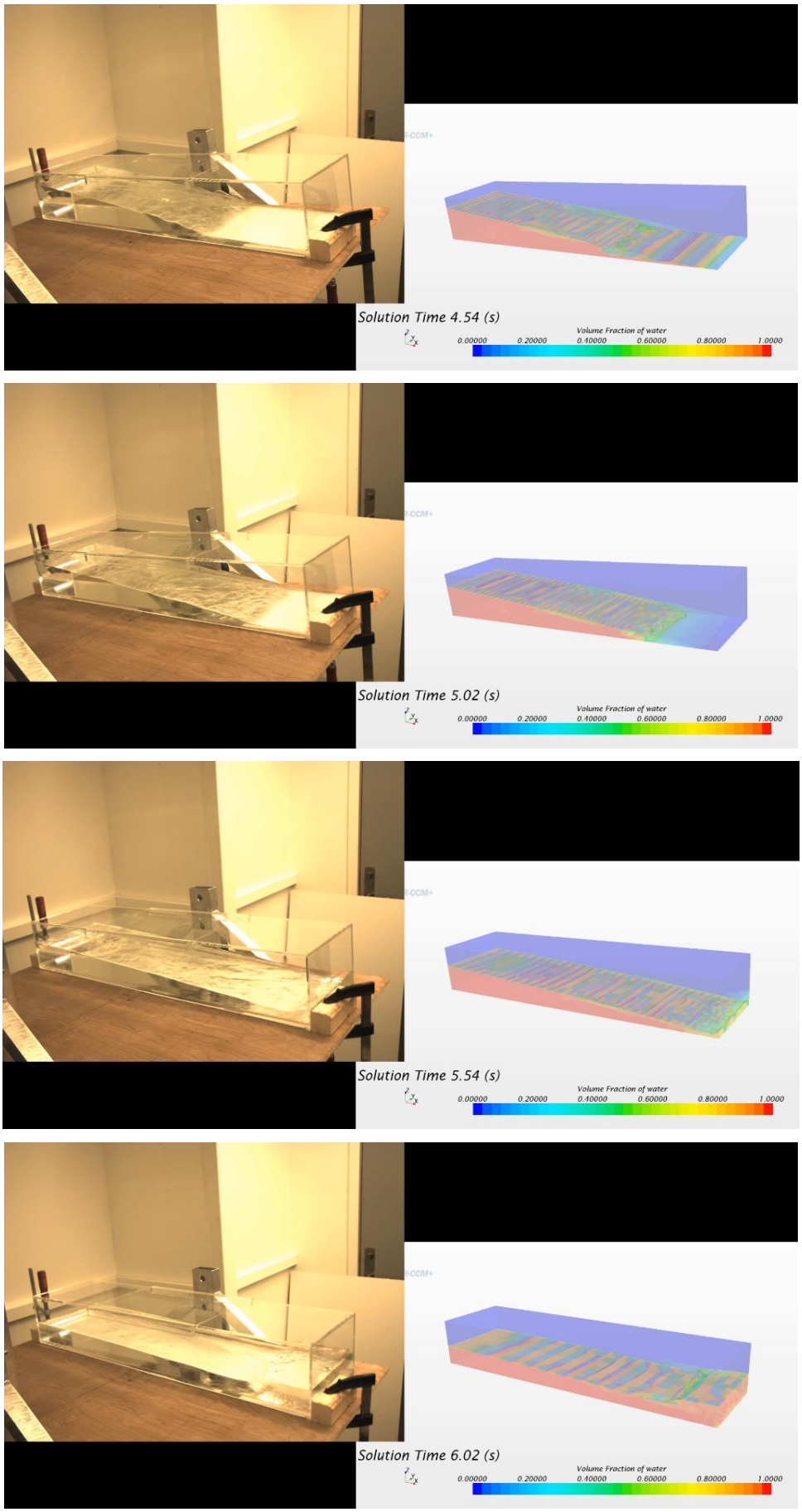

Figure 50. Comparison between model test and simulation

It can be found that the simulation has shown extremly good consistancy with the model test at excitation period of 6s. Figure 51 and 52 illustrate the moment and phase comparisons.

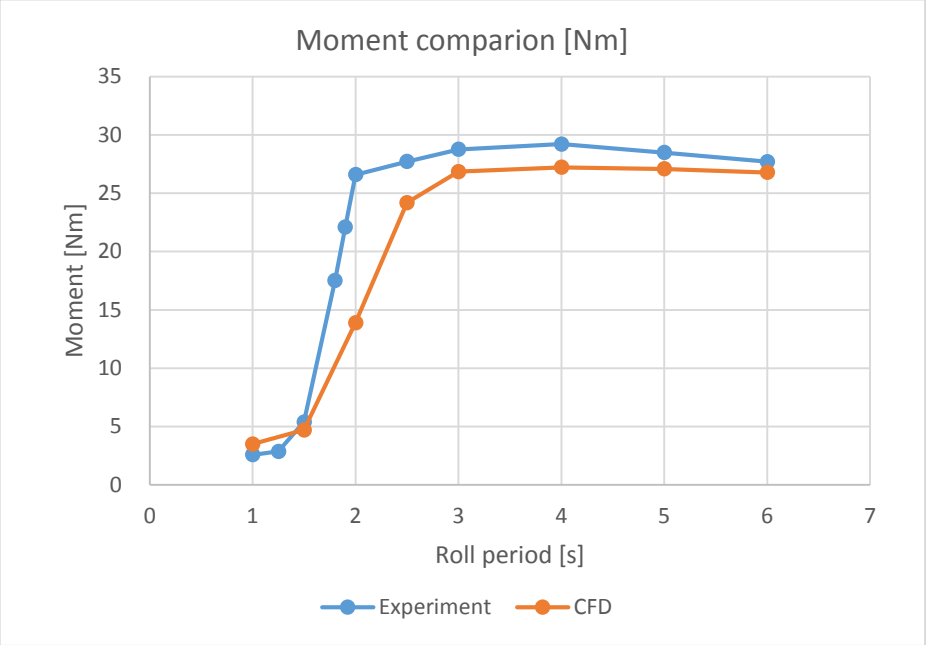

Figure 51. Moment comparison between model test and simulation

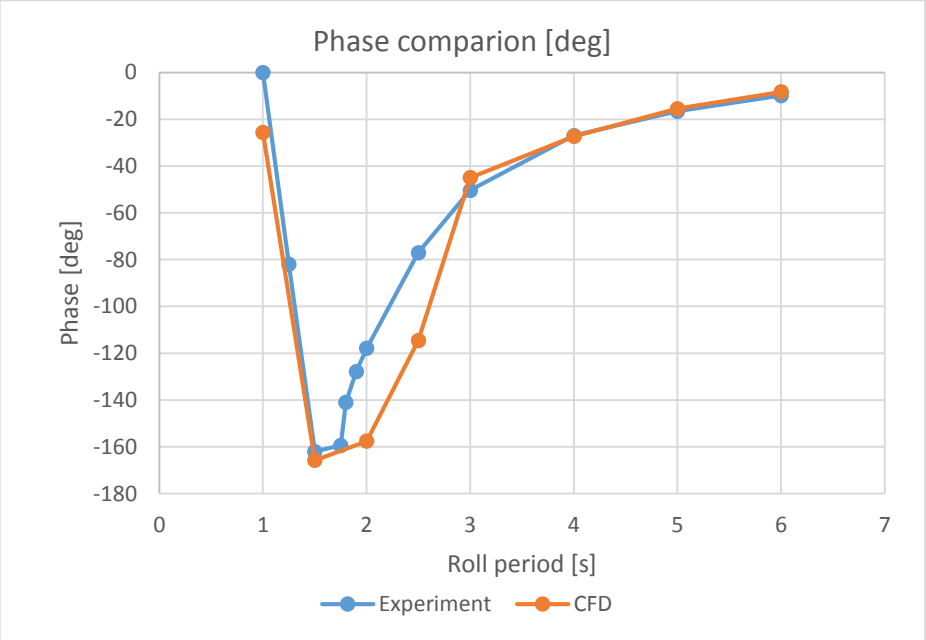

Figure 52. Phase comparison between model test and simulation

The simulations remain stable in stiffness dominated (1s-1.5s) and inertial dominated (3s-6s) regions. Both moment and phase have shown high consistency in these regions. The differences of the moment is less than 10% and the phase has a difference less than 6%.

However, in the damping dominated region (1.5s-3s), the difference between model test and simulations should not be overlooked especially when the excitation period close to the natural period of the tank where resonance occurs.

One of the reasons is the high courant number in the simulation. When the excitation amplitude is 6deg, the motion and velocity is twice as much as that at 3deg amplitude. Therefore, smaller time step is required to keep the courant numer at an acceptable level. Therefore, the results will be more realistic and reliable. Another possible solution to imporve the simulation result is to use 2nd-order temporal discretization scheme instead of 1st-order scheme. Then we can keep the numerical diffusion at a lower level.

7.2 Challenges in the thesis project

CFD has been an useful but challenging tool in applications. One should be very careful when set up the simulation models. It is easy to run a simulation but challenging to make sure that the simulation is accurate. Therefore, it is nesseary to establish a strong theoretical background to fully understand the algorithm and settings behind the software.

Model platform design and establishment took more time than expected. I started this thesis project from early February if not considering the previous literature study time. It took me approximately a month to design the model platform and make evaluation, two and half month to manufacture and install the motor, tank, camera and other components. Acturally, there was only one week for me to do the model tests which made me anxiety. Because if the simulation results were far away from the model tests, there was no time left for me to make modifications or redo the simulations. Therefore, I have to force myself to think as much as possible at the very beginning to make sure everything goes in the right way. Fortunately, the results are very positive both for the simulations and the model tests.

8 CONCLUSIONS

In this thesis project, the development of anti-tanks is summarized as well as the numerical methods. Different types of anti-roll tanks are introduced and compared.

One contribution of this project is developing guidelines for anti-roll tank simulation. A numerical model is introduced and discussed. And this particular model is suitable for a general thermostatic incompressible sloshing problem.

The main part of this project is studying the anti-roll tank performance. Firstly, the natural period of the partially filled tank is investigated and discussed.

Then different excitation amplitudes have been investigated. It has been found that roll damping increases nonlinear with increasing roll amplitude at resonance frequency region. Smaller excitation amplitude will result in higher amping moment. However, the damping moment has liner increase when the excitation period away from the damping dominated region.

Besides, different filling levels are studied and discussed. It found that the roll damping increases with increasing liquid level and the damping dominated region turned to be more narrow. If known the natural period of vessel roll motion, the optimal filling level can therefore be found.

Furthermore, it compares the results from simulations with the exsiting experimental database. The comparions have shown good consistency. The model tests, which designed and performed by the author, have given a strong validation for the numerical simulations as well.

REFERENCES

Bell J., Walker.P. "Activated and passive controlled fluid tank system for ship stabilization." *Transactions of Society of Naval Architects and Marine Engineers*, 1966: 150.

Bennett, S. "Ship stabilization: history." *Concise Encyclopedia of Traffic and Transportation Systems*, 1991: 454-459.

Bernhard Godderidge, Mingyi Tan, Stephen Turnock, Chris Earl. *A Verification and Validation Study of the Application of Computational Fluid Dynamics to the Modelling of Lateral Sloshing.* University of Southampton, 2006.

Bosch, J. J. van den and Vugts, J. H. "Roll damping by free surface tanks." *Nederlands Scheeps-Studiecentrum TNO*, 1966: 83.

Celebi, M.S., Akyildiz, H. "Nonlinear modeling of liquid sloshing in a moving rectangular tanks." *Ocean Engineering*, 2002: 1527-1553.

Charles G Speziale, Sutanu Sarkar, and Thomas B Gatsi. "Modelling the pressure-strain correlation of turbulence: An invariant dynamical systems approach." *Journal of Fluid Mechanics*, 1991: 227:245–272.

Chern, M.J., Borthwick, A.G.L, Eatock Taylor, R. "A pseudospectral transformation of 2-D non-linear waves." *Journal of Fluids Structure*, 1999: 607-630.

Consultants, WS Atkins. *MARNET best practice guidelines for marine applications of computational fluid dynamics.* MARNET, 2003.

F.R.Menter. "Two-Equation Eddy-Viscosity Turbulence Models for Engineering Applications." *AIAA Journal*, 1994: vol.32,1598-1605.

Faltinsen, O. M., Olsen, H. A., Abramson, H. N. and Bass, R. L. "Liquid Slosh in LNG." *Veritas.* Oslo, Norway, 1974.

Faltinsen, O.M., Timokha, A.N. *Sloshing.* 2009.

Fathi, Dariusz Eirik. *ShipX Vessel Responses (VERES), Motion Control Extension.* MARINTEK A/S, 2014.

Frahm, H. "Results of trails of the anti-rolling tanks at sea." *Transactions of Institution of Naval Architects*, 1911: 53.

Froude, W. "On the rolling of ships." *Transactions of Institution of Naval Architects 2*, 1861: 180.

Goudarzi, M. A. and Sabbagh-Yazdi, S. R. "Investigation of Nonlinear Sloshing." *Soil Dynamics and Earthquake Engineering*, 2012: 355-365.

Hirsch, Charles. "Fundamentals of Numerical Discretisation." *Numerical Computation of Internal and External Flows. Vol 1:.* John Wiley and Sons, 1988.

Ikeda, Y., Yoshiyama, T. "A study on Flume-type anti-rolling tank." *Journal of the Kansai society of naval architects 216*, 1991: 111.

John D Anderson, Jr. *Computational Fluid Dynamics: The Basics with Applications.* McGraw Hill, Inc., 1995.

Lee, B.S., Vassalos, D. "An investigation into the stabilization effects of anti-roll tanks with flow obstructions." *International Shipbuilding Progress.* 1996. 43(433),70.

Lewis, E. V. "Principles of Naval Architecture, Volume iii, Motions in Waves and Controllability." *Society of Naval Architects and Marine Enogneers*, 1989.

Liu, Z., Huang, Y. "A new method for large amplitude sloshing problems." *Journal of Sound and Vibration*, 1994: 185-195.

Martin, J.P. "Roll Stabilisation of Small Ships." *Marine Technology*, 1994: Vol. 31, No. 4.

Menter, F.R. "Zonal Two Equation k-w Turbulence Models for Aerodynamic Flows." *24th Fluid Dynamics Conference.* 1993. 93-2906.

Moaleji, R. and Greig, A. R. "On the Development of Ship Anti-Roll Tanks." *Ocean Engineering*, 2007: 103-121.

Palm, William J. *Mechanical Vibration.* John Wiley & Sons, Inc, 2007.

Rhee., Shin Hyung. "Unstructured grid based Reynolds-Averaged Navier-Stokes method." *Transactions of the American Society of Mechanical Engineers.* 2005. 127: 572-582.

Sames, P.C., Marcouly, D., Schellin, T.E. "Sloshing in rectangular and cylindrical tanks." *Journal of Ship Research*, 2002: 186-200.

Solaas, F. "Analytical and Numerical Studies of Sloshing in Tanks." *NTH.* Trondheim, Norway, 1995. 103.

Souto Iglesias, A., Perez Rojas, L., Zamora Rodriguez, R. "Simulation of anti-roll tanks and sloshing type problems with smoothed particle hydrodynamics." *Ocean Engineering*, 2004: 1169-1192.

Vasta, J., Gidding, A.J., Taplin, A., Stilwell, J.J. "Roll stabilization by means of passive tanks." *Transactions of Society of Naval Architects and Marine Engineers*, 1961: 411.

Wilcox, David C. *Turbulence Modelling for CFD.* DCW Industries, 1998.

Winkler, S. "FLUME® Passive Anti-Roll Tanks : Application on merchant and naval ships." *Flume GmbH*, 2012.

Zhong, Z., Falzarano, J.M., Fithen, R.M. "A numerical study of U-tube passive anti-rolling tanks." *Proceedings of the Eight International Offshore and Polar Engineering Conference.* Canada, 1998. 504-513.

APPENDIX

Appendix A	Tank Drawings
Appendix B	3D model of Tank Platform (digital)
Appendix C	Test data files (digital)
Appendix D	Simulation files (digital)
Appendix E	Animations of comparions (digital)
Appendix F	Draft paper version of the thesis work

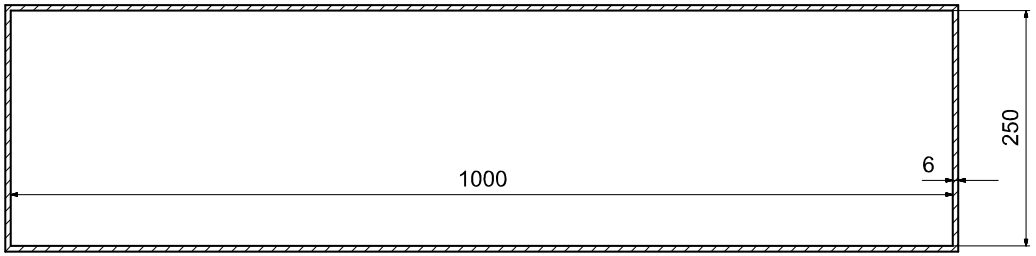

SECTION B-B

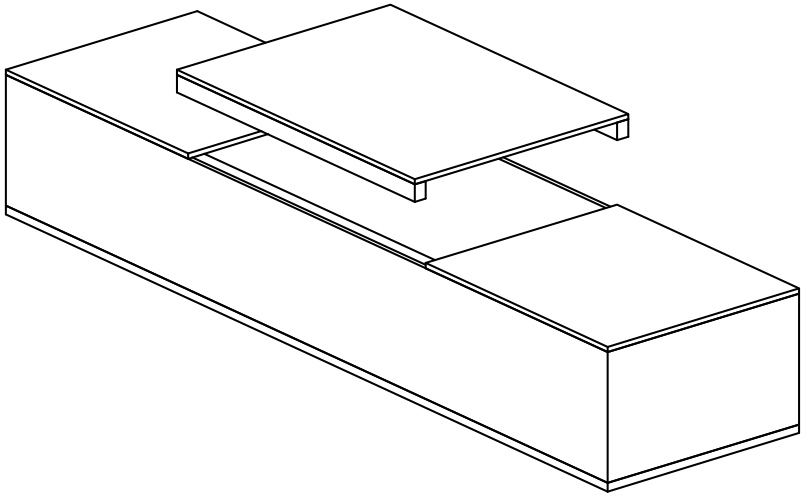

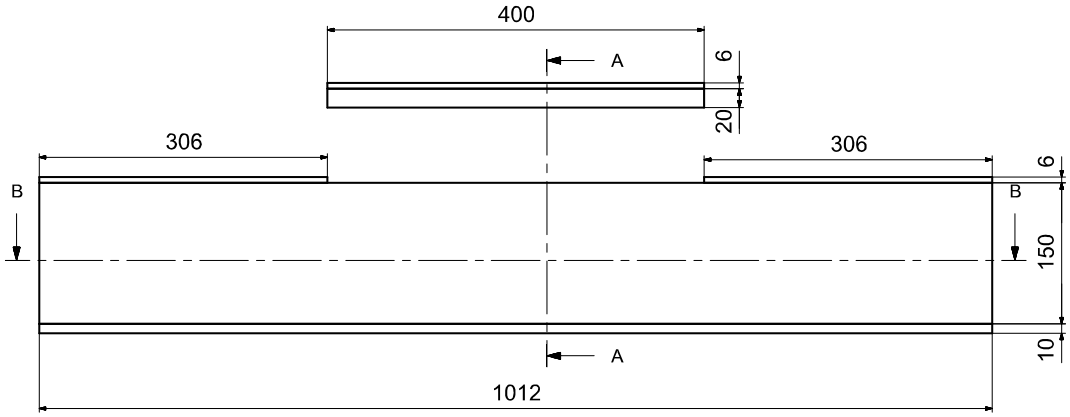

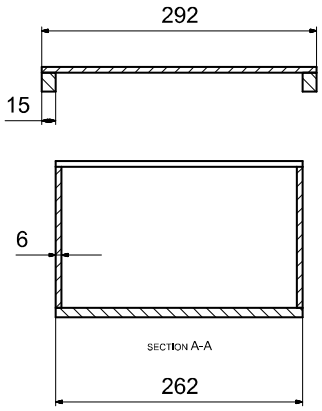

SECTION A-A

262

ALL DIMENSIONS IN MM

SIEMENS		THIS DRAWING HAS BEEN PRODUCED USING AN EXAMPLE TEMPLATE PROVIDED BY SIEMENS PLM SOFTWARE	
FIRST ISSUED		TITLE	
DRAWN BY			
CHECKED BY			
APPROVED BY		SIZE: A0	DRG NO. assembly1
		SCALE 1:1	SHEET 1 OF 1

（Initial draft）

Computational Fluid Dynamics (CFD) study on Free surface anti-roll tank and experimental validation

ABSTRACT

The excessive motion of a ship can seriously degrade the performance of machinery and personnel. Anti-roll tanks are tanks fitted onto ships in order to improve their response to roll motion, which is typically the largest amplitude of all the degrees of freedom. In this paper, a numerical model based on Volume of Fluid (VOF) is introduced to simulate the liquid sloshing inside a free surface tank (FST). Through the simulation of the model, the performance of the FST is fully investigated when the tank is excited by different periods and different amplitudes. Besides, different tank filling levels are studied to find out the optimal filling level. The results are proved by the existing experimental database. Furthermore, results from model test gives further validation to the numerical model. The comparisons between the model tests and simulations have shown good consistency. Further improvements are proposed in the end.

Key words: Volume of Fluid (VOF), free surface tank (FST), model tests, validation

INTRODUCTION

The subject of roll stabilisation has been investigated for many years by Naval Architects and designers. The main reason for this continued interest is that for roll, unlike pitch or other degrees of freedom, the forces required to create a stabilising effect are relatively small.

There are a great number of roll stabilisation devices available for use on vessels today. Many of these were initially developed for use on large ships but are increasingly being installed on smaller vessels where the subsequent benefit to the vessel's motions is often more apparent. This is due to the relatively high transverse stability, and short natural roll periods of smaller vessels (Martin 1994). The prevalence of shorter waves also means that smaller vessels are more likely to encounter resonant wave conditions and thus violent rolling. Therefore, this paper invetigated the tank performance on a offshore supply vessel (OSV) byusing CFD tool and model tests.

NUMERICAL METHOD

The motion of a fluid can be described by a set of partial differential equations expressing conservation of mass, momentum and energy per unit volume of the fluid. The Navier Stokes equations for three dimensional incompressible fluid flow can be written in conservation form as follows

$$\nabla \cdot \vec{v} = 0 \tag{1}$$

$$\frac{\partial \vec{v}}{\partial t} + \nabla \cdot (\vec{v}\vec{v}^{T}) = -\frac{1}{\rho}\nabla p + \nu(\nabla \cdot \nabla)\vec{v} - g\vec{e}_3 \tag{2}$$

where

- $\vec{v}$ is the velocity field vector;
- p is the pressure;

- ρ is the mass density;
- ν is the kinematic viscosity;
- g is the acceleration of gravity;
- $\overrightarrow{e_3}$ is the unit vector pointing upwards;
- ∇ is the gradient operator;
- ∇· is the divergence operator;
- ∇·∇ is the Laplace-operator;

The interface between the phases of the mixture is resolved by using Volume of Fluid (VOF) model.

TANK DESCRIPTION

A series of tests with free surface anti-roll tank in 1DOF harmonic motion was conducted at Aalesund University College. The results of these experiments in terms of moment amplitude and phase angle were used to validated the simulation model.

Table 1. Main dimensions of the Vessel

Parameter	Value [m]
Lpp	75.5
Breadth	21
Draught	6.8
Vertical center of gravity,VCG	7.6

Table 2. Full scale tank dimensions

Parameter	**Notation**	**Full scale**	**Model scale**
		Value [m]	**Value [mm]**
Tank width	b	20	1000
Tank length	L	5	250
Tank height	H	3	150
Filling level	h	1;1.5;2	50;75;100
Rotation point above the tank bottom	s	0	0

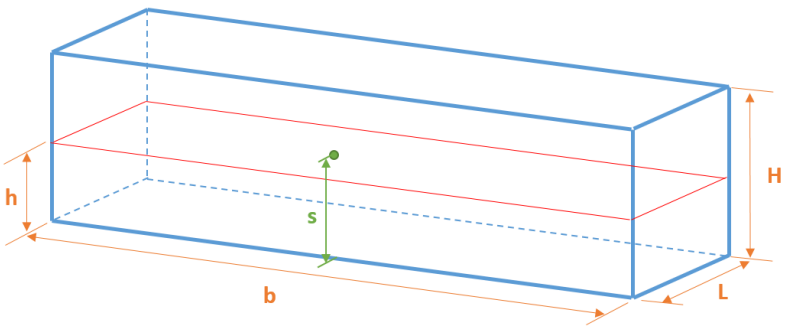

Figure 1: Definition of geometry and tank dimensions

Normally, the liquid inside free surface tank should have a weight which accounts to approximately 2-4% of the total ship displacement. The tank breath is designed as large as possible in order to provide more damping moment. Based on industrial experience, it is recommended that the designed tank length should follow:

$$L = 3 + 3\% \times Lpp$$

The full size tank is scaled to a model size tank by a scale factor 1:20. The model size tank is therefore used in both numerical calculations and model tests. The tank motion is defined as a 1-DOF sinusoidal motion with the rotation center in the middle of the tank bottom.

MODELLING

In this paper, the tank geometry is meshed by Trimmer model using a base size 0.005m. In order to get better results, volumetric control in Z direction is introduced. The relative Z size is 0.0025m which is 50% of the other two directions.

Star CCM+ offers two different time discretisation schemes, a first order and second order backward Euler scheme. Both of them are tested and recommendation will be given. A time step of 0.001s is applied in the numerical simulation. Thus, the Courant number, which is the rate of flow speed with which numerical disturbances propagate, will be controlled below 1.0. The flow inside is simulated as turbulent flow. K-Epsilon turbulence model is applied here.

2D FLOW VS 3D FLOW

Generally speaking, turbulence is a three-dimensional time-dependent phenomenon, therefore the simulations should use 3D model. However, a 2D model is computionally cheap compared to a 3D model when using same dimensions. Therefore, it is of interest to investigate the differences beteen 2D and 3D simulations.

The grids/meshes of 2D and 3D model are compared in the following table. Notice that the calculating environment is Windows 8.1 x64, Intel(R) Core(TM) i7-3635QM CPU @ 2.40GHz 2.40GHz, 8G RAM.

Table 7. 2D and 3D comparison

	cells	Interior Faces	Vertices	Computional time
2D	12000	23740	12261	20 mins for 10 s
3D	127296	376096	171609	233 mins for 10s
Ratio	1:10.6	1:15.8	1:14	12:1

Next, we will compare 2D and 3D simulations when excitation period is 2s, 2.5s, 3s, 4s, 5s, respectively. In order to make sure that 2D simulations are accurate enough, we use a smaller time step 0.001s.

When the excitation period is relatively small for instance 2.5s as shown in Figure 2, some differences appears between 2D and 3D simulations. An obvious reason is that 2D simulation neglect the vortex in tank length direction. Besides, it does not include the effect of the tank side walls. However, these two aspects may affect the result only when the flow inside the tank is fully turbulent. When we increase the excitation period to 3s, 4s and 5s, it can be found that the differences between 2D and 3D simulations become smaller and smaller.

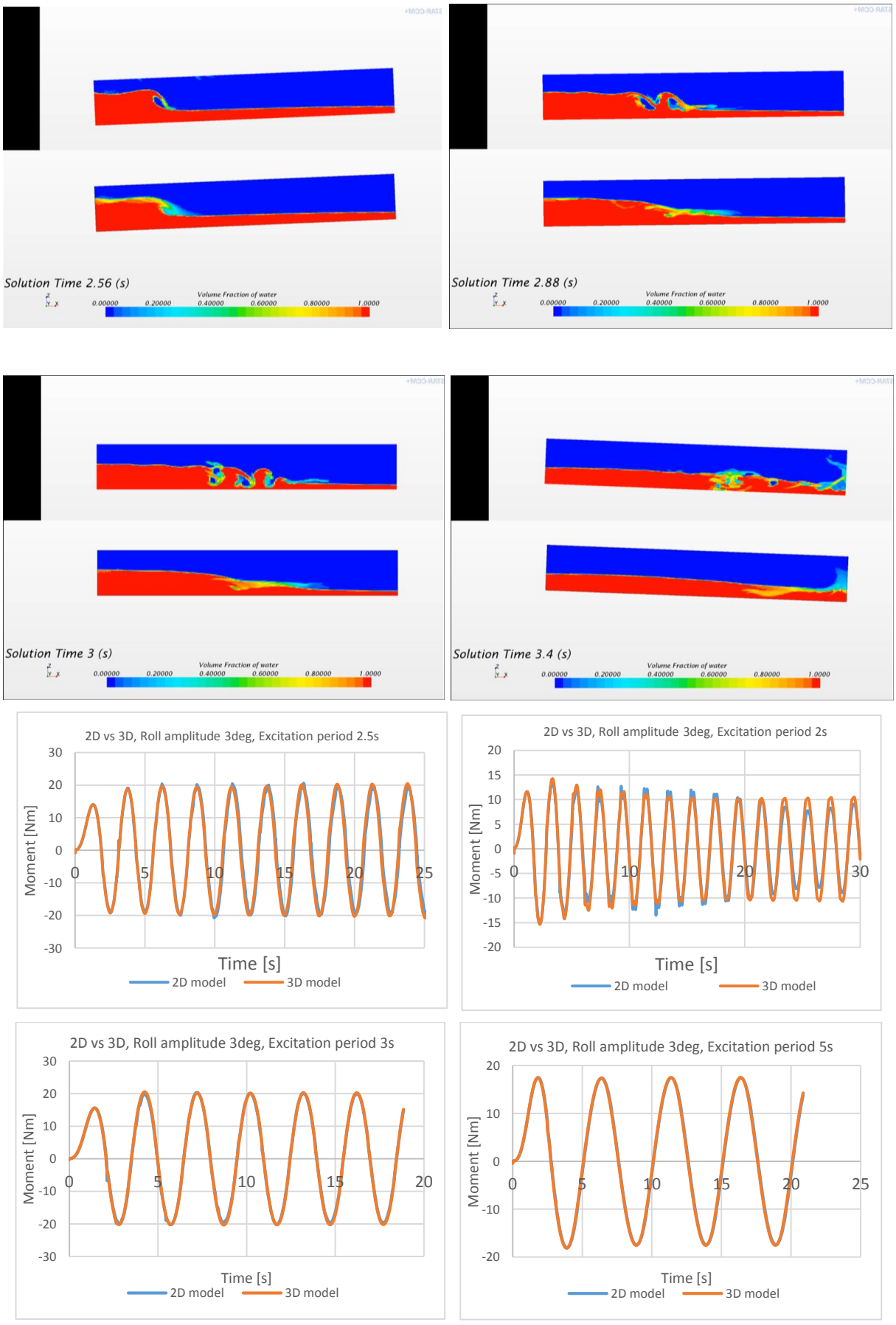

Figure 2: Comparison between 2D and 3D flow

Based on previous discussion, the moment differences between 2D and 3D simulations are rather small. Therefore, we may accept 2D simulations only in our specific cases. Though turbulence is a three-dimensional time-dependent phenomenon, we may use 2D simulations to initial iterations, initial screening of alternative designs, and parametric studies because it is easy to implement and computationally cheap.

However, when the excitation period is very small and the sloshing inside is severe, 3D simulation is recommended and it is more reliable than a 2D simulation.

EXCITATION AMPLITUDES

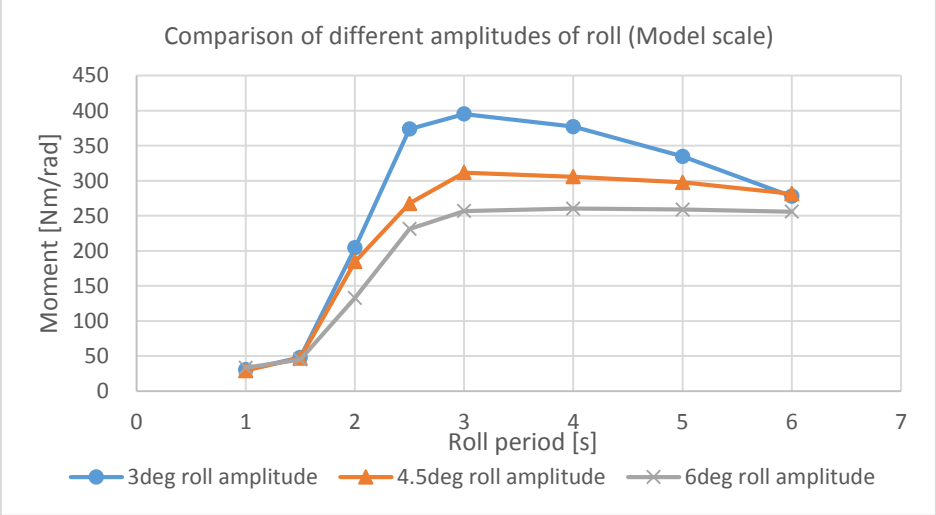

Figure 3. Moment comparison of different excitation amplitudes (Model scale)

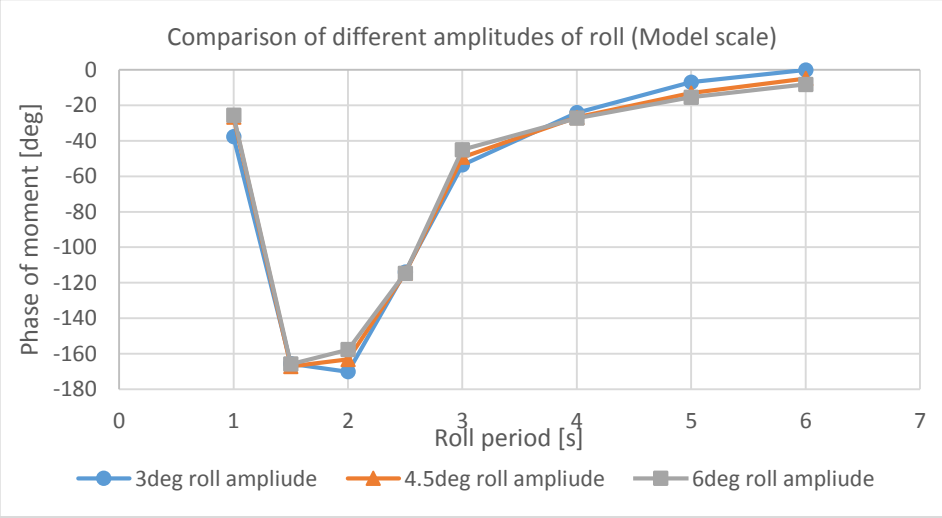

Figure 4. Phase comparison of different excitation amplitudes (Model scale)

In figure 3, the moment is expressed as moment per unit roll to make the values comparable with other amplitudes of roll. The total moment can be found by multiplying with the amplitude of roll motion. The amplitude of the moment can also be read out of the time series.

When multiplying each curve by its roll amplitude it is clear that the black curve multiplied by six gives higher values than the blue curve multiplied by two. A higher roll amplitude represented by the black curve gives therefore higher damping moments. Another aspect can be seen from the graph: The distances between the single curves are not equal. The damping moment increases not linear with the roll amplitude.

The lower graph in figure 4 shows the phase of the moment relative to the rig motion in degrees over the roll periods. For the first period of four seconds and for the large periods towards the end, there is nearly no phase difference because either the water is too inert to follow the rig motions or it can easily follow the motions at large periods. The phase of the moment can be read out of the recorded time series after the measured forces are multiplied by the lever arm to the centre of gravity.

FILLING LEVELS

The main dimensions of a ART are defined in design phase. Therfore, change the filling percentage becomes the only way to ajust the natural frequency of the tank. In this part, we will discuss three different filling levels: 5cm, 7.5cm and 10cm, corresponding to 33%, 50% and 66% filling percentage.

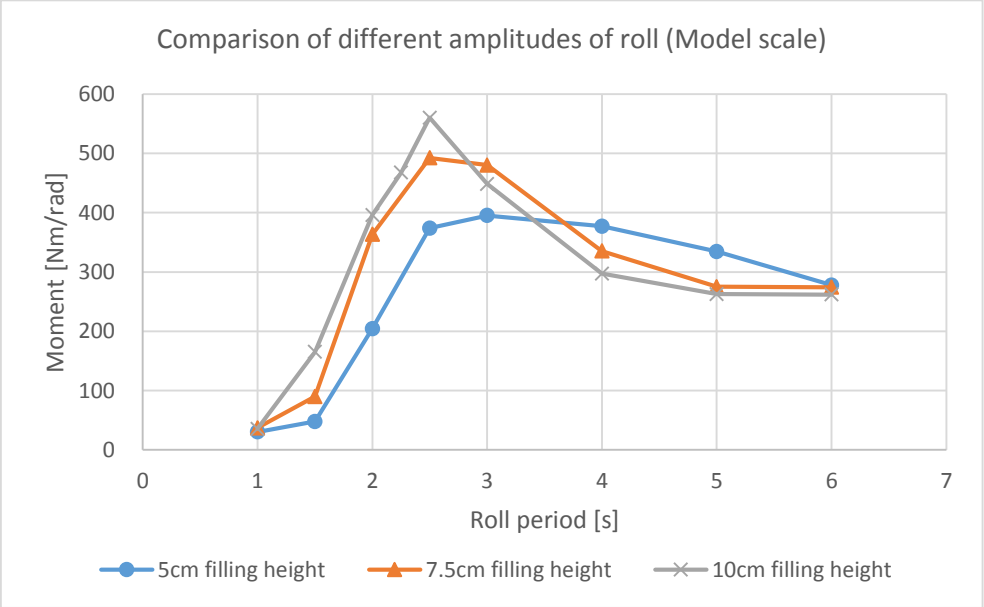

Figure 5. Moment comparison of different filling levels (Model scale)

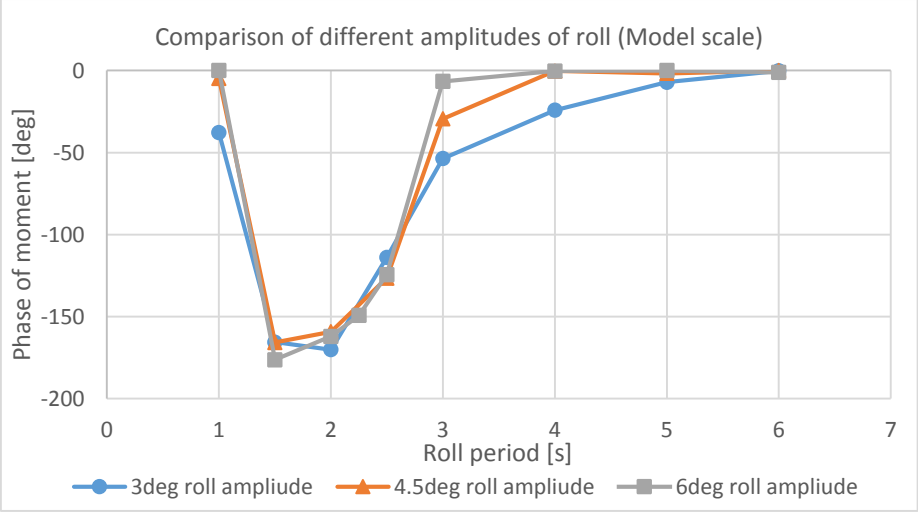

Figure 6. Phase comparison of different filling levels (Model scale)

Normally, higher filling level means more liquid inside the tank which will provide more static forece thus create more damping moment. This phenomenon can be found from 1s to 2.5s in Figure 5.

The natural period of the tank reduces as the filling level increases. It can be found that higher filling level create higher peak moment.

When the sytem enters in inertial dominated region, the tank with more liquid generates less moment. More liquid inside the tank means more mass, which creates more inertial impact. Therefore, it is more difficult to excite the liquid motion. Besides, the system with more mass enters in inertial dominated region much more early than those with less mass. This can also be found in the phase curve.

When the phase close to 0 (after 3.0s), the system enters in interial dominated region. Besides, it indicates the resonance occurs when the phase angle close to -90deg.

Then we transfer the model scale result to full scale result as shown in Figure 6. Considering the resonance period of the vessel is around 13s (Figure 37), we can found the tank performance at 50% filling is much better that it with 33% filling. The optimal filling level for this particular tank is between 50% and 66%.

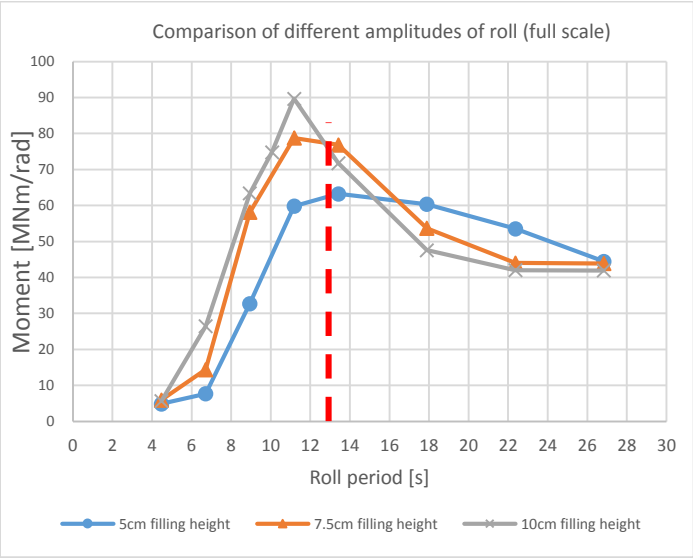

Figure 7. Comparison of different filling levels (Full scale)

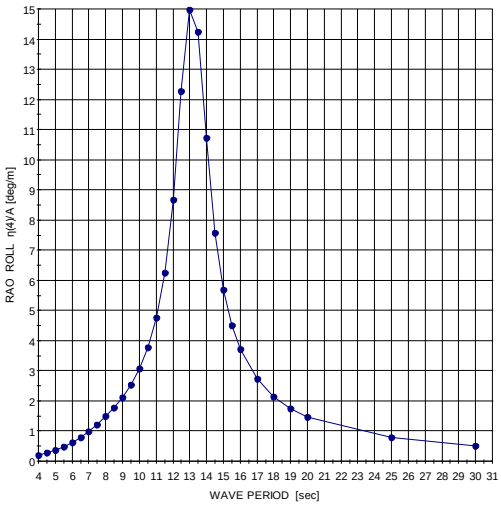

Figure 8. Roll RAO of the OSV

EXPERIMENTAL VALIDATION

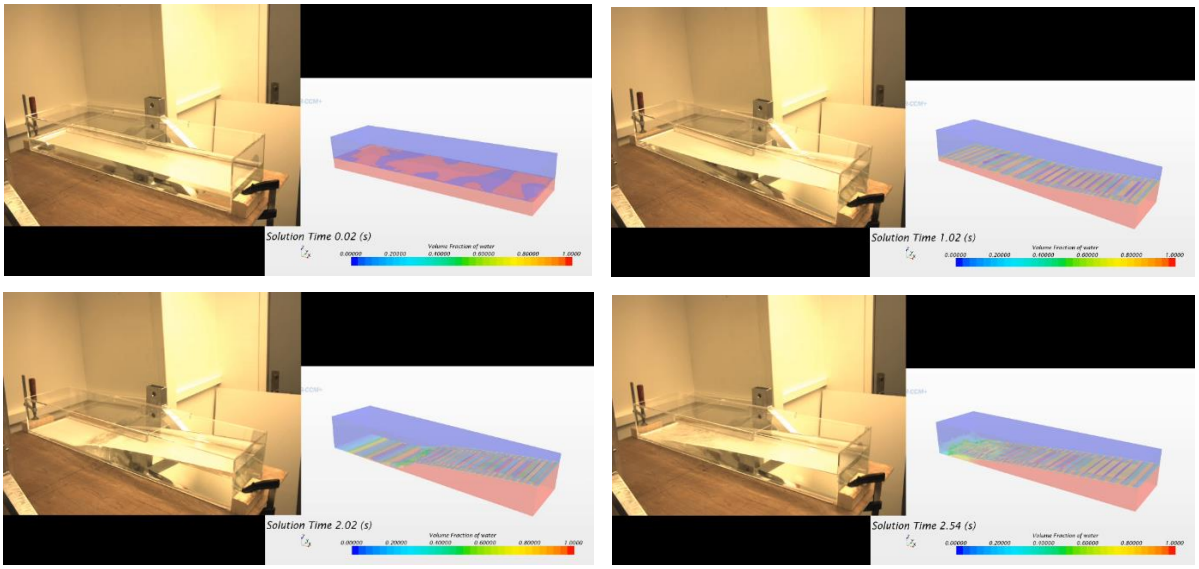

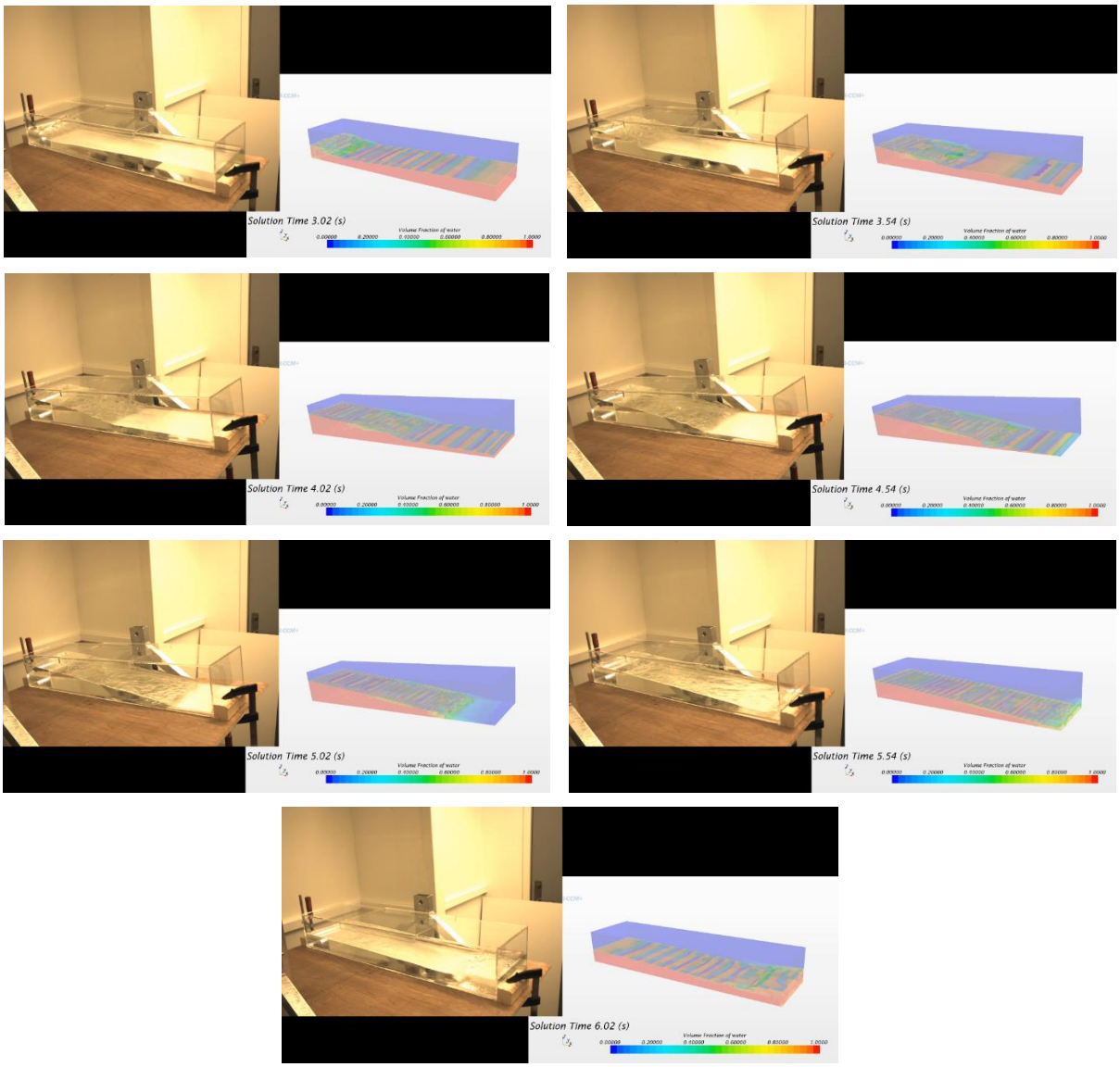

Figure 9. Comparison between model test and simulation at period 6s

It can be found that the simulation has shown extremly good consistancy with the model test at excitation period of 6s. Figure 51 and 52 illustrate the moment and phase comparisons.

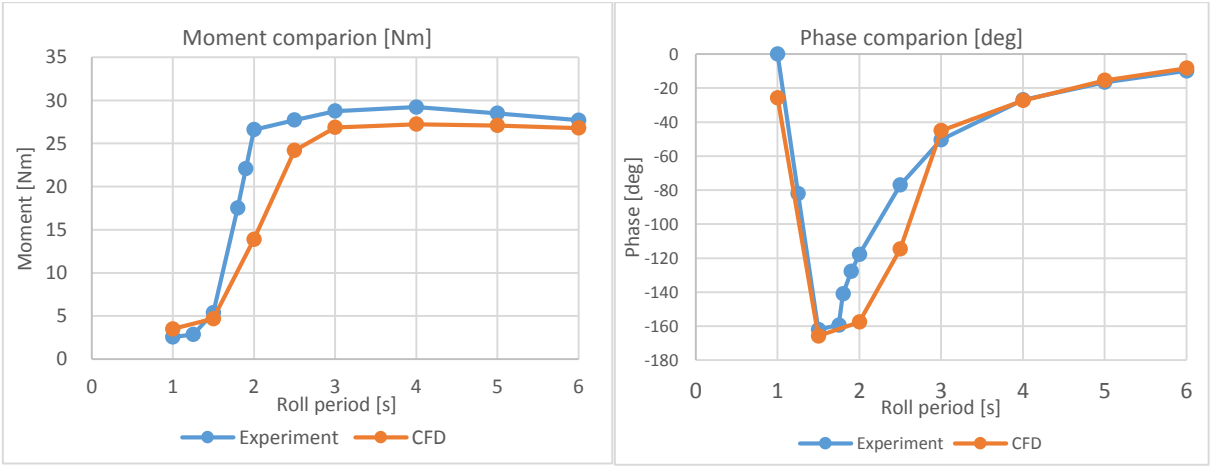

Figure 10. Moment and phase comparison between model test and simulation

The simulations remain stable in stiffness dominated (1s-1.5s) and inertial dominated (3s-6s) regions. Both moment and phase have shown high consistency in these regions. The differences of the moment is less than 10% and the phase has a difference less than 6%.

However, in the damping dominated region (1.5s-3s), the difference between model test and simulations should not be overlooked especially when the excitation period close to the natural period of the tank where resonance occurs.

One of the reasons is the high courant number in the simulation. When the excitation amplitude is 6deg, the motion and velocity is twice as much as that at 3deg amplitude. Therefore, smaller time step is required to keep the courant numer at an acceptable level. Therefore, the results will be more realistic and reliable. Another possible solution to imporve the simulation result is to use 2nd-order temporal discretization scheme instead of 1st-order scheme. Then we can keep the numerical diffusion at a lower level.

CONCLUSIONS

A numerical model is introduced and discussed. And it has been proved that this particular model is suitable for a general thermostatic incompressible sloshing problem.

The main part of this project is studying the anti-roll tank performance. Different excitation amplitudes have been investigated. It has been found that roll damping increases nonlinear with increasing roll amplitude at resonance frequency region. Smaller excitation amplitude will result in higher amping moment. However, the damping moment has liner increase when the excitation period away from the damping dominated region.

Besides, different filling levels are studied and discussed. It found that the roll damping increases with increasing liquid level and the damping dominated region turned to be more narrow. If known the natural period of vessel roll motion, the optimal filling level can therefore be found.

Furthermore, it compares the results from simulations with the exsiting experimental database. The comparions have shown good consistency. The model tests, which designed and performed by the author, have given a strong validation for the numerical simulations as well.